National Library
of Canada

Bibliothèque nationale
du Canada

Canadian Theses Service   Service des thèses canadiennes

Ottawa, Canada
K1A 0N4

NOTICE

The quality of this microform is heavily dependent upon the quality of the original thesis submitted for microfilming. Every effort has been made to ensure the highest quality of reproduction possible.

If pages are missing, contact the university which granted the degree.

Some pages may have indistinct print especially if the original pages were typed with a poor typewriter ribbon or if the university sent us an inferior photocopy.

Previously copyrighted materials (journal articles, published tests, etc.) are not filmed.

Reproduction in full or in part of this microform is governed by the Canadian Copyright Act, R.S.C. 1970, c. C-30.

AVIS

La qualité de cette microforme dépend grandement de la qualité de la thèse soumise au microfilmage Nous avons tout fait pour assurer une qualité supérieure de reproduction.

S'il manque des pages, veuillez communiquer avec l'université qui a conféré le grade

La qualité d'impression de certaines pages peut laisser à désirer, surtout si les pages originales ont été dactylographiées à l'aide d'un ruban usé ou si l'université nous a fait parvenir une photocopie de qualité inférieure.

Les documents qui font déjà l'objet d'un droit d'auteur (articles de revue, tests publiés, etc.) ne sont pas microfilmés.

La reproduction, même partielle, de cette microforme est soumise à la Loi canadienne sur le droit d'auteur, SRC 1970, c. C-30.

Canada

Anatomical and Physiological Characteristics of
Mesencephalic and
Pontine Substrates of Reward

Sandra Boye

A Thesis

in

The Department

of

Psychology

Presented in Partial Fulfillment of the Requirements
for the Degree of Master of Arts at
Concordia University
Montréal, Québec, Canada

September 1988

© Sandra Boye, 1988

ABSTRACT

Anatomical and Physiological Characteristics of

Mesencephalic and Pontine Substrates of Reward

Sandra Boye

The objective of this study was to determine anatomical

and physiological characteristics of mesencephalic and

pontine substrates of reward.

Male hooded rats were implanted with a fixed monopolar

stimulating electrode aimed at the ventral tegmental area

and a moveable electrode aimed at the medial pons. After

stabilization of self-stimulation, the existence of reward-

relevant axonal linkage between fixed mesencephalic self-

stimulation sites and several dorsoventral pontine sites was

investigated using the behavioral version of the collision

test. A combination of eight mesencephalic and 44 pontine

sites were sampled in eight subjects. Evidence of direct

axonal linkage was found between the lateral hypothalamus-

ventral tegmental area and eleven sites in the medial pons.

In a second experiment, estimates of the refractory

periods and the conduction velocities of the reward-relevant

neurons linking the lateral hypothalamus-ventral tegmental area and the medial pons were obtained in six of the subjects. Results show that the most excitable reward-relevant neurons have absolute refractory periods and conduction velocities in the range of 0.35 to 0.73 msec and 3.96 to 14-m/sec respectively.

Acknowledgements

My sincerest gratitude goes out to Dr. Pierre-Paul Rompré, my thesis supervisor, for all the help and guidance he has provided throughout the past two years. Pierre-Paul has always been an enlightening source of new ideas and insight and for this, I am grateful.

Thanks to Dwayne Schindler, all aspects of data analysis for this thesis were made simple and quick. Dwayne's enormous patience and helpful comments have made this thesis a little easier to complete.

I wish to thank Dr. Peter Shizgal for helpful comments and advice at all stages of my work. Peter's enthusiasm for the field has always been a source of encouragement.

Many thanks to my office mates Beverley Murray, Margaret Forgie, Renee Segal and Beth Noel, for sharing the good times and laughing at the bad. I am especially grateful to Margaret and Beverley for their support, encouragement, and helpful advice throughout the preparation of this thesis.

Finally, I'd like to thank my family, mom, dad, Silvia and Peter for having supported and encouraged me from the beginning.

Dedication

This thesis is dedicated to my parents, Nydia and Ramon

Table of Contents

List of Figures

List of Tables

List of Appendices

An important goal in the study of the physiological basis
of motivation is the identification of the neural
substrate(s) responsible for the transmission and
integration of reward signals. In this respect, electrical
brain self-stimulation, discovered by Olds and Milner
(1954), constitutes a powerful tool. Electrical brain
stimulation studies have often employed the self-stimulation
paradigm as a model of appetitively motivated behavior: the
self-stimulating rat emits an instrumental response with the
goal of attaining the delivery of a train of stimulating
pulses to a reward-related brain site. Electrical
stimulation of the brain can thus be used as a reinforcer of
operant behavior. Consequently, by studying goal-directed
behavior, such as self-stimulation, we may be in a better
position to understand the neural circuitry that mediates
reward.

Most of the previous research aimed at identifying and
characterizing the substrate(s) for self-stimulation has
focussed on the medial forebrain bundle (MFB). Stimulation
along this fiber bundle produces strong reward and few
concomitant aversive and/or motoric reactions. It has been
shown that at least some reward-relevant neurons in the MFB
link the lateral hypothalamus and the ventral tegmental area
(Shizgal, Bielajew, Corbett, Skelton and Yeomans, 1980;
Bielajew and Shizgal, 1980, 1982, 1986; Durivage and
Miliaressis, 1987; Gratton and Wise 1988; Malette and

Miliaressis, 1987). Bielajew and Shizgal (1986) have
further shown that the normal direction of propagation of at
least some reward-relevant neurons in the MFB is descending
(action potentials travel in a rostro-caudal direction).
Other studies have shown that the refractory periods and
conduction velocities of reward-relevant neurons in the MFB
are in the range of 0.4 to 1.2 msec (Yeomans 1975, 1979;
Rompré and Miliaressis, 1980; Miliaressis and Rompré, 1980;
Bielajew, Jordan, Ferme-Enright and Shizgal, 1981; Bielajew
and Shizgal, 1982, 1986; Macmillan, Simantirakis and
Shizgal, 1985; Bielajew, Thrasher and Fouriezos; 1987) and 1
to 8.3 m/sec, respectively (Shizgal et al., 1980; Bielajew
and Shizgal, 1982, 1986; Durivage and Miliaressis, 1987;
Gratton and Wise, 1988). These physiological
characteristics suggest that at least a portion of the
reward-relevant substrate(s) travelling through the MFB
comprises neurons with myelinated axons of small diameter
that descend towards the mesencephalon. These findings
constitute a major step towards the identification of the
reward substrate(s). Unfortunately, inferences of this kind
cannot yet be drawn concerning most other neural structures
that support self-stimulation because the critical data
either have not been collected or are incomplete.

In a previous topographical study, Rompré and Miliaressis
(1985) have identified a large and sensitive reward system
in the brain stem. The region of positive self-stimulation

sites extends at least four millimeters in the anterior-posterior axis, between the rostral mesencephalon and the caudal pons. In the pons, continuous positive sites were found on the midline between the cerebral aqueduct and the pontine nuclei. Reward thresholds (defined as the minimum stimulation frequency that just failed to induce self-stimulation, see Rompré and Miliaressis, 1985) were lowest in the ventral region of the dorsal raphe, near its junction with the decussation of the superior cerebellar peduncle. In the rostral mesencephalon, a large column of positive sites were found up to 1 mm lateral to the midline, between the central gray and the ventral tegmental area. When going from caudal to rostral areas, the low-threshold sites shifted from dorsal to ventral and from medial to lateral regions, following the trajectory of the tegmental radiations. Rompré and Miliaressis (1985) also observed that self-stimulation thresholds increased substantially in midline regions posterior to the coronal level passing through the dorsal raphe, and suggested that reward-relevant neurons in this area bifurcate laterally as they travel towards the caudal brain stem. Because such an unexpectedly large area of the brain stem appears to contain reward-relevant neurons, it seems reasonable to suspect that the MFB can no longer be considered as the sole point of focus for stimulation-induced reward. One point of interest is the possibility that reward-relevant neurons link the ventral tegmental area and brain stem sites. Indeed, the

continuity of positive sites throughout the mesencephalon in Rompré and Miliaressis' study supports such a hypothesis. The present study was designed to investigate this possibility and to characterize the physiology of the fibers forming this hypothetical link.

In the first experiment, the behavioral version of the collision technique developed by Shizgal et al (1980) was used to reveal the existence of direct axonal linkage between reward-relevant neurons in the rostral mesencephalon and the brain stem. In the second experiment, Yeomans' (1975) double-pulse technique was used to determine the refractory periods of the directly stimulated reward-relevant neurons that link the two sites. Combination of the results stemming from these two experiments will constitute a step forward towards the identification of the reward substrate(s).

EXPERIMENT 1

Introduction

A major challenge in brain stimulation studies is to
determine which neurons located within the stimulation field
are responsible for the observed behavior. Stimulation of
reward-relevant sites has been found to elicit, in addition
to self-stimulation, other behaviors such as feeding (Hoebel
and Teitelbaum, 1962), drinking (Mogenson and Stevenson,
1966), copulation (Caggiula and Hoebel, 1966), exploration
(Rolls and Kelly, 1972), escape (Bower and Miller, 1958),
circling (Miliaressis and Rompré, 1980), and predatory
attack (MacDonnel and Flynn, 1964). One hypothesis proposed
to explain the multiple behavioral effects is the presence
of functionally different fiber pathways coursing through
the stimulation field. Indeed, Nieuwenhuys, Geeraedts, and
Veening (1982) have shown that more than 50 different fiber
systems run through the MFB. Anatomical overlap prevents
easy dissociation of the relevant fibers and thus more
sophisticated methods for characterizing, and therefore
distinguishing, those stimulated fibers responsible for the
rewarding effect are required.

Deutsch (1964) developed an approach that circumvents the
problem of non-selectivity of intracerebral stimulation.

This approach consists of studying the trade-off between the stimulation parameters required to maintain self-stimulation performance at a constant level. The hypothesis is that the rules governing the trade-off functions reflect the unique physiological characteristics of the neurons that are responsible for the behavior under study. By combining this psychophysical approach and the collision technique, Shizgal et. al. (1980) revealed a reward-relevant axonal link between the lateral hypothalamus and the ventral tegmental area. Their technique is based on the physiological phenomenon of collision -- the conduction failure that occurs when anti- and orthodromic action potentials travelling along the same axon collide and cancel out. Electrical stimulation of an axon produces orthodromic action potentials that propagate towards the terminal and antidromic action potentials that propagate towards the soma. Suppose a two-electrode arrangement implanted in series along an axon, (see Figure 1). If a first (conditioning or C-) pulse is delivered through the electrode closest to the terminal (downstream) and a second (test or T-) pulse is delivered in close succession via the electrode closest to the soma (upstream), the antidromic action potential generated by the downstream electrode will collide with the orthodromic action potential triggered at the upstream electrode, and neither will propagate past the point of collision. Consequently, only the orthodromic signal triggered by the downstream electrode will reach the terminal. If, however, the interval between

Figure 1. Stimulation condition for the collision test.
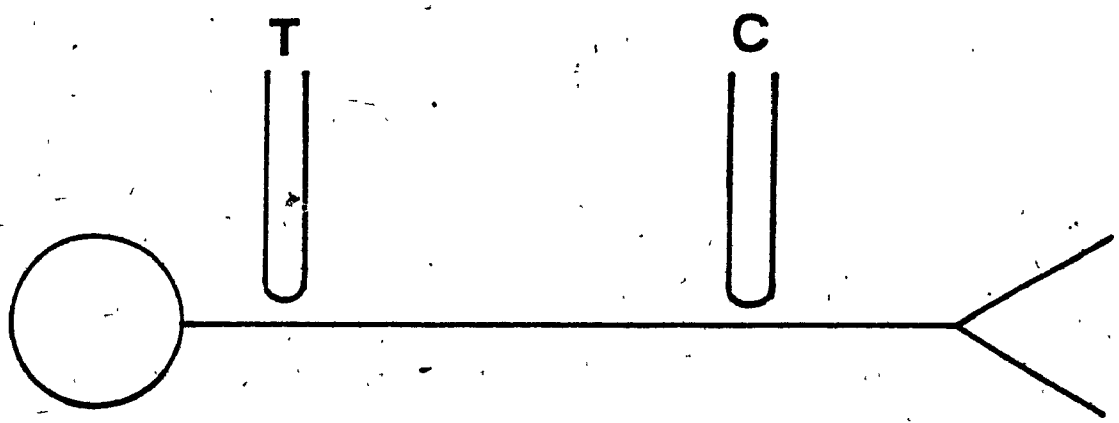
the delivery of the two pulses is delayed enough to allow the antidromic action potential triggered by the C-pulse and its trailing refractory zone to clear the site of the proximal electrode before the T-pulse is delivered, then collision will not occur and two action potentials will reach the terminal instead of one. The longest inter-pulse interval at which collision occurs is referred to as the collision interval and it represents the sum of the inter-electrode conduction time and the refractory period of the axonal segment beneath the tip of the electrode used to deliver the T-pulse.

The application of the collision technique to the study of behavioral substrates consists of measuring, at different C-T intervals, the frequency of pulse-pairs required to maintain a fixed level of behavior. A collision effect is evidenced by an increase in the required frequency as the C-T interval is reduced. The presence of such an effect indicates that the axons of the neurons responsible for the behavior under study travel through both stimulation fields.

As mentioned earlier, the collision technique has been successfully employed to establish the existence of reward-relevant axonal linkage within the medial forebrain bundle, between the lateral hypothalamus and the ventral tegmental area. More recently, Bielajew et al. (1987) have shown that reward-relevant neurons also directly link the lateral

preoptic area and the lateral hypothalamus, a finding that
would suggest continuity between the ventral tegmental area
and basal forebrain regions.   The present experiment is
aimed at extending our knowledge about the anatomy of the
reward system by investigating the possibility of a reward-
relevant link between the ventral tegmental area and sites
within the brain stem.

Method

Subjects

Subjects were eleven male hooded rats of the Long Evans
strain from Charles River breeding farms, weighing between
300-450 g at the time of surgery. They were individually
housed in plastic cages and were maintained on a 12 hr
light/dark cycle. Food and water were available ad libitum
before and after surgery.

Electrodes and Surgery

Each subject was implanted with a moveable and a fixed
monopolar electrode. Fixed electrodes were constructed from
(0.25 mm) stainless steel wires insulated with Formvar, and
crimped to a male amphenol connection. Moveable electrodes
consisted of a plastic guide and a stainless steel moveable
wire also insulated with Formvar (for further details, see
Miliaressis, 1981); the tip of each electrode was honed to a
hemispherical shape. An indifferent electrode was wrapped
around four to five skull screws. Dental cement was used to
fixate the electrode assembly.

Surgery was conducted under general anesthesia induced by
sodium pentobarbital (65 mg/kg). With the skull held

horizontally between bregma and lambda, fixed electrodes
were aimed at 5.5 mm behind bregma, 1.0 mm lateral to the
midline, and 7.8 mm below dura.   Moveable electrodes were
aimed at the midline, 7.7 mm behind bregma and 6.0 mm below
the surface of the skull.

Apparatus

Bar-pressing behavior was shaped in a manually-operated
set-up and subsequently tested in computer-controlled
equipment.   Testing chambers measured 25 cm X 25 cm X 70 cm.
A rodent lever protruded into the chamber, 6 cm above the
floor.   Above the lever was a 1.5 cm yellow jewel light
which came on when stimulation was available.   In the hand-
operated set-up, all temporal parameters were controlled by
manually-set integrated circuit pulse generators, whereas in
the computer-controlled equipment they were controlled by a
dedicated microprocessor.

Stimulation pulses were produced by dual constant-current
generators (Mundl, 1980).   Electric charge build-up át the
brain-electrode interface was prevented by connecting
stimulator outputs through a 1K resistor during the pulse
interval.   Current intensity was monitored with an
oscilloscope by reading the voltage drop across a 1K
resistor in series with the rat.

Procedure

Training and Stabilization

One week after surgery, subjects were shaped to bar-press for electrical stimulation of the ventral tegmental area using 500 msec trains of cathodal rectangular pulses of constant duration (0.1 msec). During the training phase, current intensity and pulse frequency were varied and adjusted to produce maximal response rates. Once vigorous responding was established, subjects were allowed to bar-press freely for one hour daily, for three consecutive days. Subjects were then trained, for an additional three days, to bar-press for trials of 30 sec separated by rest periods of the same duration. Only subjects that could be trained to bar-press for stimulation of the ventral tegmental area were included in the study.

After the initial training session, subjects were trained to bar-press for stimulation at the implantation site of the moveable electrode. If the subject could not be trained, the electrode was descended by 0.32 mm and the new site was tested the following day; the electrode was descended until a site was found where stimulation induced consistent bar-pressing.

Once subjects were shaped to bar-press for stimulation applied through each electrode, current intensities were adjusted to produce a frequency threshold of approximately 26 HZ at each brain site. Frequency thresholds were estimated from the function relating rate of bar-pressing to the stimulation frequency. These functions were obtained by establishing the number of pulse-pairs per stimulation train required to support maximal responding, and then systematically reducing this number until the behavior extinguished. Thresholds were estimated by interpolation and operationally defined as the stimulation frequency required to induce a half-maximal rate of responding. After the completion of the training phase, subjects were transferred to the computer-controlled equipment for collision testing.

Collision Test

The collision test consisted of frequency-threshold determinations for single- and two-electrode stimulation conditions. In the single electrode stimulation condition, frequency thresholds were determined for each electrode independently. In the two-electrode stimulation condition, frequency thresholds were determined using pulse pairs: in the anterior-posterior test, the C-pulse was delivered via the anterior electrode and the T-pulse was delivered via the posterior electrode; this sequence was reversed for the

posterior-anterior test. In the paired-pulse stimulation condition, frequency threshold was defined as the number of pulse pairs required to support a half-maximal rate of bar-pressing.

A given session began with two warm-up single-pulse threshold determinations for each site. Eight single-pulse threshold determinations from each stimulation site were estimated throughout a single session, interspersed among two-electrode threshold determinations. The data from a session were discarded if the standard error of the mean for single-pulse frequency thresholds for one or both electrodes varied by more than 10% (S.E.M./MEAN >10%). Paired-pulse frequency thresholds were determined at 17 different C-T intervals that ranged from 0.2 to 10.0 msec. The order in which different C-T intervals were tested was counterbalanced from day to day.

The effectiveness of paired-pulse stimulation at a given C-T interval was assessed using the formula of Bielajew et al. (1981):

$$E=(FT_{SP_L}/FT_{C-T})-1/(FT_{SP_L}/FT_{SP_H})$$

where   E = effectiveness of paired-pulse
              stimulation

FT_{SP_L} = lower of the two single-pulse frequency

thresholds,

FT_{C-T} = frequency threshold for paired pulses,

FT_H = higher of the two single-pulse frequency

thresholds.

In the formula above, an effectiveness value (E-value) of 0 results from cases in which one pulse from each pair is lost to collision, and paired-pulse stimulation therefore has the same behavioral weight as single-pulse stimulation; the same number of pulse pairs as single pulses is required to maintain behavioral output at a criterial level. Conversely, an E-value of 1 will result from cases in which both pulses in each pair are effective in triggering action potentials that reach the terminals; the paired-pulse frequency threshold is one-half the frequency threshold for single pulses. For each subject, current intensities were adjusted so as to equate single-pulse frequency thresholds for both stimulation sites. However, because this was not always possible, the denominator of the above-mentioned formula provides a correction factor to compensate for these discrepancies.

At every site, the collision test was first replicated three to four times in the anterior/posterior sequence. If, based on visual inspection, the curve relating paired-pulse

effectiveness to C-T intervals (collision curve) did not show evidence of a collision effect (i.e., no decrease in E-values as the C-T interval is shortened), the electrode was lowered by 0.16 mm and the new site was tested the following day. If, however, an effect was evident (i.e., decreased E-values at short C-T intervals), the collision test was replicated 12 times, alternating between the anterior/posterior and posterior/anterior test sequences.

Histology

At the end of the experiments, subjects were given a lethal dose of sodium pentobarbital and the tissue surrounding the electrode tips was marked by passing a direct anodal current of 100 uA for 15 sec. Subjects were then intracardially perfused with saline (0.9%), followed by a solution containing potassium ferrocyanide (3%), potassium ferricyanide (3%), and trichloroacetic acid (0.5%). The combination of this solution with the iron ion deposits caused by the anodal current results in a blue staining of the lesion site. Brains were then removed and kept in 10% formalin. Forty-eight hours prior to sectioning, brains were immersed in 30% sucrose. Brains were sectioned in 40 um sections and drawings were made under magnification of the fresh slices containing the electrode tracks; they were later stained with Thionin dissolved in 10% formalin.

Curve Fitting

In order to obtain an objective estimate of the collision interval, a non-arbitrary curve-fitting procedure was employed. The procedure basically determines if the data are best represented by a 2- or 3-segment line. In the case where the rise in the curve is abrupt and occurs between two adjacent C-T intervals, the data can be best described by a 2-segment fit composed of a lower segment representing the average of the E-values before the rise and a higher segment representing the average of the E-values after the rise. The longest C-T interval of the lower segment is then joined to the shortest C-T interval of the higher segment to illustrate that the abrupt rise occurs somewhere within this interval. In cases where the rise is gradual and occurs over more than one C-T interval, the collision curve is better described by a 3-segment fit composed of a lower and higher segment, as noted above, and a regression line representing the points that lie along the rise. The procedure calculates the residual sum of squares of the points scattered around all possible combinations of 2- and 3-segment lines fit to the data. The curve which yielded the smallest residual sum of squares was then fit to the data.

Results

The results of the collision experiment are shown first, followed by comparison of the results obtained with the anterior-posterior and posterior-anterior test sequences. Figures 2 to 10 show the results of the anterior-posterior collision tests obtained for each animal. Alpha-numerical digits on the upper-left side of each figure refer to the subjects' identification. The left panel shows histologically verified electrode placements for the fixed electrode. The middle panel shows the individual sites tested with the moveable electrode: open circles represent sites at which evidence of collision was not obtained and filled circles represent sites at which a collision effect was evidenced; open squares represent sites which did not support self-stimulation. The right panel shows the curves obtained from each site. Currents used for testing individual sites are presented in Appendix A.

Figure 2 shows the data for subject M7. The fixed electrode was located 4.3 mm behind bregma, in the posterior part of the lateral hypothalamus. The moveable electrode was located 6.8 mm behind bregma, within the central gray. Evidence of collision was obtained at the first site that was tested (site A). Inspection of the curve reveals stable E-values between the C-T intervals of 10.0 and 1.2 msec. As the inter-pulse interval is shortened from 1.2 to 1.0 msec

Figure 2.   Collision data for subject M7.   Histology drawings for this and all subsequent figures were made from the Paxinos and Watson (1986) atlas of the rat brain. Numbers on the upper-left of histology drawings refer to the plate numbers of the same atlas.

# M7

A

E

C-T INTERVAL (msec)

1.0
0.8
0.6
0.4
0.2
0.0

0.1   0.2   0.5   1.0   2.0   5.0   10.0

CG

dtg

mlf

dtgx

scp CLi

rs

ml

cp

Pn

45

PR

ml

LH

cp

35
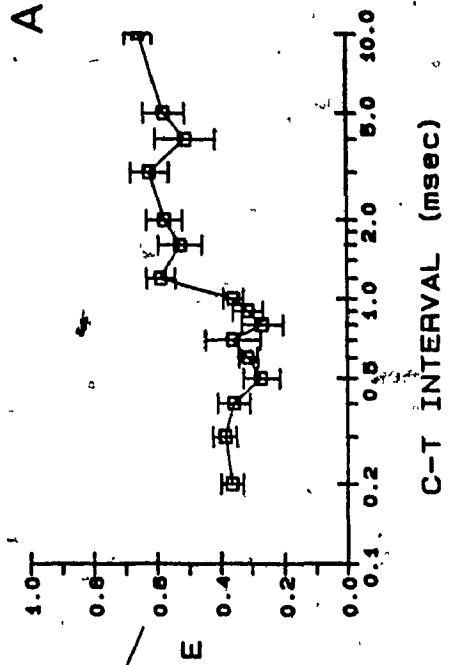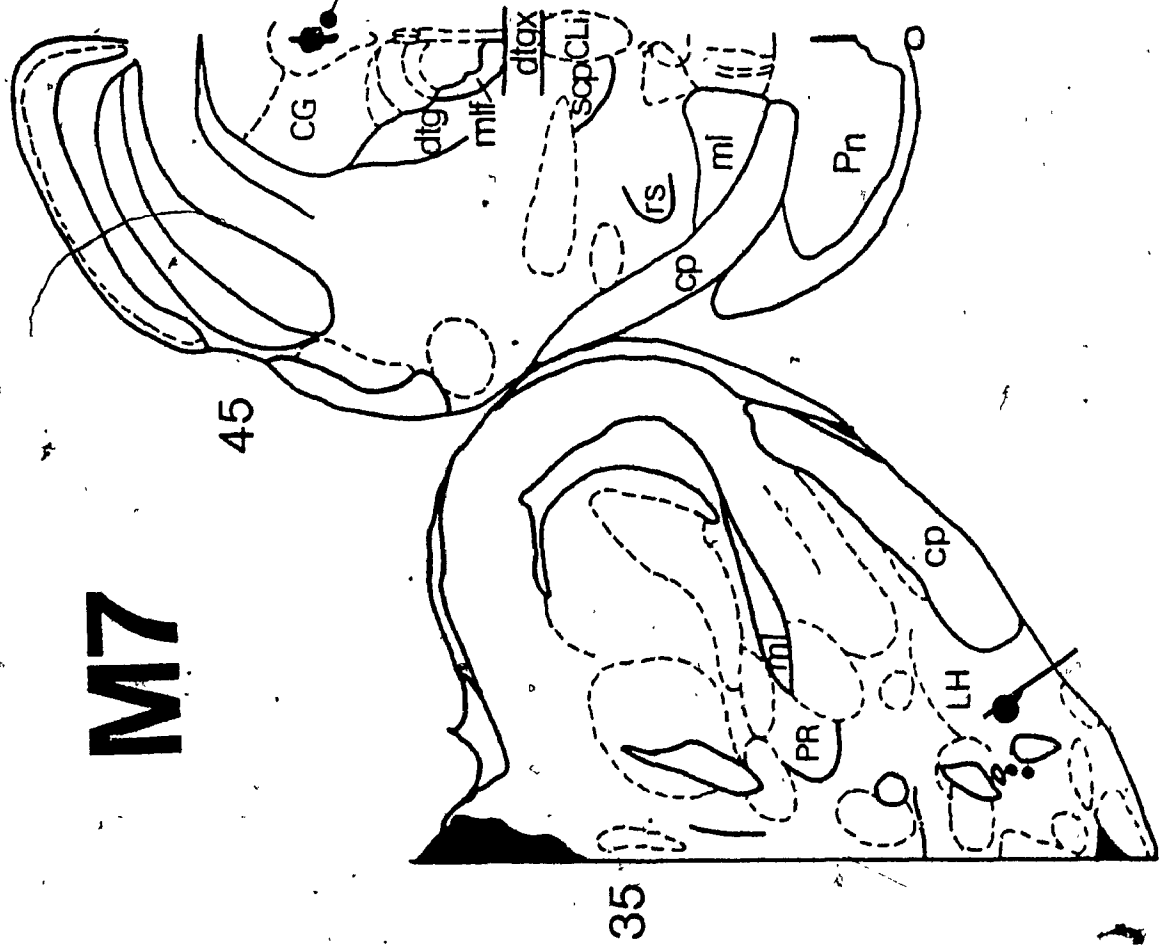
however, we observe a decrease in E-values. This decrease in paired-pulse effectiveness as the inter-pulse interval is shortened reflects collision of anti- and orthodromic action potentials travelling along the same axons and suggests direct linkage of the two stimulation sites by reward-relevant neurons.

Figure 3 shows the data for subject M1. The fixed electrode was located 5.3 mm behind bregma, within the mammillary peduncle, just ventral to the paranigral nucleus of the ventral tegmental area. The moveable electrode was located 6.8 mm behind bregma. Five sites were tested with the moveable electrode over a dorso-ventral distance of approximately 0.8 mm. Evidence of collision was obtained at the first site that was tested with the moveable electrode at a site lateral to the Edinger-Westphal nucleus (site A). Inspection of this curve reveals relatively stable E-values between the C-T intervals of 10.0 and 1.6 msec. A decrease in E-values is observed as the inter-pulse interval is shortened from 1.6 to 1.2 msec. E-values remain low between the C-T intervals of 1.2 and 0.2 msec. Lowering of the electrode by 0.16 mm was sufficient to eliminate the step-like function (site B). We did not obtain evidence of direct axonal linkage between the ventral tegmental area and either site B or C. Evidence of axonal linkage was again obtained near the ventral part of the central gray (site D). Once again, we observe stable E-values at long C-T intervals

<u>Figure 3</u>.   Collision data for subject M1.

M1

A

B

C

E

C-T INTERVAL (msec)

CG

mlf

dtgx

scp

ll

cp

ml

Pn

45

ml

SNR

VTA

39
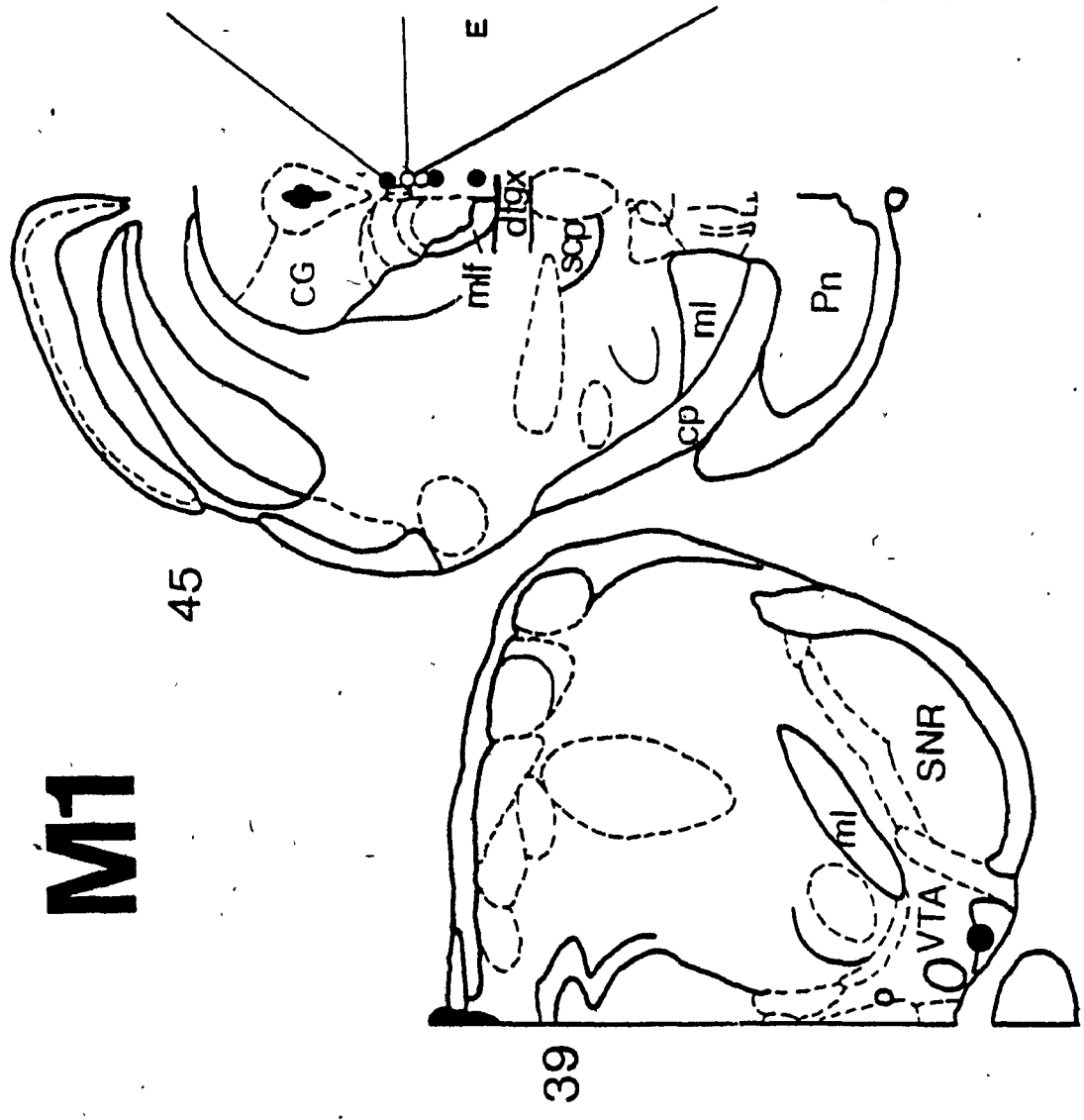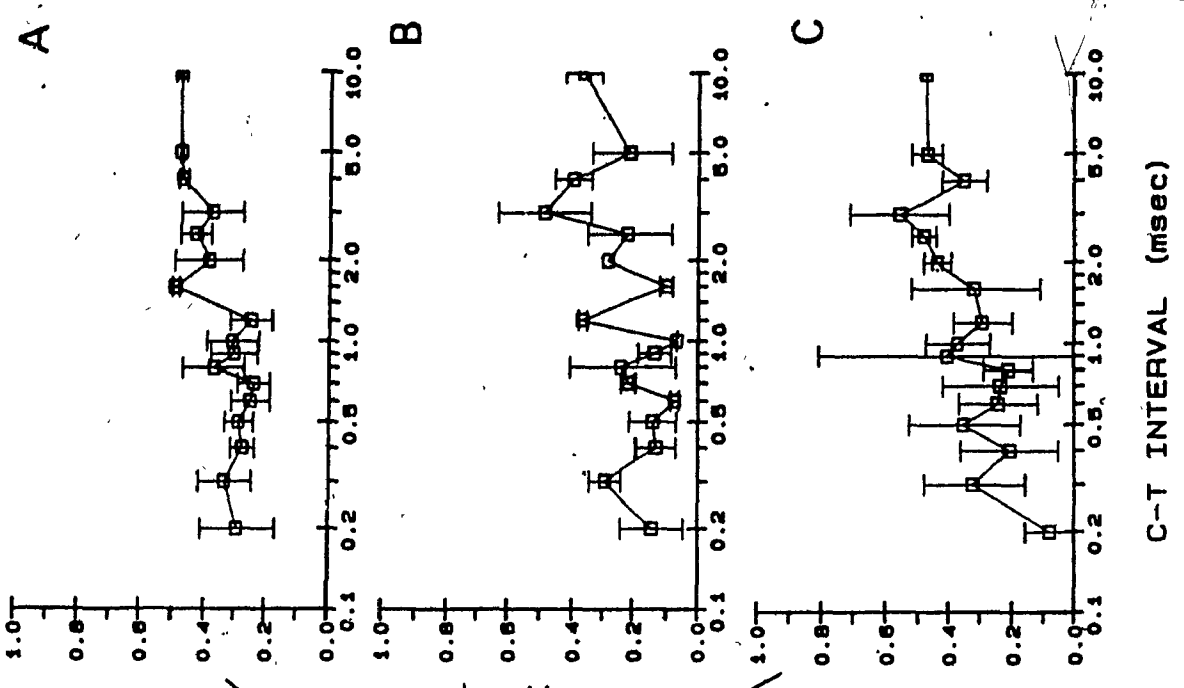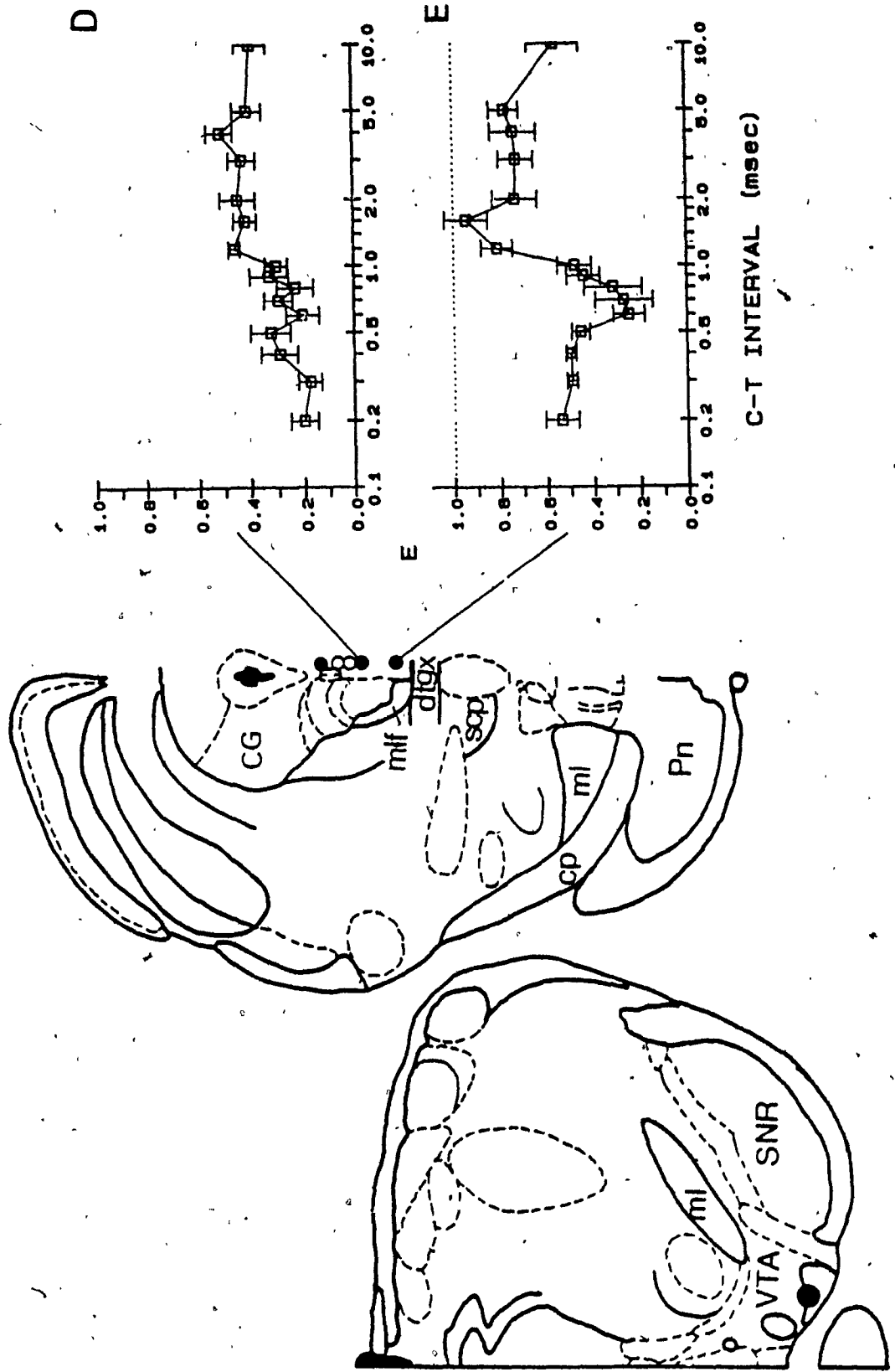
(10.0 to 1.2 msec), and a decrease in E-values as the inter-
pulse interval is shortened below 1.2 msec. A collision
effect was evidenced a third time in this subject when the
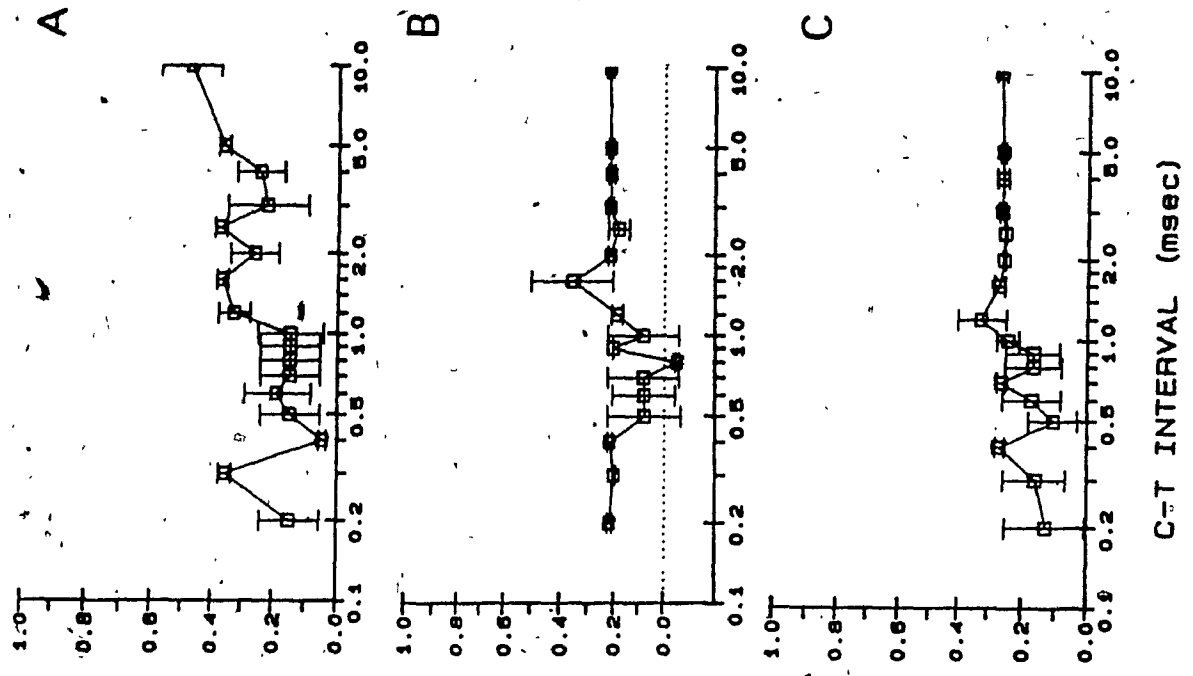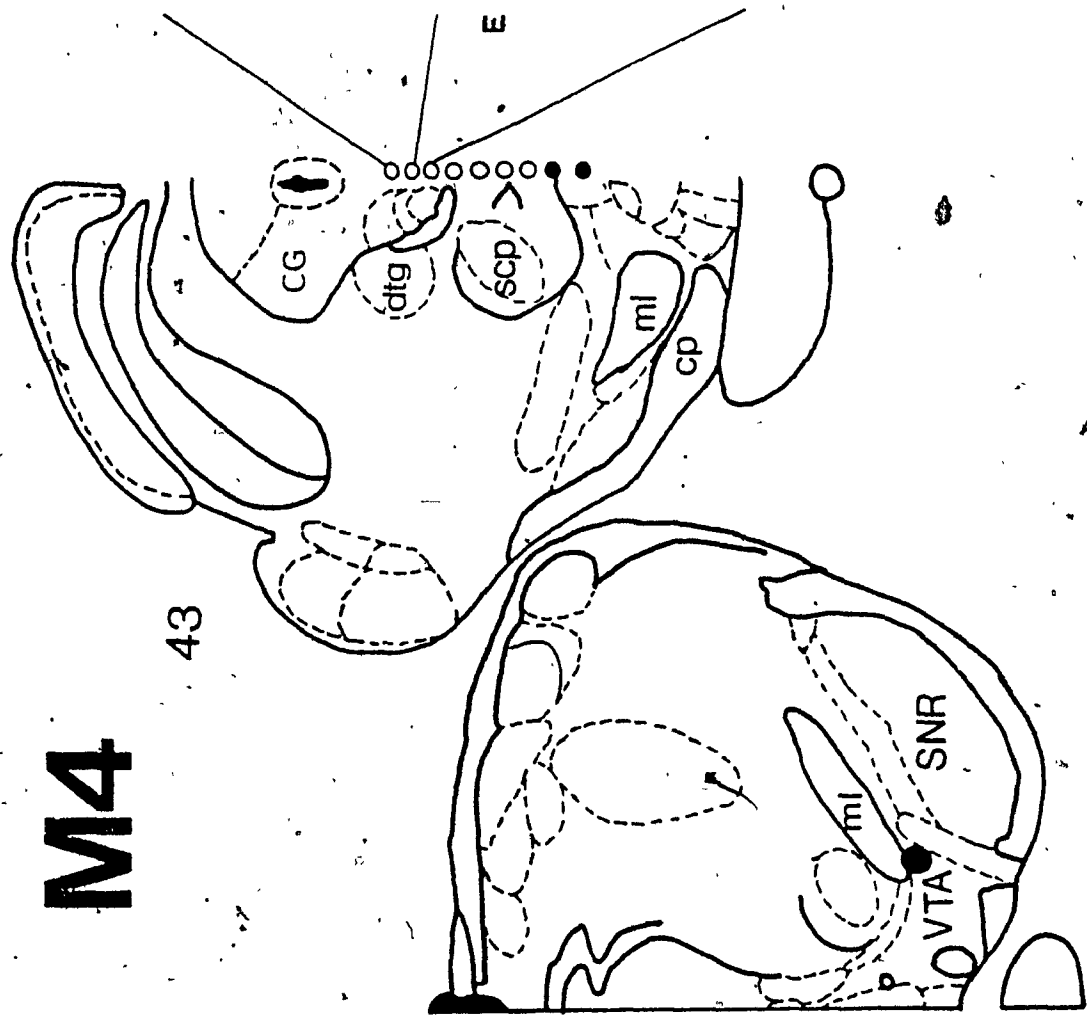electrode was lowered by 0.32 mm to the ventral part of the
central gray (site E).

Figure 4 shows the results of the collision tests for
subject M4. The fixed electrode was located 5.3 mm behind
bregma, within the dorsolateral part of the ventral
tegmental area. The moveable electrode was found on the
midline, 6.3 mm behind bregma. A total of nine sites were
tested with the moveable electrode, spanning a dorso-ventral
distance of approximately 1.7 mm. A collision effect was
not obtained from sites A to G. Evidence of axonal linkage
was first obtained at a site dorsal to the caudal linear
nucleus (site H). The decision to acknowledge site H as a
site linked by reward-relevant fibers to the ventral
tegmental area was based on comparison of this curve with
the curve obtained with the posterior-anterior test sequence
(Figure 15). In contrast to the posterior-anterior curve,
the curve obtained with the anterior-posterior test sequence
has three points which deviate from the general trend in the
data, and thus results in asymmetry between the two curves.
Low E-values are observed at 1.6, 3.0, and 4.0 msec (Figure
4H). The small size of the standard errors around these
points further suggests that the low E-values associated
with each C-T interval are not due to random variability.
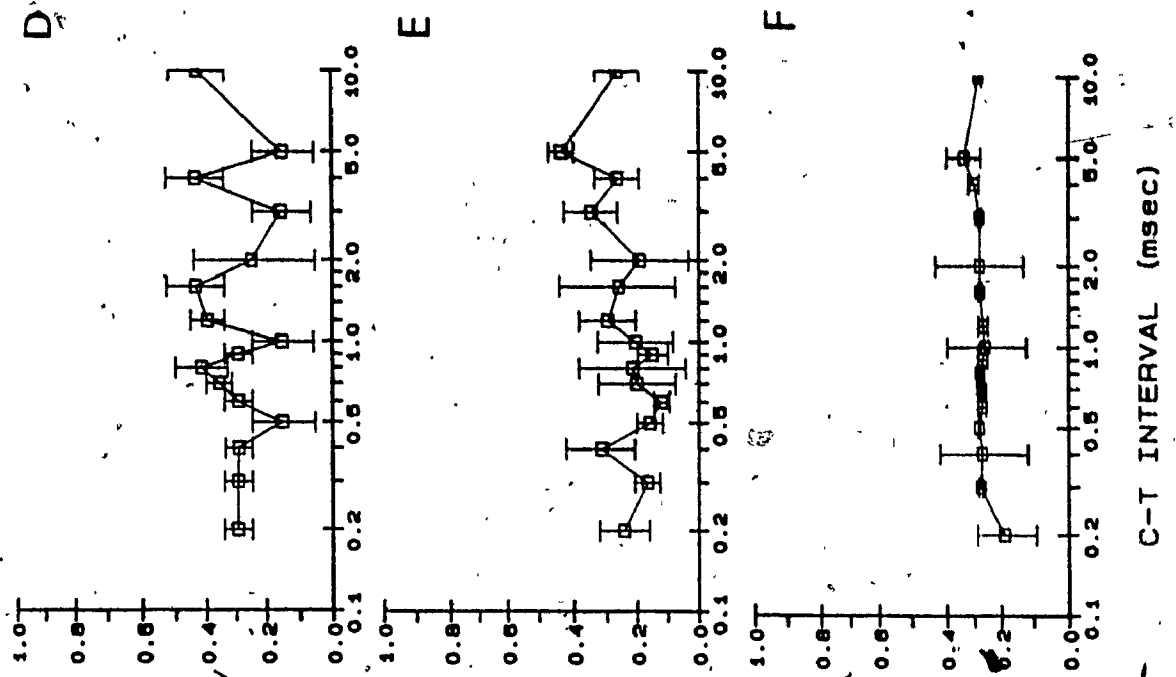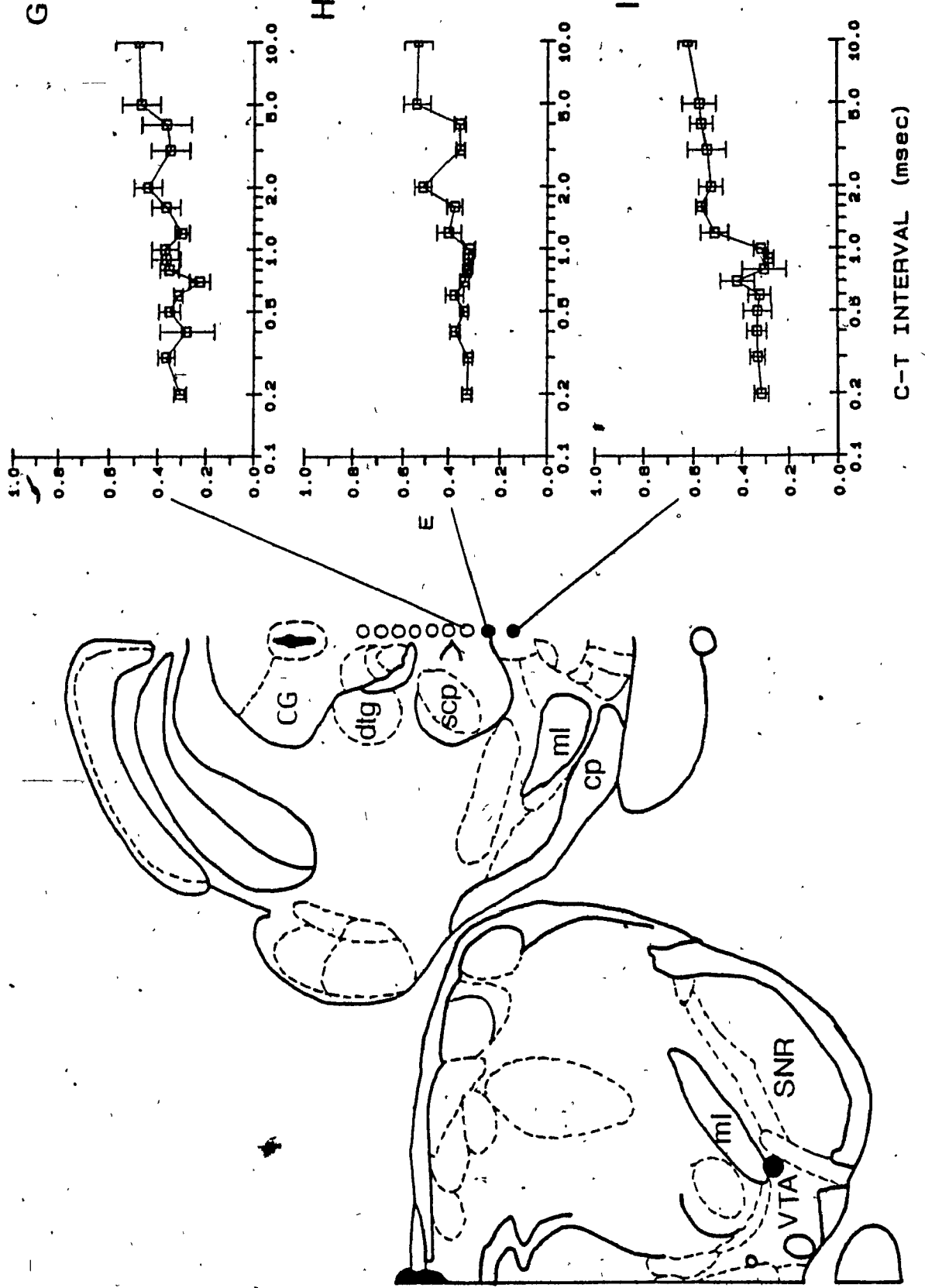
Figure 4. Collision data for subject M4.

A

B

C

E

10.0

5.0

2.0

1.0

0.5

0.2

0.1

1.0

0.8

0.6

0.4

0.2

0.0

C-T INTERVAL (msec)

M4

43

39

CG

dtg

scp

ml

cp

ml

VTA

SNR
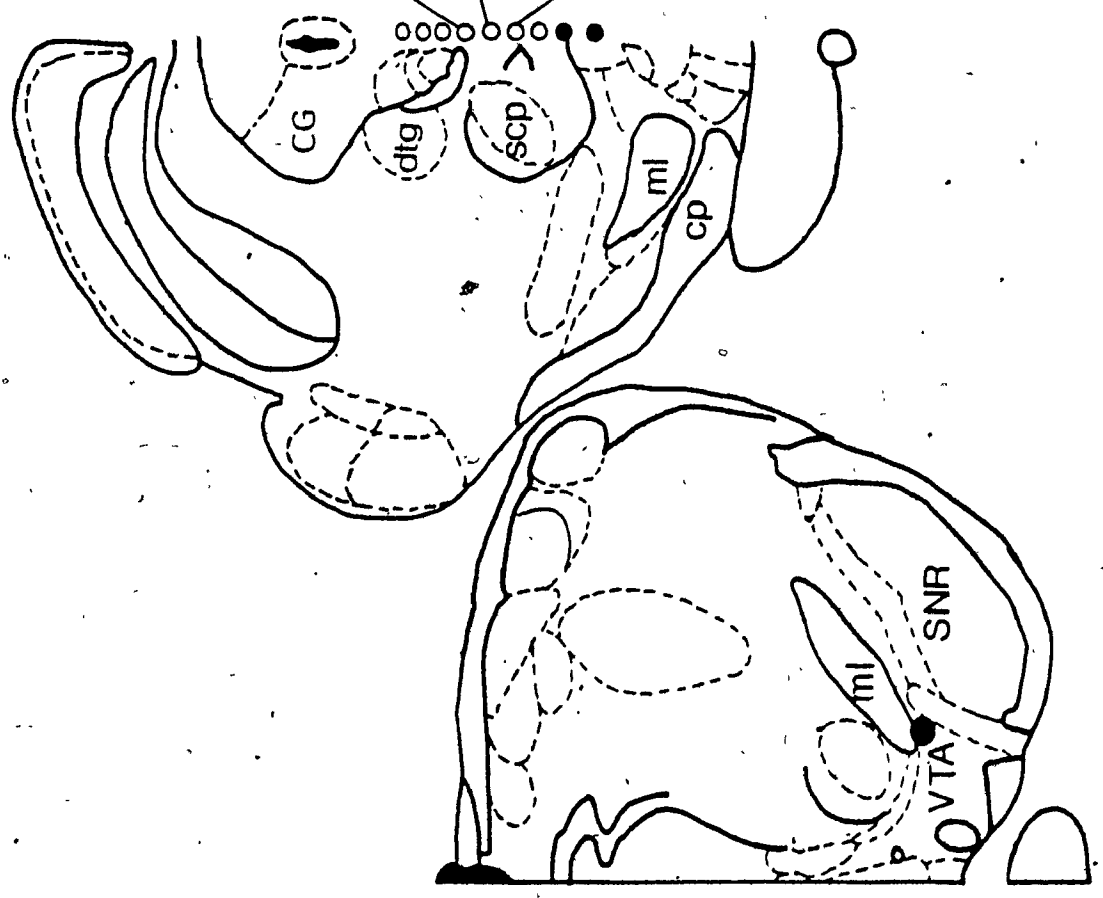
C-T INTERVAL (msec)

The lack of congruence between the anterior-posterior and posterior-anterior curve implies that the reward-relevant link between this site and the ventral tegmental area is not direct. Such asymmetry between curves obtained with each of the two test sequences will be discussed below. Evidence of collision was again obtained, after the electrode was descended by 0.32 mm, in the caudal linear nucleus (site I). We observe stable E-values at long C-T intervals and a decrease in E-values as the C-T interval is reduced from 1.2 to 1.0 msec. Stability in E-values is maintained at inter-pulse intervals below 1.0 msec.

Figure 5 shows the data obtained from subject M6. The fixed electrode was located 5.3 mm behind bregma, at the lateral part of the ventral tegmental area. The moveable electrode was located on the midline, 7.3 mm behind bregma. Subject M6 did not self-stimulate at the site of implantation of the moveable electrode. The behavior was established at site A and a total of three sites were tested for collision, over a dorso-ventral distance spanning approximately 0.4 mm. E-values were variable across C-T intervals for sites A and B. A slight lowering of the electrode by 0.16 mm was sufficient to reveal reward-relevant linkage between the ventral tegmental area and the ventral part of the dorsal raphe (site C).

Figure 5. Collision data for subject M6.

A

B

C

C-T INTERVAL (msec)

M6

47

39

CG
DR
btg
mlf
xscp
rs
ml
Pn

ml
SNR
VTA
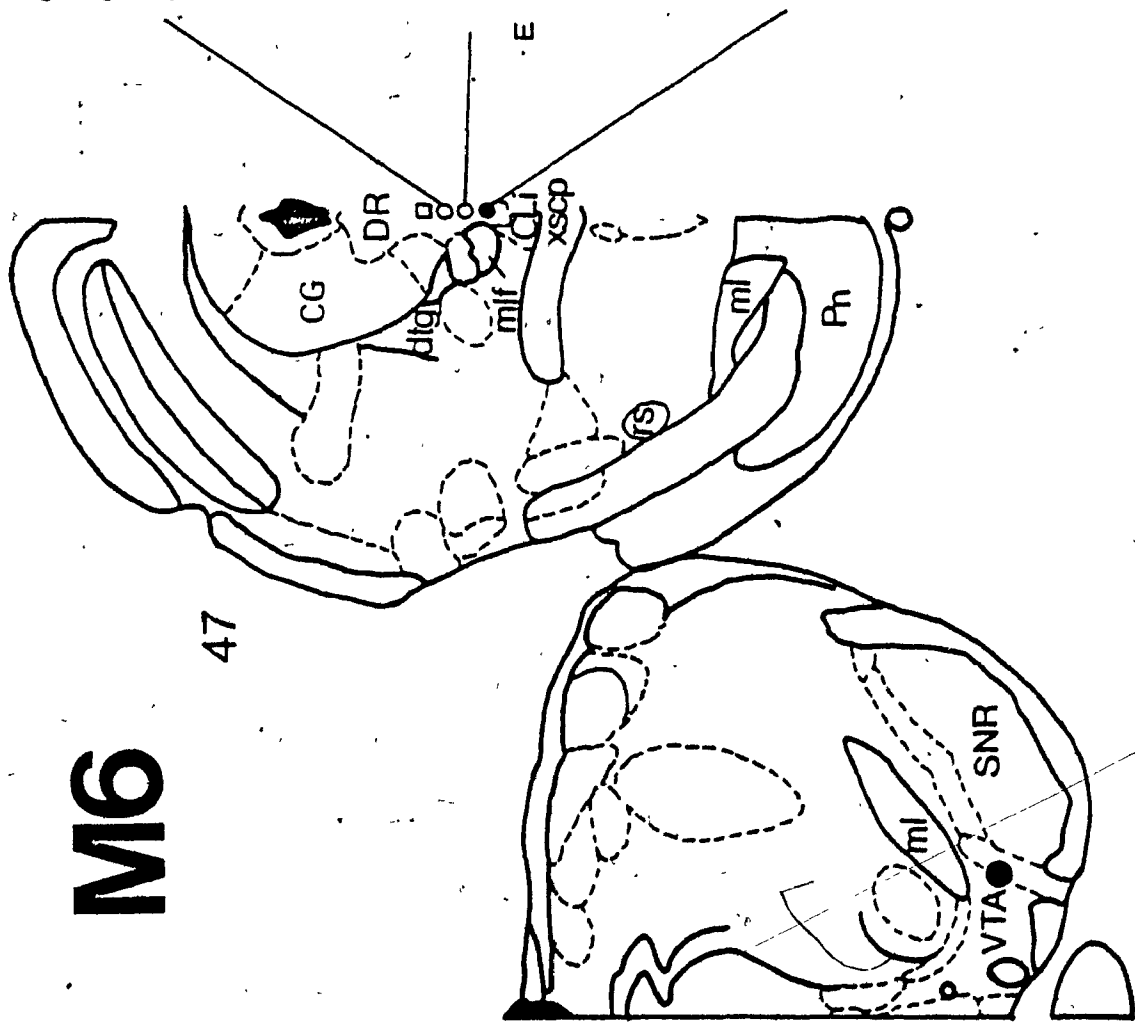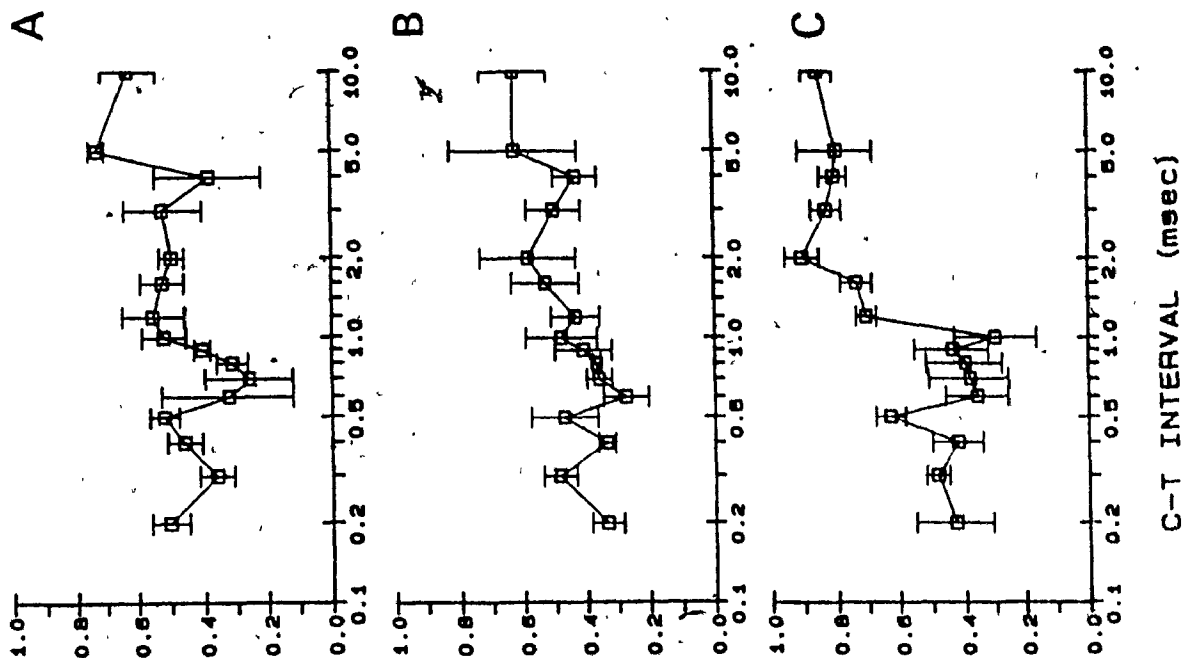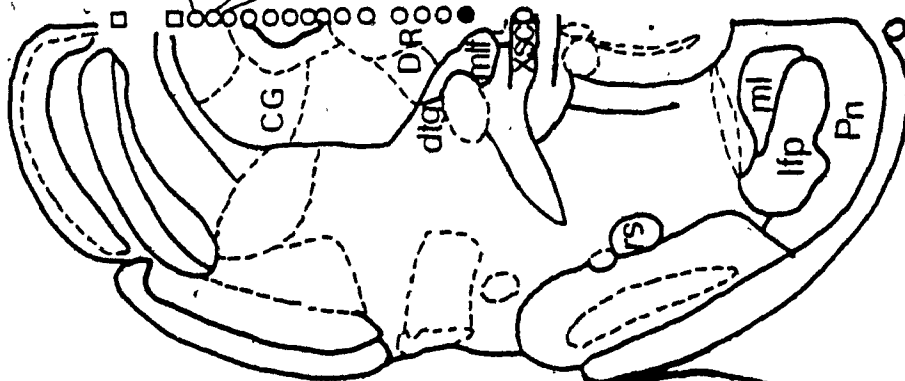
Figure 6 shows the data for subject M8. The fixed electrode was located at 5.3 mm behind bregma, within the dorsolateral part of the ventral tegmental area. The moveable electrode was located on the midline, 7.64 mm behind bregma. Self-stimulation was not obtained from the implantation site nor from the site below it. The behavior was established at site A and a total of 14 sites were tested with the moveable electrode, over a dorso-ventral distance of approximately 2.5 mm. Evidence of collision was not obtained from sites A to M. Inspection of the curves obtained from these sites reveals that E-values remained variable across C-T intervals for each site. It should be noted that for those sites that were located within the cerebral aqueduct (sites D to H), the neural tissue that was actually stimulated during behavioral testing can be thought of as being located anywhere within the perimeter of the aqueduct, but not below and above the tip of the stimulating electrode; the locations of the stimulated neurons at these sites are therefore undetermined. A collision effect was obtained when the electrode reached the ventral part of the dorsal raphe (site N), a site approximately 0.34 mm posterior to the site at which evidence of collision was obtained in subject M6. The general trend in the data shows a decrease in E-values as the C-T interval is reduced from 1.2 to 1.0 msec, followed by low effectiveness values at C-T intervals less than 1.0 msec. E-values at long C-T intervals are low, however, at 2.0, 3.0, and 5.0 msec, and
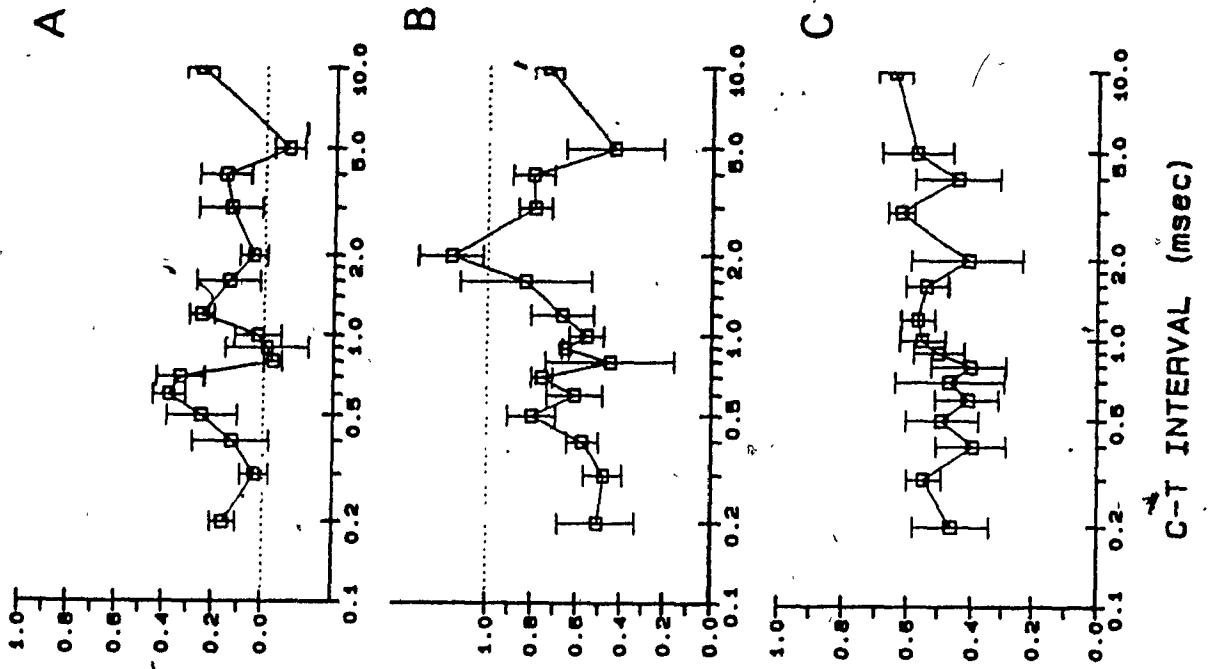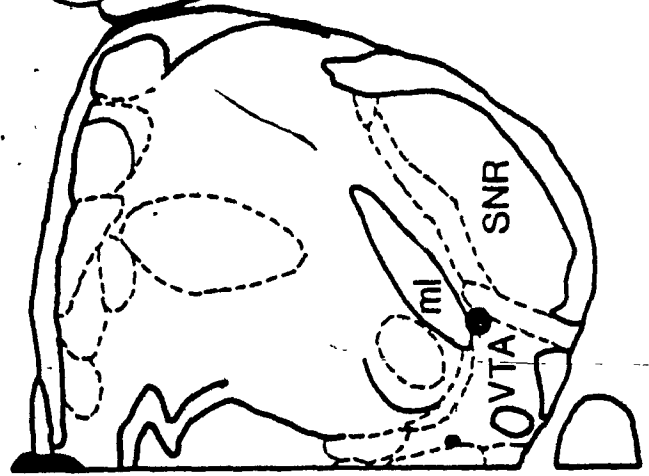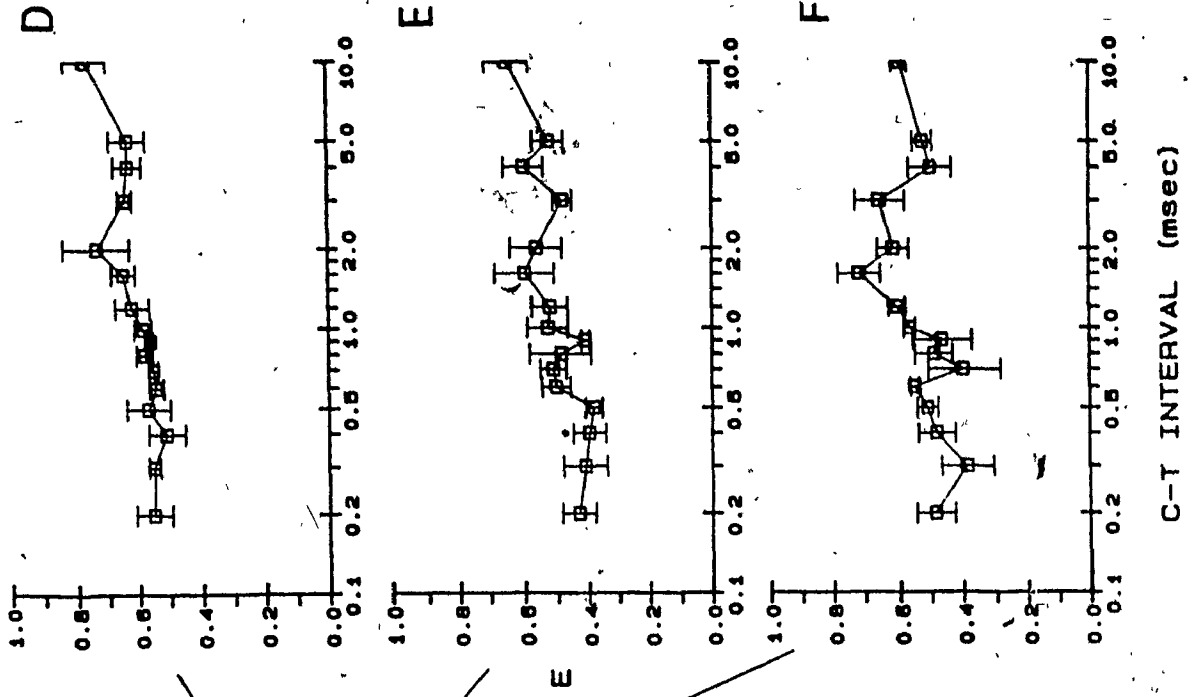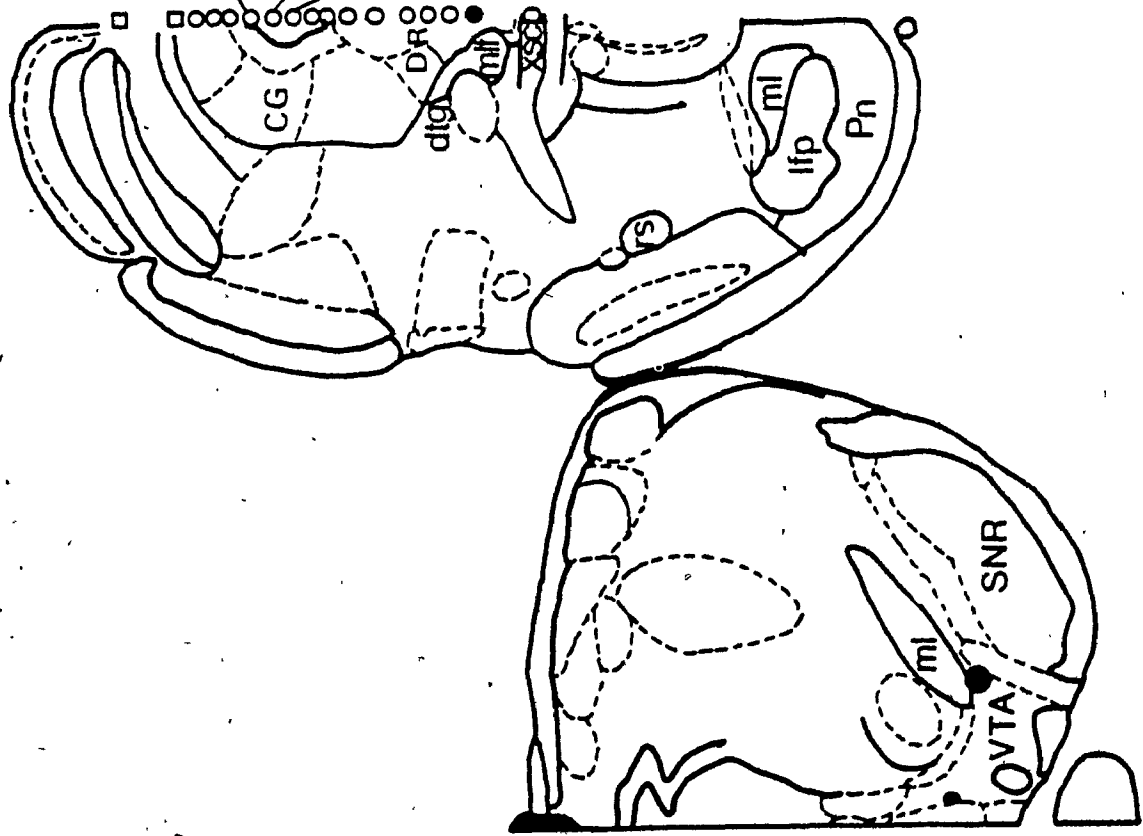
Figure 6. Collision data for subject M8.

36

D
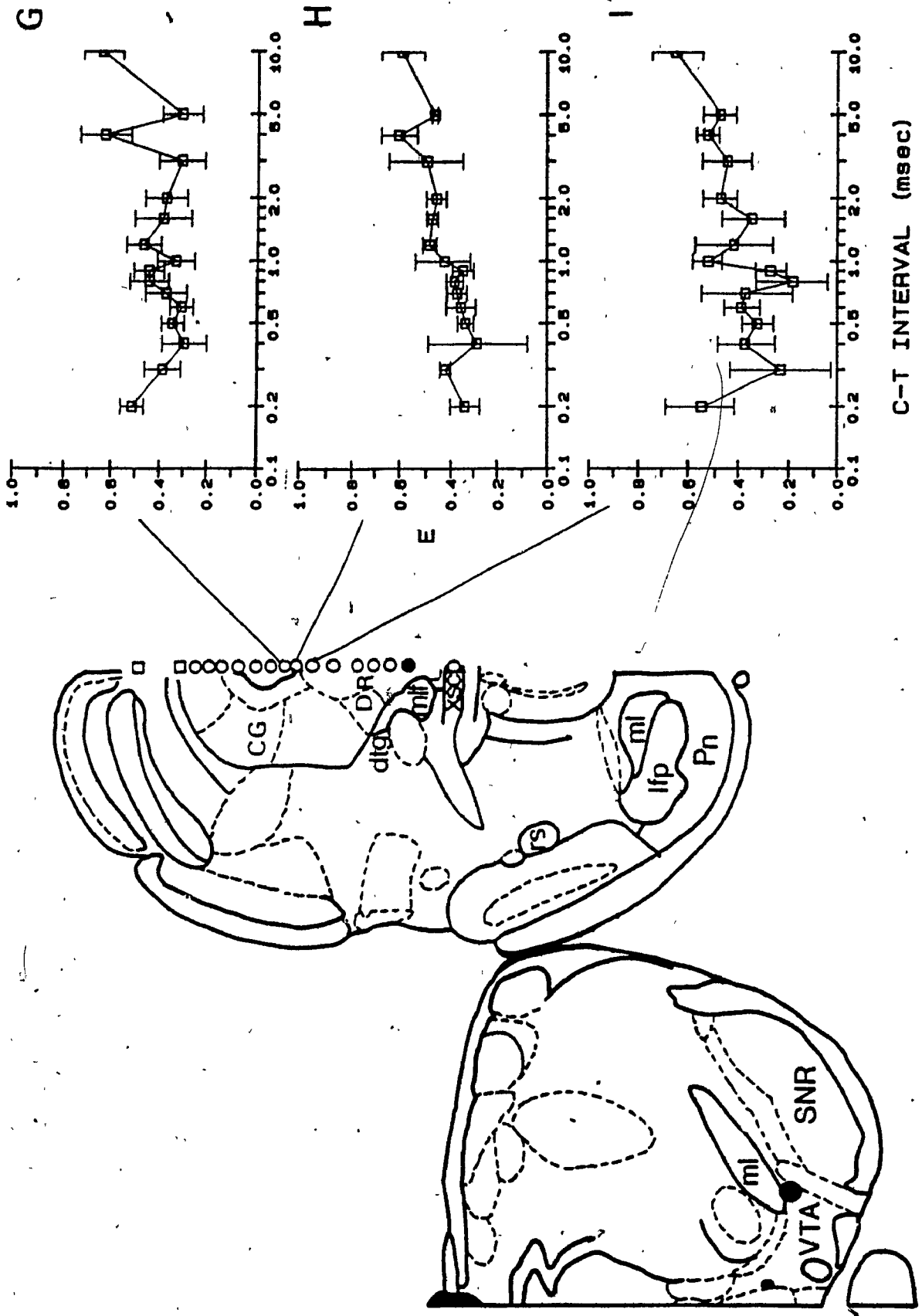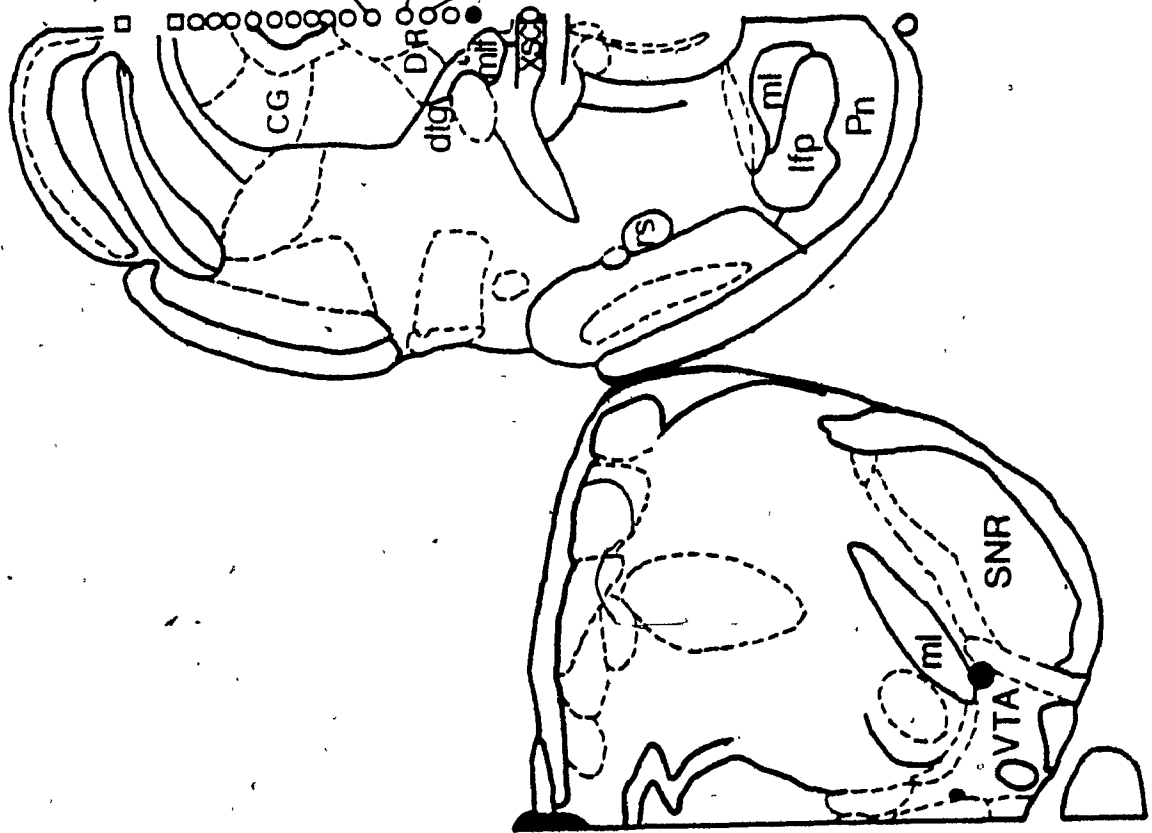
E

F

C-T INTERVAL (msec)

CG
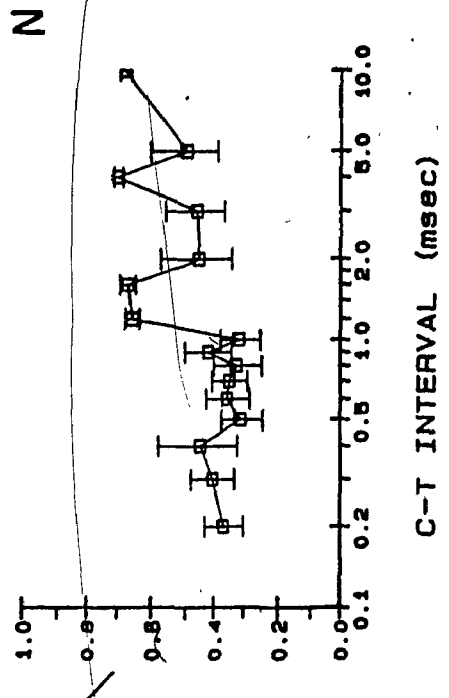DR
dtg
mlf
xscp
rs
ml
lfp
Pn

ml
VTA
SNR

C-T INTERVAL (msec)

M

N

C-T INTERVAL (msec)

E

CG

DR

dtg

mlf

xscp

ml

lfp

Pn

s

ml

VTA

SNR
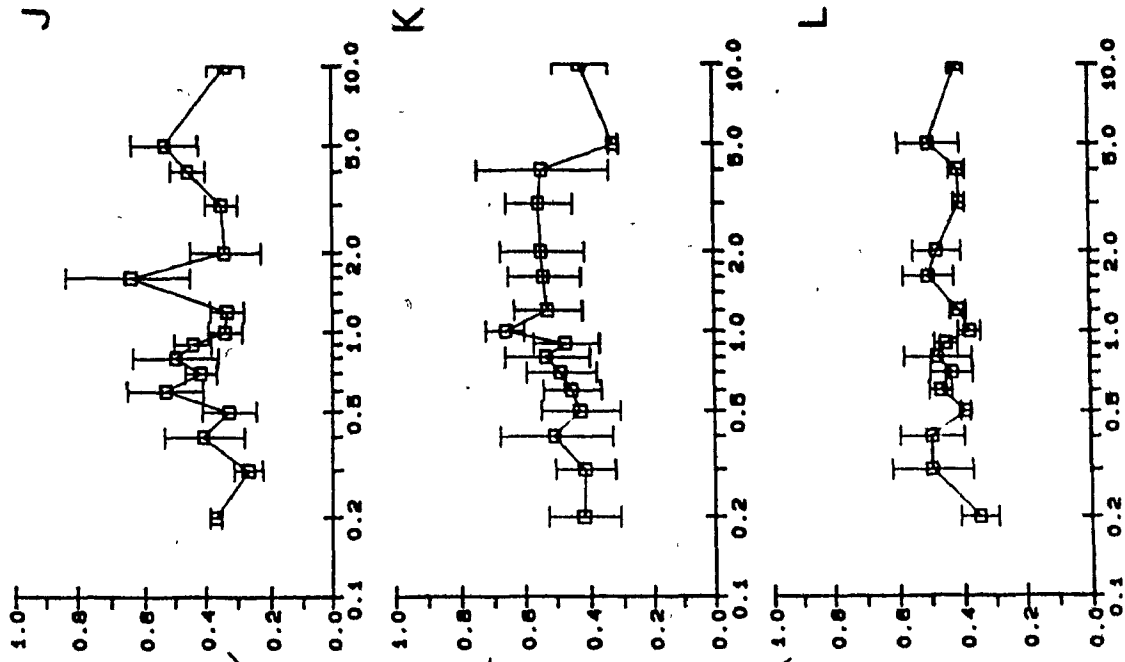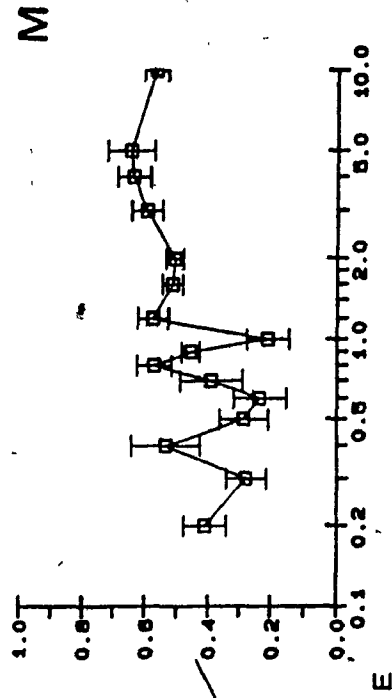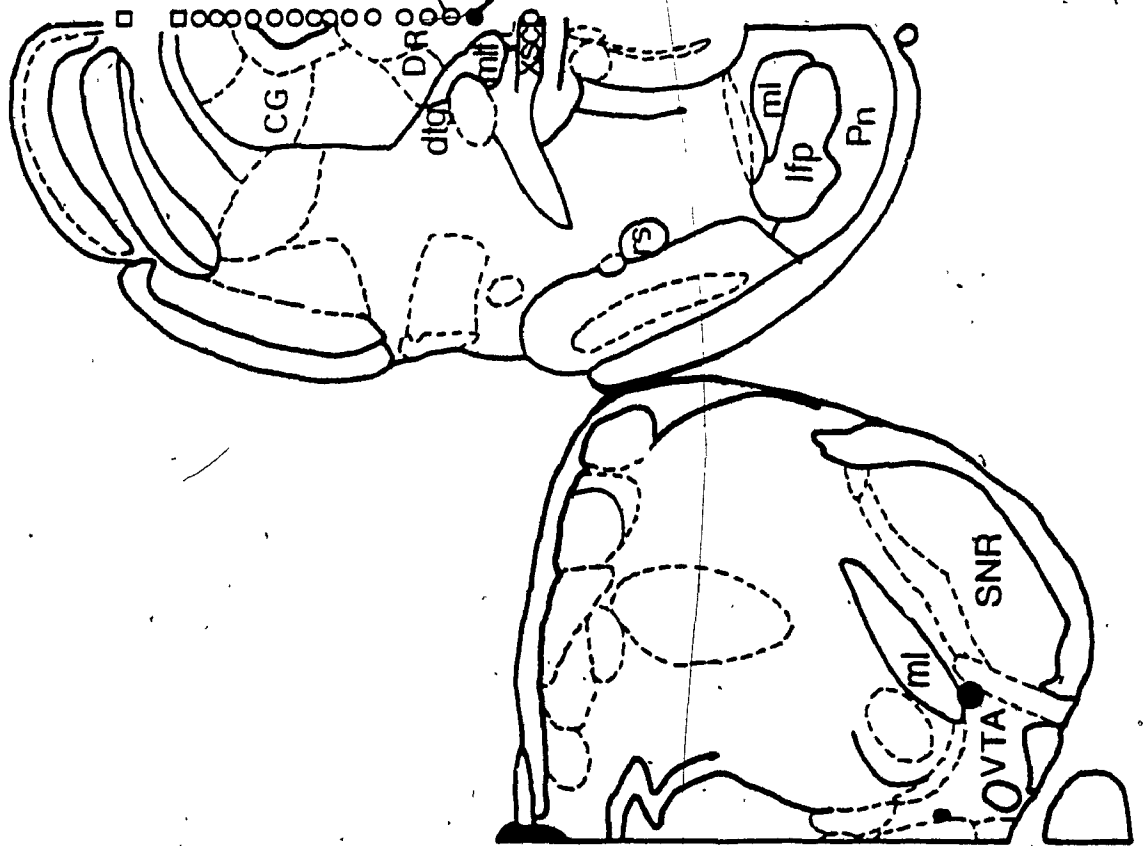
have large standard errors compared with those points at
1.2, 1.6, 4.0, and 10.0 msec. We observed some signs of
infection around the electrode assembly which suggests that
the electrodes were probably unstable during behavioral
testing. This instability could provide an explanation to
the high variability in E-values. Indeed, as has been shown
with the data of subjects M1, M4 and M6, a small movement of
the electrode tip can result in the stimulation of different
reward-relevant fibers. This hypothesis is supported by
inspection of Figure 7 which shows the progressive changes
occuring in the collision curve obtained from site N with
repetitive testing. A clear collision effect was obtained
the first time that this site was tested. Notice the
stability in E-values at C-T intervals between 10.0 and 1.2
msec. Collision at this site occurs at inter-pulse
intervals shorter than 1.2 msec. During subsequent
replications of the collision test at this site, the curve
degenerated progressively due to the variability of the
points at 2.0, 3.0, and 5.0 msec. Because the animal lost
its electrode assembly at the end of the sixth replication,
a lesion was not made at the tip of the electrode; therefore
the location of the sites tested with the moveable electrode
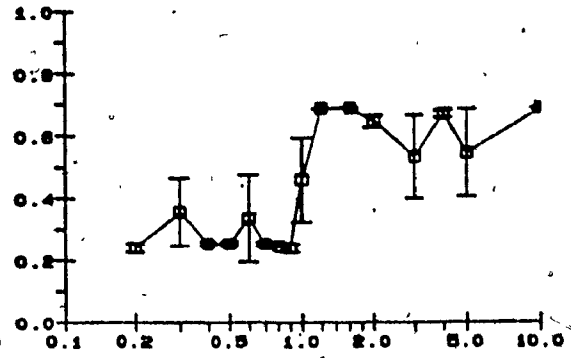may not be as precise as for the other subjects.

Figure 8 shows the data for subject X2. Contrary to the
other subjects, the fixed electrode of subject X2 was
located on the right side of the brain, 4.8 mm behind

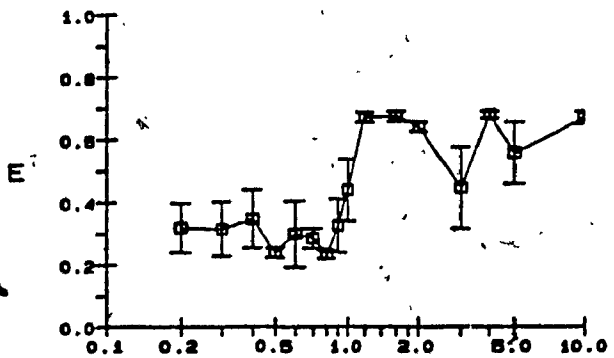Figure 7. Averaged collision curves for site N of subject
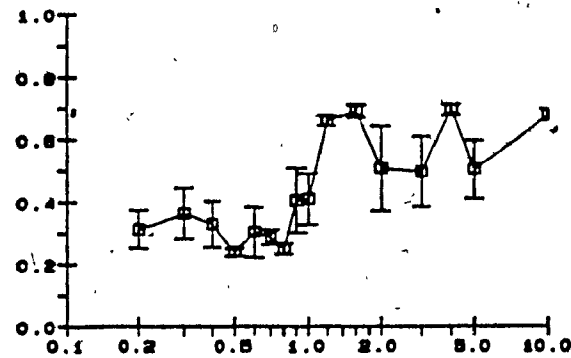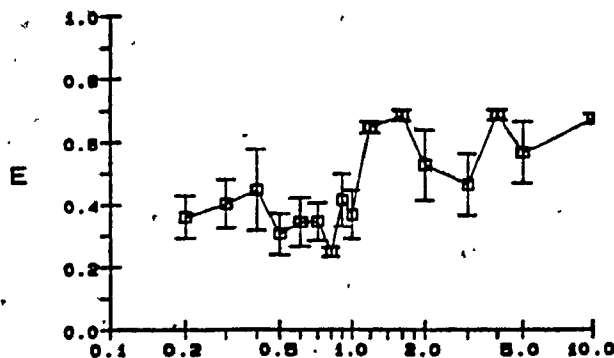
M8.
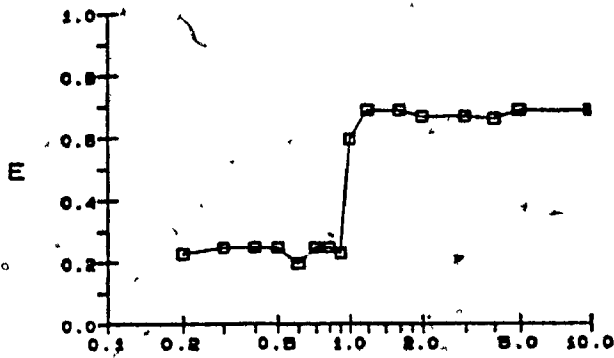
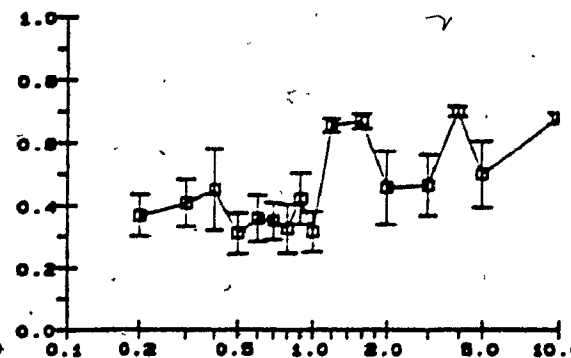REPLICATION #1

REPLICATION #2

REPLICATION #3

REPLICATION #4

REPLICATION #5

REPLICATION #6

C-T INTERVAL (msec)
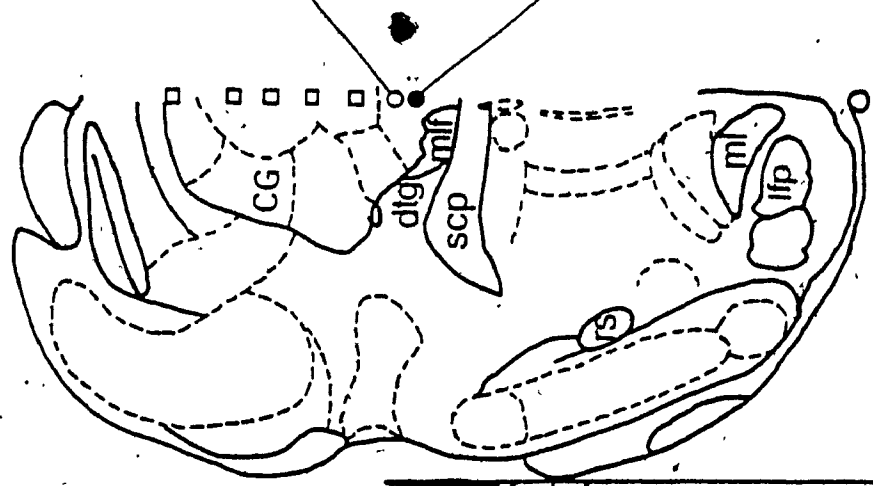
C-T INTERVAL (msec)

Figure 8. Collision data for subject X2.

A

B

10.0 5.0 2.0 1.0 0.5 0.2 0.1

1.0 0.8 0.6 0.4 0.2 0.0

C—T INTERVAL (msec)

E

CG

dtg

mlf

scp

ml

lfp

s

X2

50

37

scp
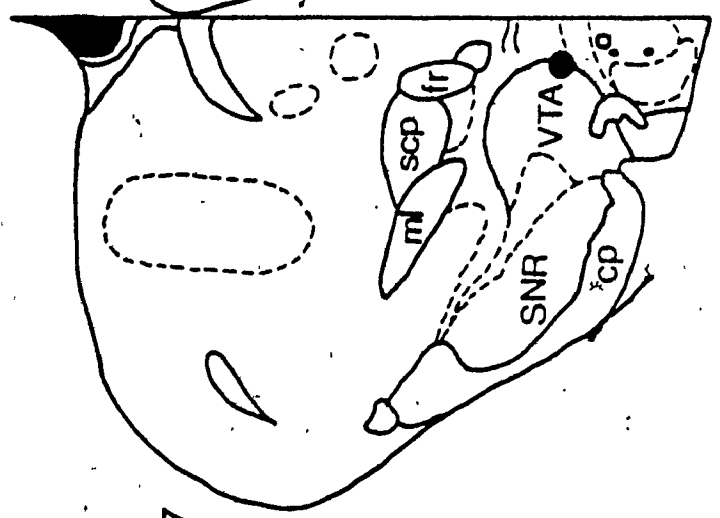
fr

ml

VTA

SNR

cp
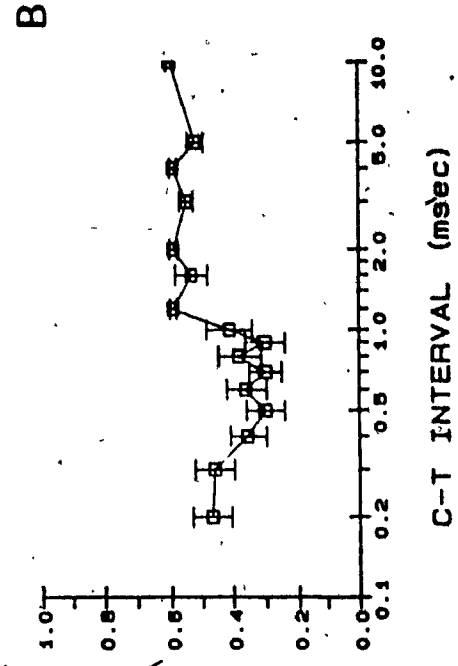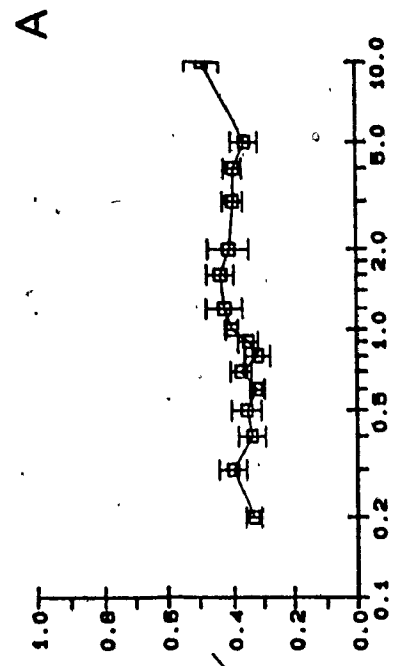
bregma, at the medial border of the ventral tegmental area.
The moveable electrode was implanted 3.0 mm from the surface
of the skull because, based on the data from subject M8, we
suspected that self-stimulation could be obtained at more
dorsal sites in the central gray. The moveable electrode
was located on the midline, 8.0 mm behind bregma. Self-
stimulation was not obtained from the first 5 sites that
were tested. The behavior was established at site A and two
sites were tested for collision over a dorso-ventral
distance extending approximately 0.2 mm. We did not obtain
evidence of direct axonal linkage between site A and the
ventral tegmental area. Inspection of the curve obtained
from site A reveals stable E-values across all C-T
intervals. Again, lowering of the electrode by as little as
0.16 mm was sufficient to reveal evidence of direct axonal
linkage of site B with the ventral tegmental area.

Figure 9 shows the data for subject B1. The fixed
electrode was located 4.8 mm behind bregma, on the dorsal
border of the ventral tegmental area. The moveable
electrode was located 8.0 mm behind bregma, within the
central gray, just ventrolateral to the aqueduct. Evidence
of direct axonal linkage was obtained at the site of
implantation of the moveable electrode. The general trend
in the data shows a decrease in E-values as the C-T interval
is decreased from 1.2 to 1.0 msec, followed by low E-values
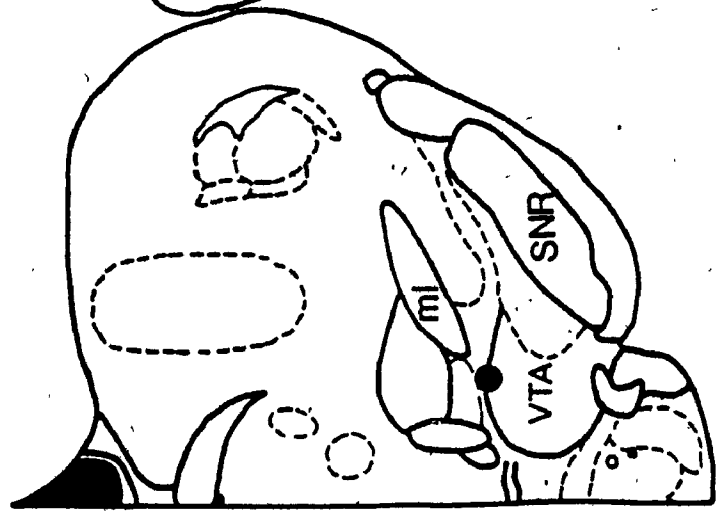at the shorter C-T intervals.

Figure 9.   Collision data for subject B1.

A

C-T INTERVAL (msec)

E

B1

CG   DR
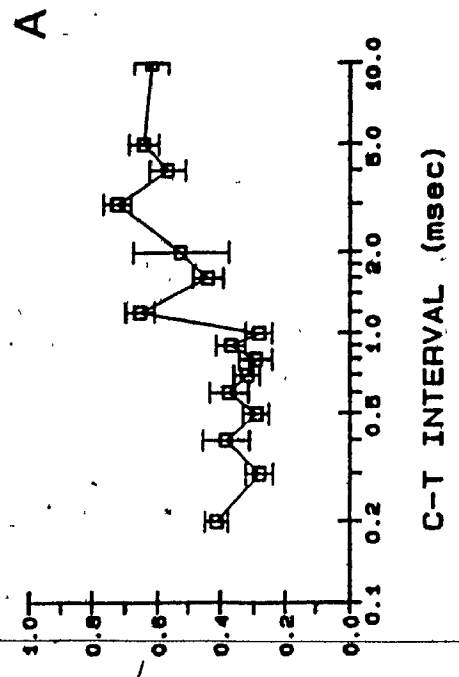dtg   mlf
scp

50

ml
llp

ml
SNR
VTA
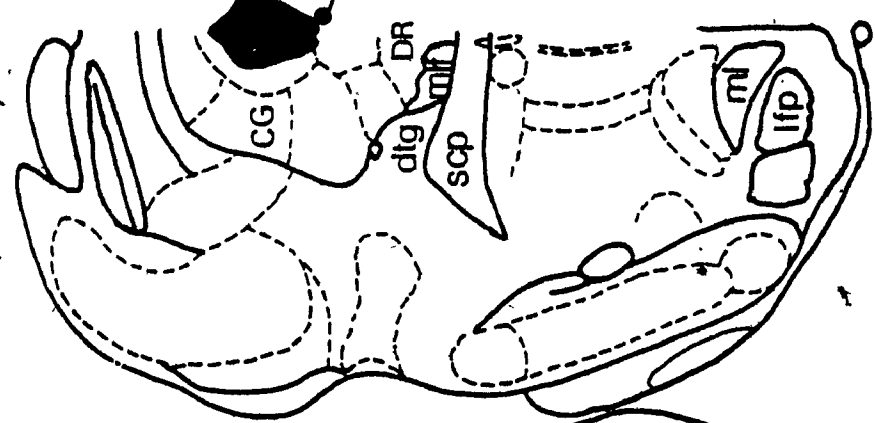
37

Figure 10 shows the data for subject MO. The fixed electrode was found at 5.3 mm behind bregma, on the lateral part of the ventral tegmental area. The moveable electrode was located 8.8 mm behind bregma, on the lateral border of the dorsolateral tegmental nucleus. Evidence of collision was obtained at the site of implantation of the moveable electrode (site A). Inspection of the collision curve obtained from this site reveals stable E-values at long C-T intervals which are interrupted by a decrease in the effectiveness of paired-pulse stimulation at C-T intervals shorter than 1.2 msec. E-values at short C-T intervals are variable in comparison to E-values at long C-T intervals.

Figures 11 to 21 have been compiled for comparison of the anterior-posterior and posterior-anterior collision curves for each site at which a collision effect was evidenced. Numbers on the upper-left part of the figures refer to the subjects' identification. Curves fitted to the data are shown below each individual graph. The curved line joining the upper and lower portions of the collision data results from plotting a linear function in semi-logarithmic space. Posterior-anterior collision curves were not obtained for site N of subject M8 (Figure 18). Due to the changes occuring in the collision curve with subsequent replications, we decided to obtain six replications of the curve before beginning the posterior-anterior test sequence.

Figure 10.   Collision data for subject MO.

Figure 11. Anterior-posterior and posterior-anterior collision curves for subject M7.

POSTERIOR-ANTERIOR

ANTERIOR-POSTERIOR

C-T INTERVAL (msec)

C-T INTERVAL (msec)

M7
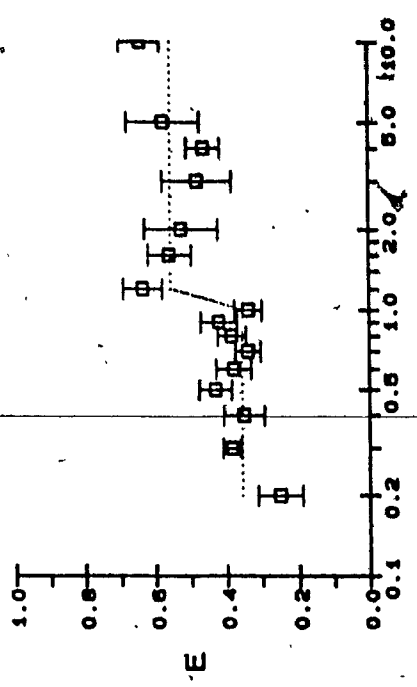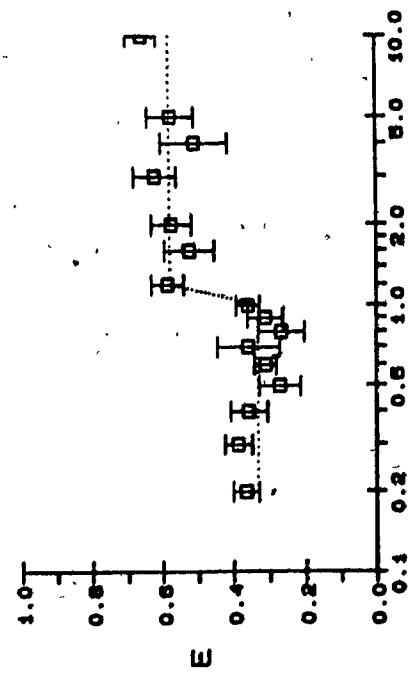
Figure 12. Anterior-posterior and posterior-anterior collision curves for subject M1, site A.

POSTERIOR-ANTERIOR

ANTERIOR-POSTERIOR

C-T INTERVAL (msec)

C-T INTERVAL (msec)

M1
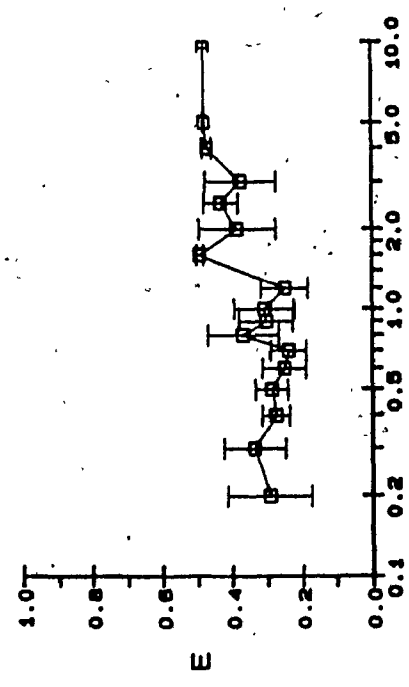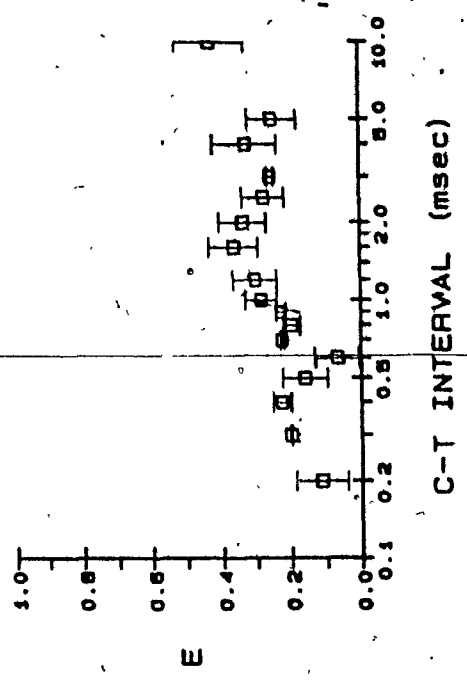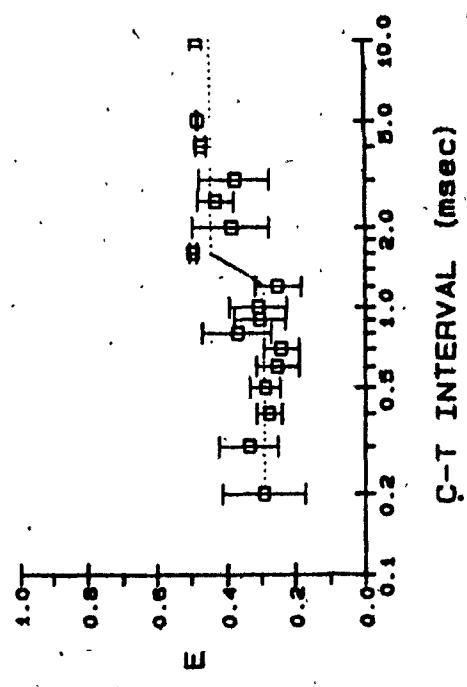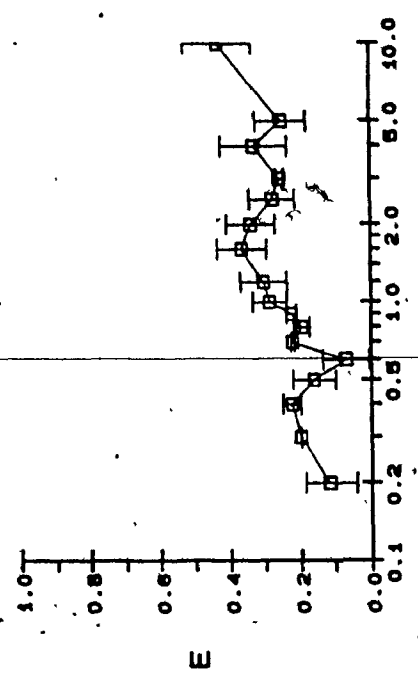
Figure 13. Anterior-posterior and posterior-anterior
collision curves for subject M1, site D.

POSTERIOR-ANTERIOR

ANTERIOR-POSTERIOR

M1
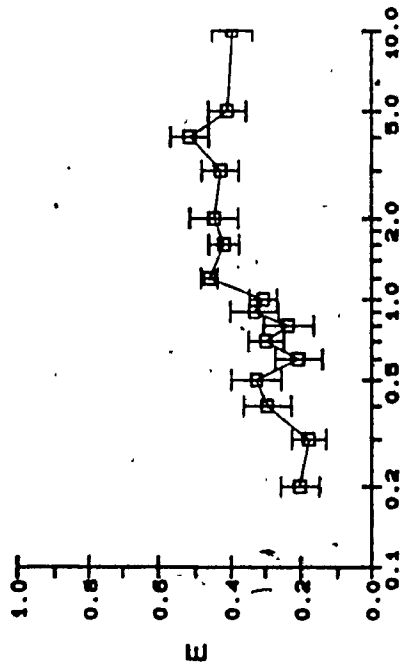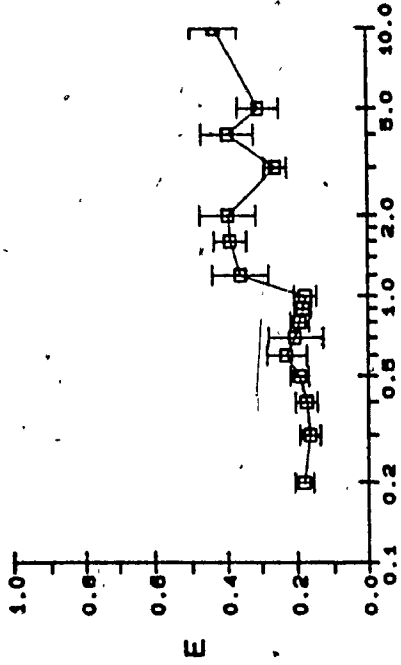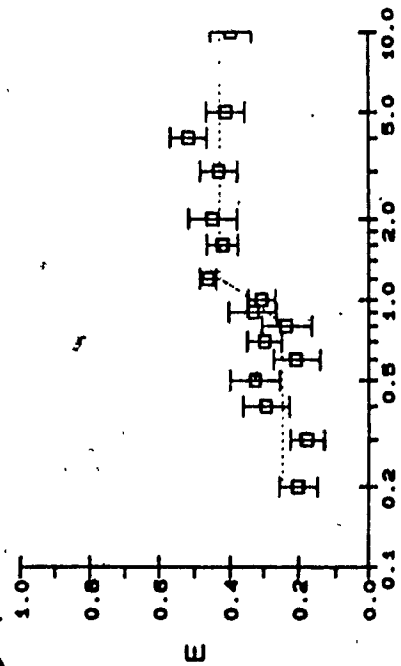
C-T INTERVAL (msec)
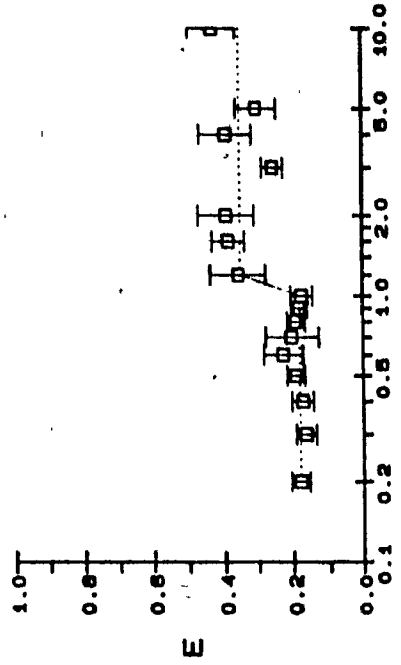
C-T INTERVAL (msec)

Figure 14. Anterior-posterior and posterior-anterior collision curves for subject MI; site E.
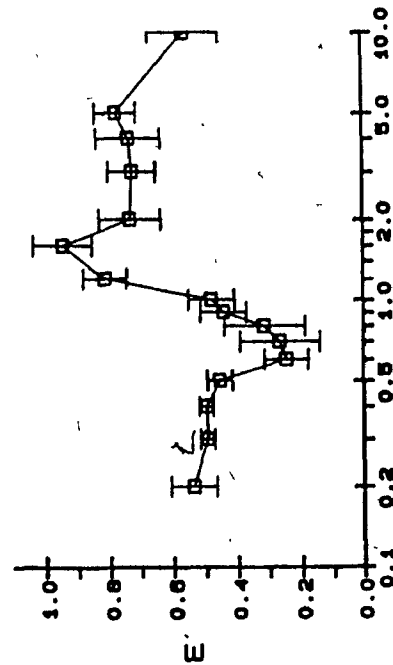
POSTERIOR-ANTERIOR

ANTERIOR-POSTERIOR

C-T INTERVAL (msec)

C-T INTERVAL (msec)
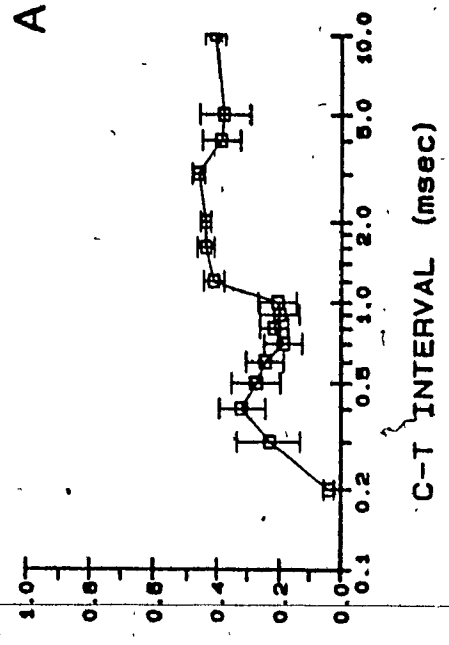
M1

Figure 15. Anterior-posterior and posterior-anterior collision curves for subject M4, site H.
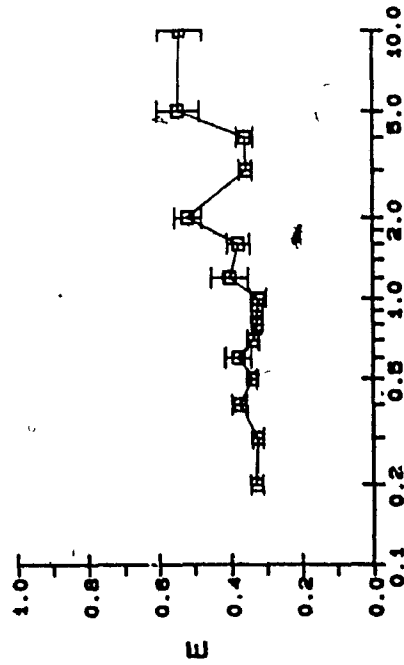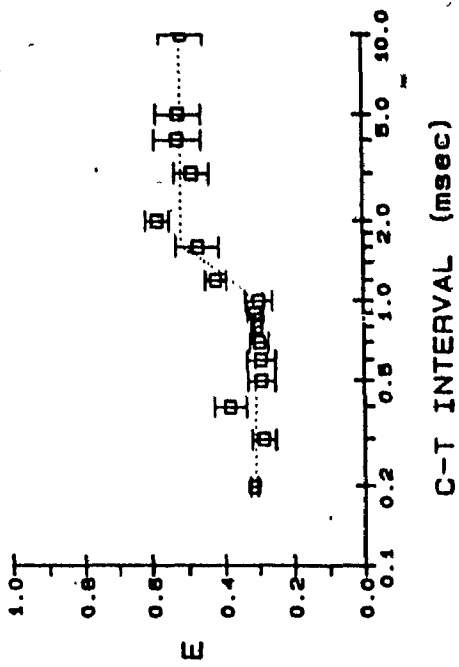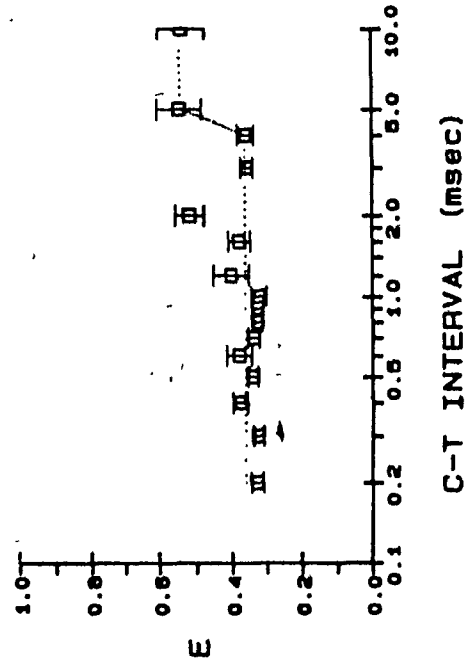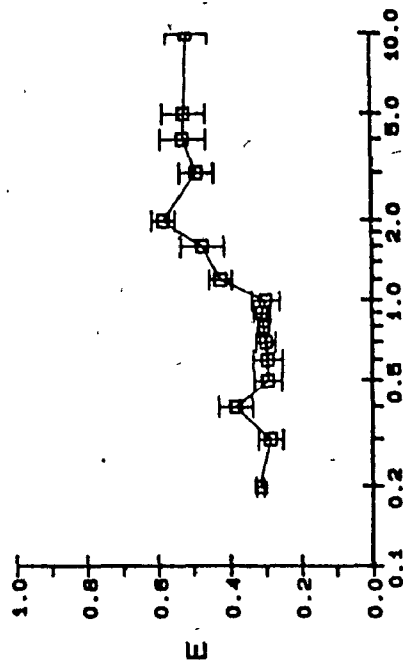
Figure 16. Anterior-posterior and posterior-anterior collision curves for subject M4, site I.
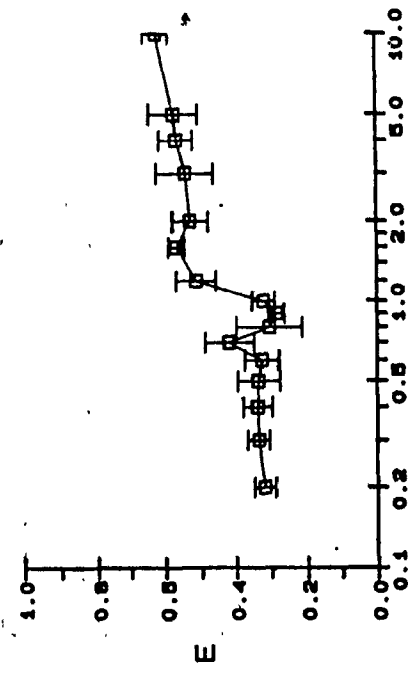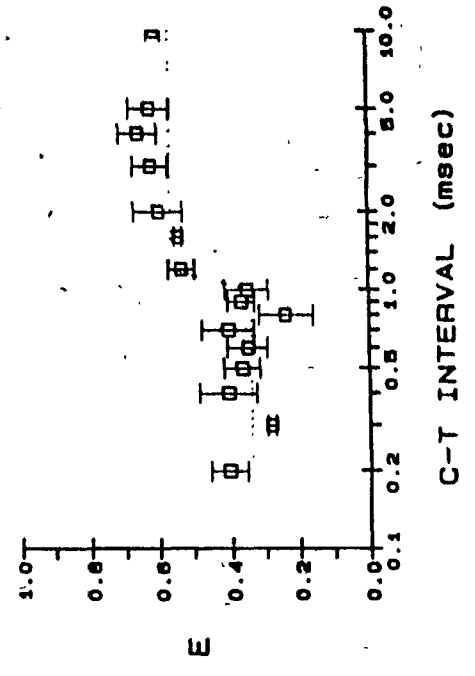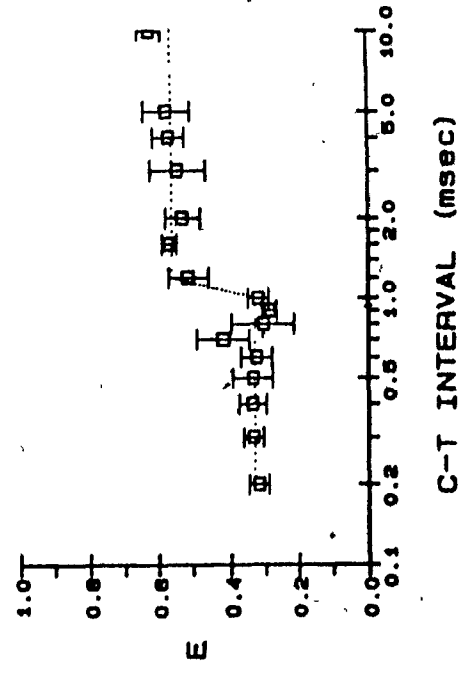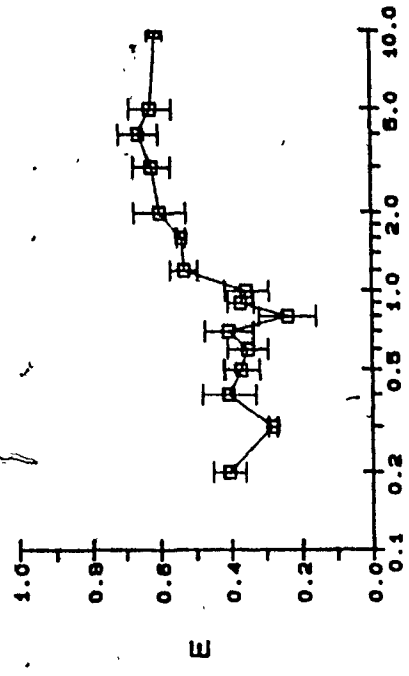
Figure 17. Anterior-posterior and posterior-anterior
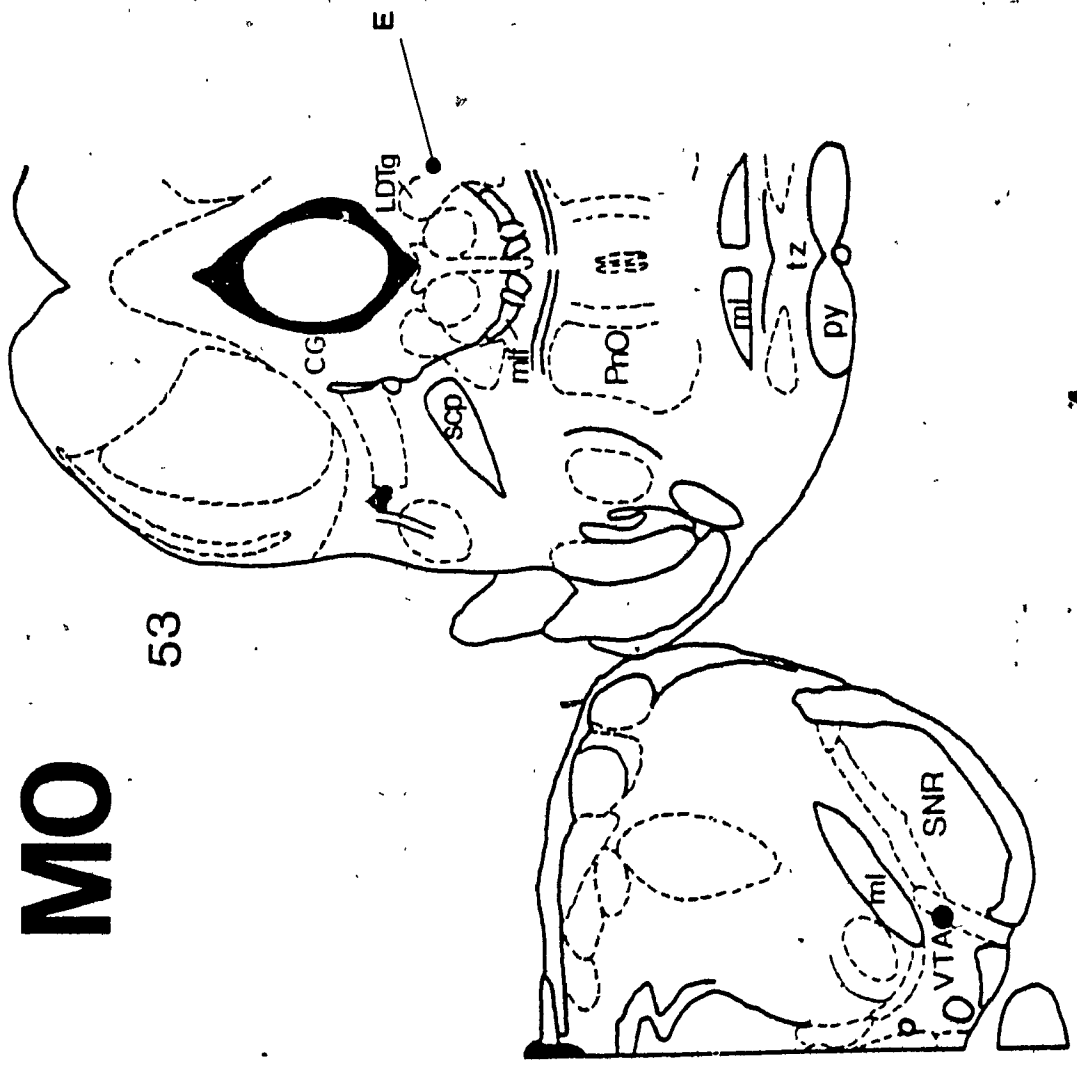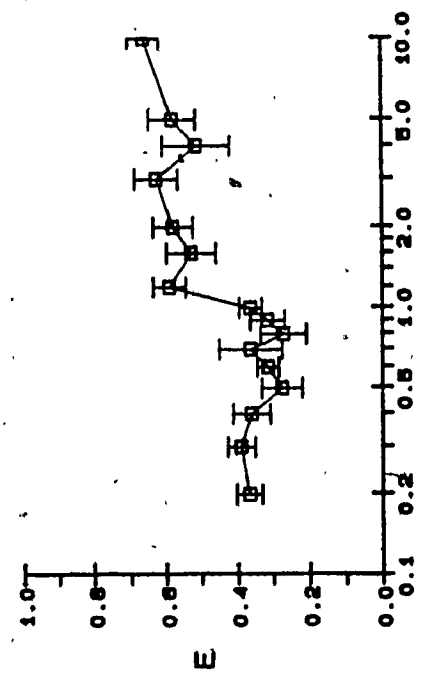collision curves for subject M6.
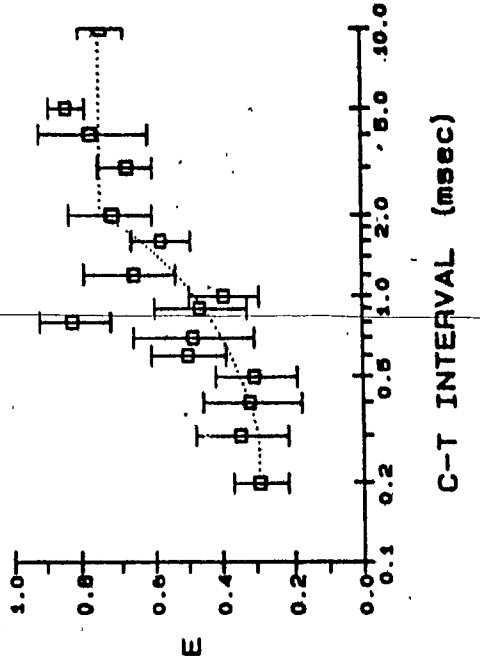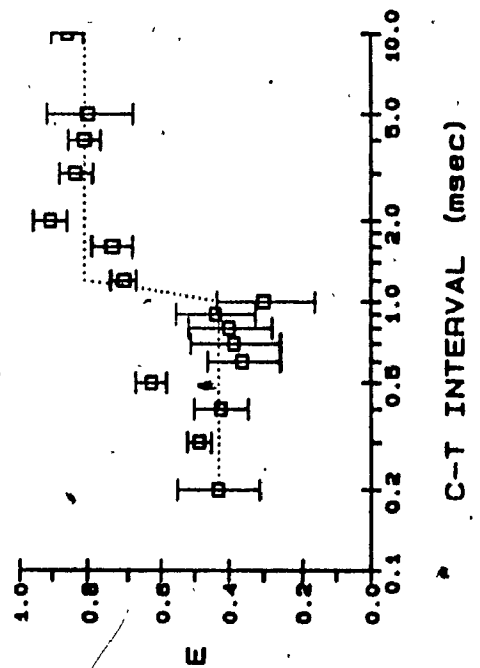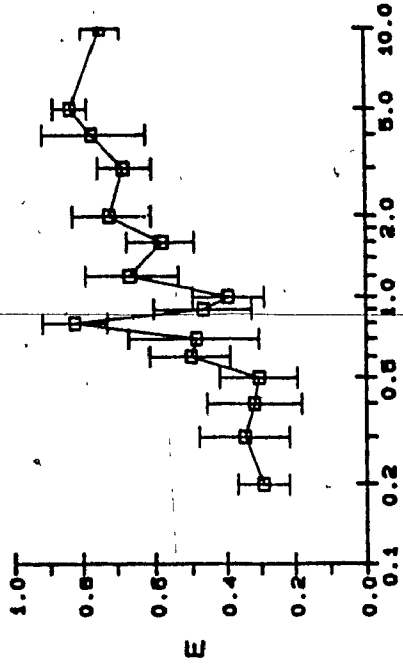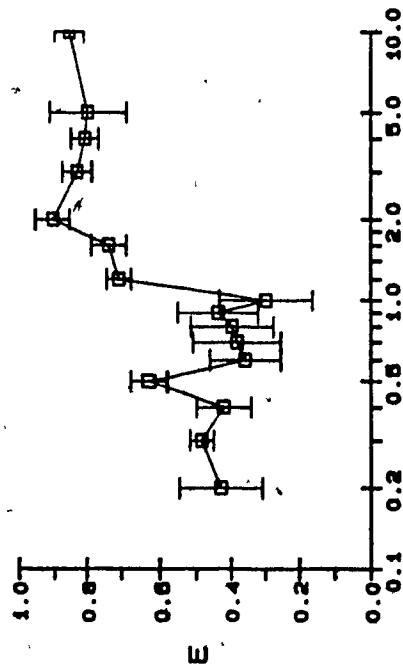
Figure 18. Anterior-posterior and posterior-anterior collision curves for subject M8.

M8

ANTERIOR-POSTERIOR
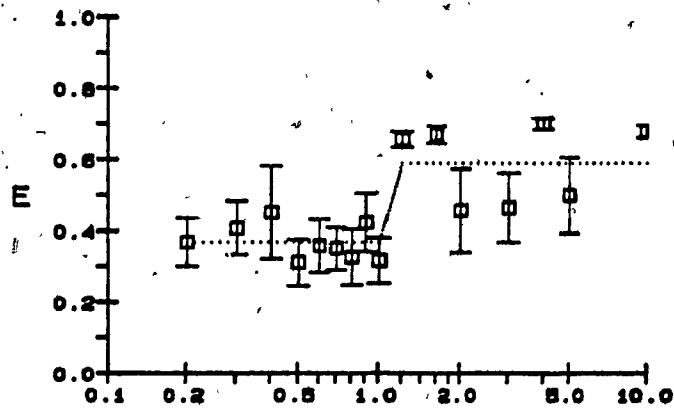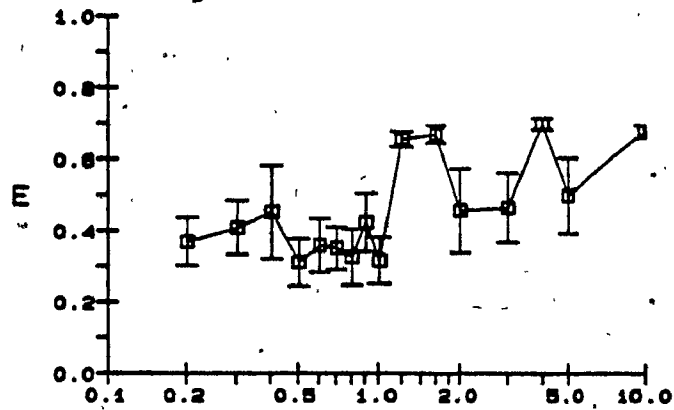
Figure 19. Anterior-posterior and posterior-anterior collision curves for subject X2.

POSTERIOR-ANTERIOR

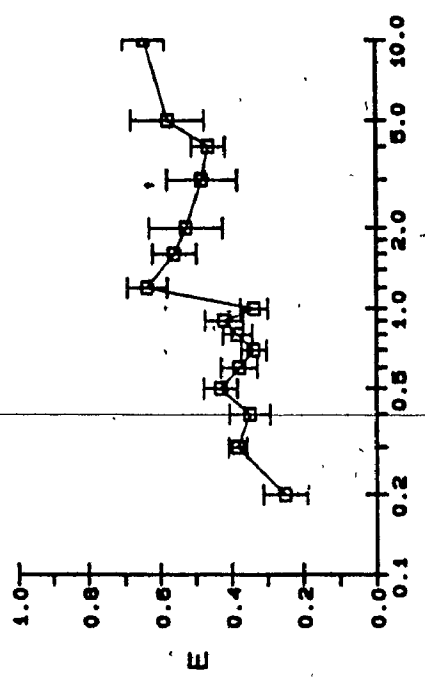ANTERIOR-POSTERIOR

X2
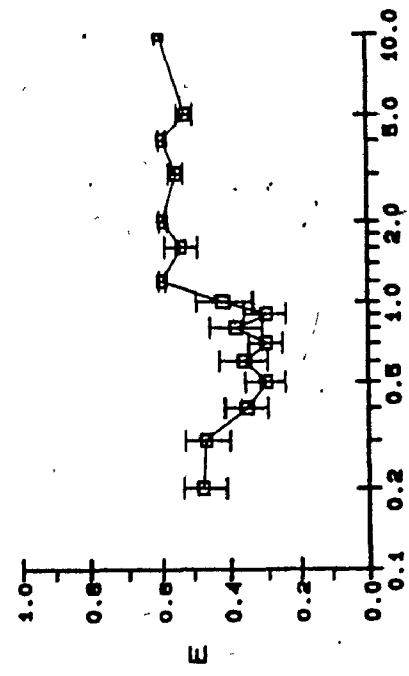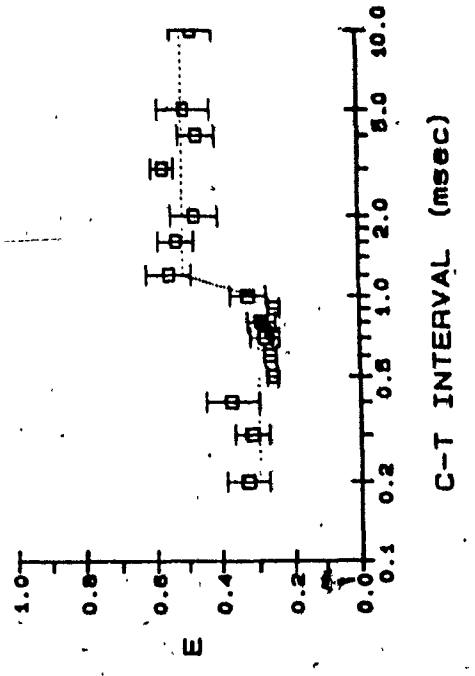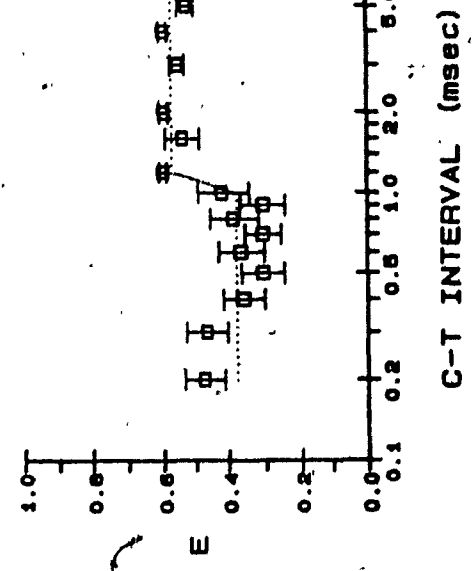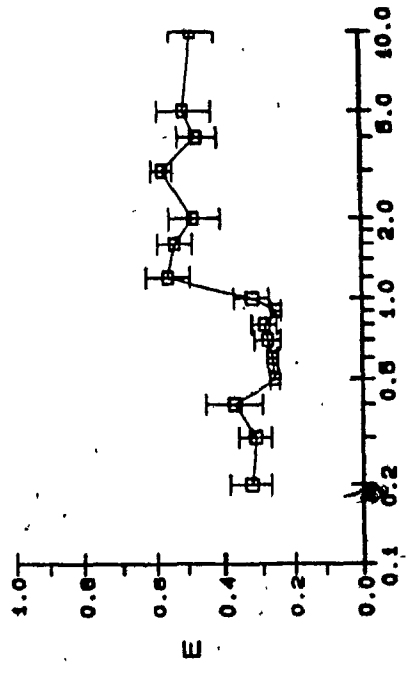
C-T INTERVAL (msec)

Figure 20: Anterior-posterior and posterior-anterior collision curves for subject Bl.

71

POSTERIOR-ANTERIOR

ANTERIOR-POSTERIOR

C-T INTERVAL (msec)

C-T INTERVAL (msec)

B1
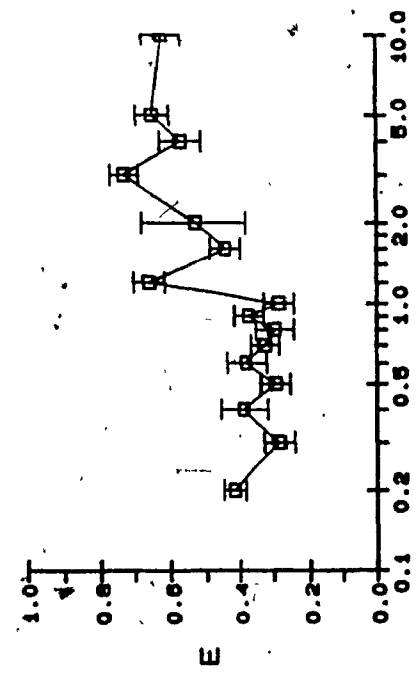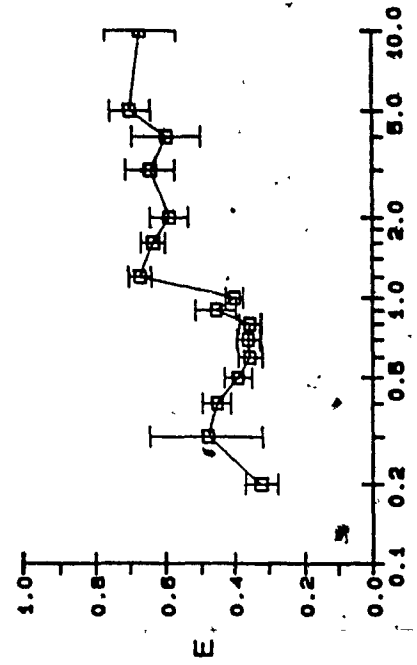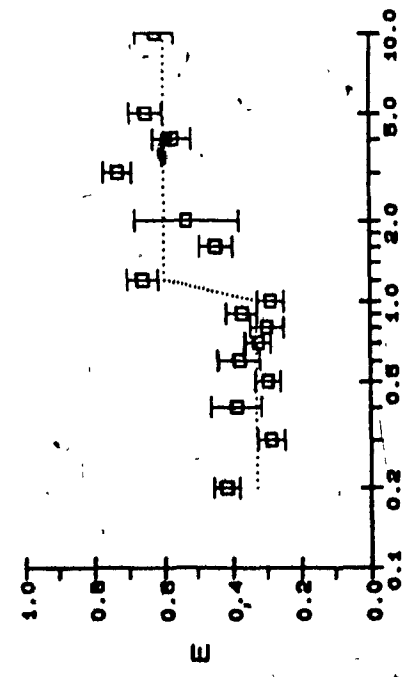
Figure 21. Anterior-posterior and posterior-anterior
collision curves for subject MO.

POSTERIOR-ANTERIOR

ANTERIOR-POSTERIOR

C-T INTERVAL (msec)

C-T INTERVAL (msec)

MO
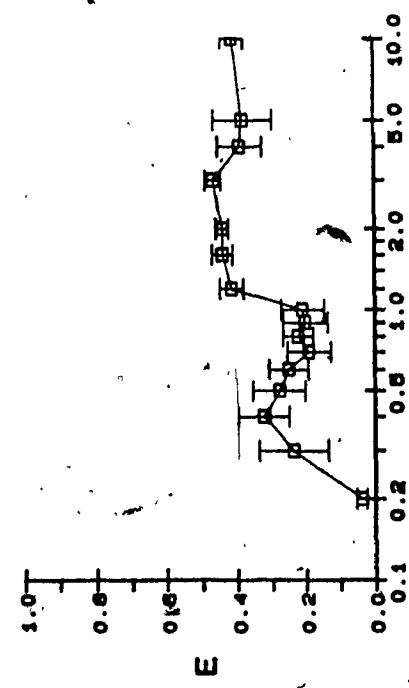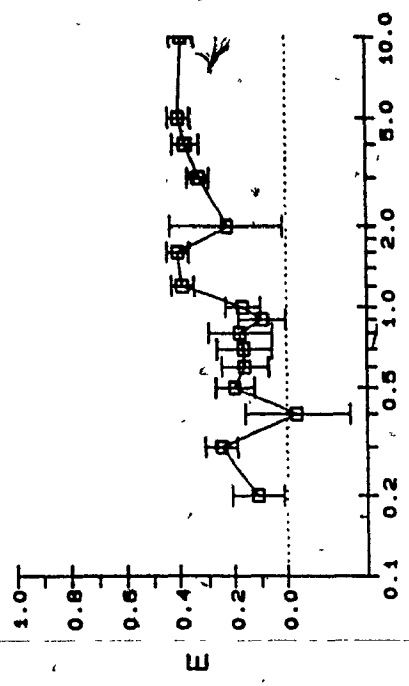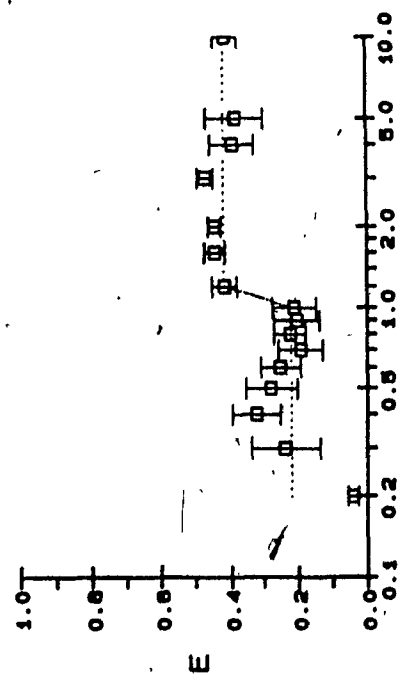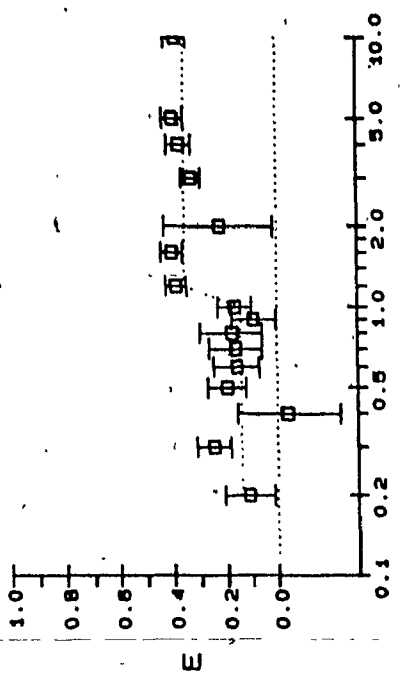
As mentioned earlier, subject M8 lost his electrode assembly at the end of the sixth replication.

Inspection of the anterior-posterior and posterior-anterior collision curves obtained from the remaining seven subjects reveals that most of the curves are very similar across test sequences: both have a step-like function which is preceded and followed by relatively stable E-values, and the collision intervals are the same. However, some of the collision curves are not congruent, differing in shape and/or the C-T interval at which collision occurs. The curves obtained from subjects M1, and M4 site H, show such discrepancies (Figures 12 to 15). The differences in the curves obtained from subject M6 (Figure 17) could be due to imbalances in the currents used to test the two sequences. Currents used for the anterior-posterior sequence were 363uA for each site; those for the posterior-anterior sequence were 269uA for the anterior site and 363uA for the posterior site.

Discussion

The most parsimonious interpretation of the collision results obtained from this first experiment is that common reward-relevant fibers are shared by both stimulation sites. These results thus imply that the lateral hypothalamus and the ventral tegmental area are linked by reward-relevant fibers with nontine sites. In a previous collision study, Bielajew et al. (1981) failed to reveal axonal linkage between reward-relevant neurons in the mesencephalic central gray and the anterior medial forebrain bundle. One possibility is that the failure to reveal a direct link was due to the use of fixed stimulating electrodes. It has previously been shown (Rompré and Miliaressis, 1985; Rompré and Boye, submitted) that the range of positive reward-relevant sites in the mesencephalon extend approximately 4 mm in the dorso-ventral plane. Accordingly, the probability of activating common reward-relevant fibers using fixed stimulating electrodes is very low. Miliaressis and Philippe (1983) have shown that the probability of revealing the existence of direct axonal linkage is much greater when moveable electrodes ate used; this conclusion is supported by the present results showing that lowering of the electrode by as little as 0.16 mm can make the difference between positive and negative collision results.

The results of this collision experiment place anatomical
constraints on neural substrates considered as likely
carriers of the reward signal. At least part of the
trajectory of the substrate should travel between the
central gray-dorsal raphe region and the ventral tegmental
area. The results of subject M7 further imply that the
extent of this path may be greater, linking the lateral
hypothalamus and the medial pons. A summary of the location
of sites at which evidence of axonal linkage was obtained is
presented in Figure 22. The tips of all rostral electrodes
but one were located in the ventral tegmental area; the tip
of the rostral electrode of subject M7 was located in the
posterior part of the lateral hypothalamus. With the
exceptions of subjects M0 and M4, which were the subjects
with the longest and shortest inter-electrode distances
respectively, evidence of collision was obtained when the
tip of the posterior electrode was located between the floor
of the cerebral aqueduct and the ventral part of the
central-gray. The most caudal site that was tested was
located more laterally compared to the other sites (Figure
22, panel B). Note the deviation of this point from the
cluster of points found on the midline.

Histological analysis tends to suggest that reward-
relevant neurons that travel between the mesencephalon and
the pons respect a certain anatomical pattern. First,
reward-relevant fibers linking the posterior part of the

Figure 22.   Schematic representation of results obtained
from the collision test in eight subjects.

A

B
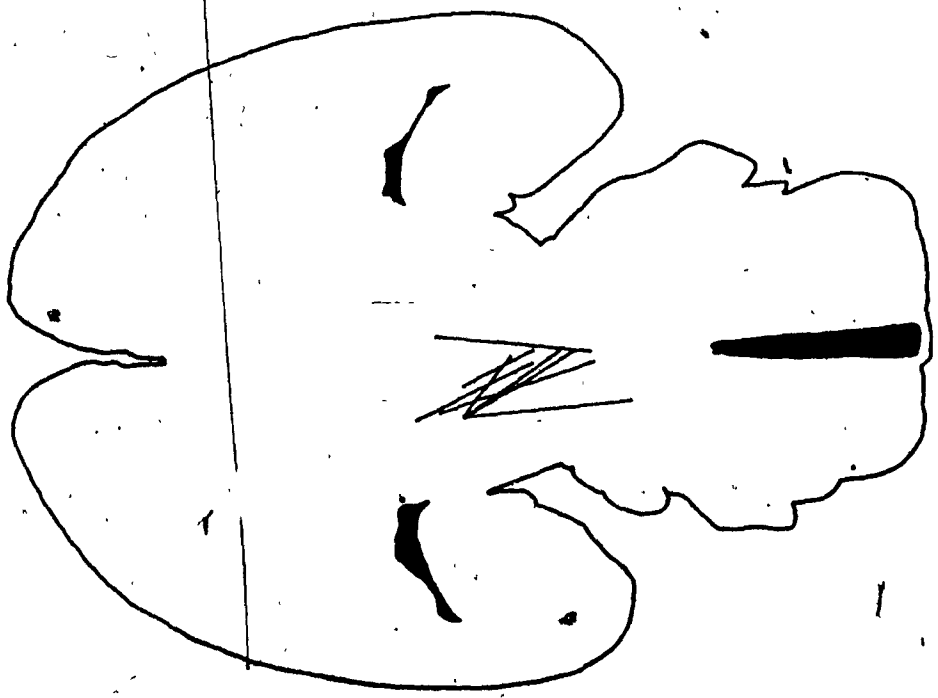
lateral hypothalamus and the rostral part of the ventral
tegmental area to the pons seem to spread between the
cerebral aqueduct and the ventral central gray. Reward-
relevant neurons linking the caudal part of the ventral
tegmental area to the pons seem to pass through more ventral
regions of the pons. Second, the reward substrate either
bifurcates or converges, depending on the natural direction
of propagation, on the midline pons. In effect, evidence of
a direct axonal link was found between the dorsal raphe and
the right (subject X2) and left (subject B1) ventral
tegmental area. Third, histological analysis of the brain
of subject MO revealed that the rostral electrode was
located in the left ventral tegmental area and the moveable
electrode was located on the left side of the pons at about
1 mm off the midline. Two possible trajectorial
arrangements can explain the evidence of collision. A first
possibility is that some reward-relevant neurons remain
ipsilateral as they travel between the pons and the ventral
tegmental area. A second possibility is that reward-
relevant fibers cross the midline twice, thereby returning
to the same side of the brain. Although confirmation of
these anatomical arrangements requires additional empirical
support, they provide a useful feature that can help
identify the reward substrate.

An interesting feature stemming from the collision data
is the asymmetry between collision curves obtained with the

anterior-posterior and posterior-anterior test sequences. These differences reveal interesting characteristics about the reward-substrate in regions posterior to the ventral tegmental area. According to the model of Shizgal et al. (1980), if paired-pulse effectiveness reflects the summation of neural activity along a fiber bundle not interrupted by any synapses (pure axonal model), th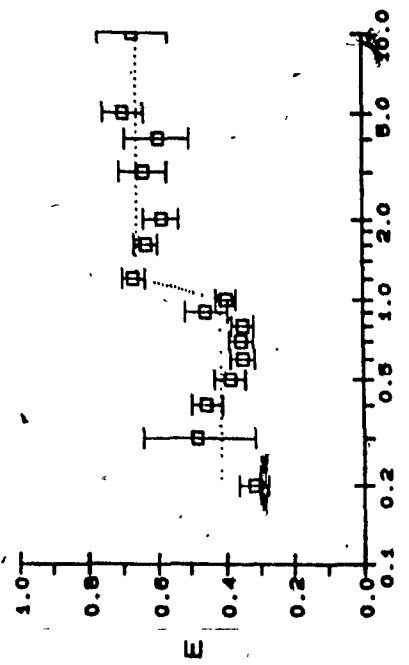e anterior-posterior and posterior-anterior collision tests should yield identical curves. In our study, however, we sometimes observed differences between the collision curves derived with each of the two test sequences. These differences may suggest that other neural mechanisms, which are not yet well understood, contribute to the E-values. One possible neural event that would account for differences in either the shape of the curves or the collision intervals, is the presence of synaptic link(s) between reward-relevant neurons activated by the two electrodes. Due to the unidirectional nature of synaptic transmission, a given curve might exhibit peculiarities which are not observed on the counterpart curve obtained with the opposite test sequence.

With the exception of the collision curves obtained from subjects M1, site E, and subject M6, site C, (Figures 3 and 5), summation levels are relatively low across all sites. The levels of summation obtained from concurrent stimulation of rostral and caudal sites in the present study is lower than those obtained from concurrent stimulation of

ipsilateral sites within the MFB (see Shizgal et al., 1980; Bielajew and Shizgal, 1982) but is comparable to the summation levels observed in the bilateral MFB collision test in Shizgal et al's study (1980). Low summation levels were also obtained by Bielajew et al. (1980) when concurrent stimulation was applied to the lateral hypothalamus and the periaqueductal gray. It was proposed by these authors that this was due to stimulation of different reward-relevant fibers with a common output. In the present study, based on the collision data of subjects X2 and B1, it can be assumed that reward-relevant fibers in the medial pons either bifurcate as they travel bilaterally to more rostral areas or that they course bilaterally towards the midline pons where they converge. If this is the case, then reward-relevant fibers projecting to, or descending through, the right hemisphere and stimulated by the pontine electrode could never be stimulated by a mesencephalic electrode located in the left hemisphere, and this would result in an incomplete collision effect. The contralateral reward-relevant fibers stimulated only by the moveable electrode will never undergo collision. If the outputs of these two reward-relevant bundles converge on a common integrator, then summation levels at long C-T intervals should be close to 1. Indeed, the counter model predicts that the process which integrates neural activity triggered by the stimulation electrodes is indifferent to the spatiotemporal distribution of incoming signals (see Gallistel, Shizgal,

and Yeomans, 1981). However, the low summation levels observed in the present study suggest other possibilities. The first possibility is that reward-relevant neural signals transmitted from contralateral sides of the brain are integrated independently by separate integrative processes. A second possibility is that the outputs of the two bundles converge on a common integrator that has poorer spatial integration than temporal integration. Such differences in spatial and temporal summation have been found in the peripheral nervous system (Chung and Wurster, 1978).

Another interesting feature of the collision curves is the increase in paired-pulse effectiveness values at short C-T intervals seen in some of the positive collision curves (see Figures 2,3E,8). Such effects would appear to suggest the contribution of latent addition--action potentials triggered by the summation of two subthreshold stimuli. However, the fact that in these cases, the inter-electrode distances ranged from 2.4 to 4.36 mm and that the highest current intensity was 542 uA, does not provide strong support for the hypothesis of overlapping stimulation fields. Some mechanism(s) other than latent addition, and not understood yet, may have contributed to the E-values at these short C-T intervals.

The results of the present experiment have revealed anatomical characteristics about the reward substrate. The

next experiment was designed to reveal physiological characteristics of the same neurons.

EXPERIMENT 2

Introduction

In addition to providing evidence of axonal linkage between two brain sites, positive collision results offer a means for estimating the conduction velocity of those fibers undergoing collision. As stated earlier, the collision interval represents the sum of the inter-electrode conduction time and the refractory period of the axonal segment underneath the tip of the electrode delivering the second pulse in each pair. If the refractory period can be estimated and subtracted from this total, then we are left with the time required for action potentials to travel from the site of one electrode tip to the other. This time estimate can then be divided into the distance between the electrode tips to yield an estimate of the conduction velocity of those fibers responsible for the collision effect. Such valuable information can further characterize first-stage reward neurons and narrow the selection of candidate pathways.

The excitability cycle of a neuron is estimated in a way that is analogous to the collision test, but with both pulses (C and T) delivered via the same electrode. The delivery of a subthreshold C-pulse causes a local

disturbance in the membrane potential of the cell but does not trigger an action potential. If, however, a T-pulse of equal intensity is delivered immediately after the C-pulse, the two subthreshold stimuli may summate and cause the cell to fire. This effect is called local potential summation and decays as the C-T interval is increased. If a suprathreshold C-pulse is applied to the membrane, an action potential is triggered and this marks the beginning of the absolute refractory period. During this phase, a T-pulse cannot trigger another action potential in the refractory fibers regardless of the amplitude of the pulse. The absolute refractory period is followed by the relative refractory period. During this time, the threshold for firing is elevated and an action potential can be triggered by a T-pulse only if it is of greater intensity than is required at resting potential.

Early work on the refractory periods of self-stimulation neurons employed one of the techniques developed by Deutsch (1964), which involves measuring bar-pressing rates as a function of C-T interval. Yeomans (1975) has argued that because the relation between pulse frequency and response rate is not linear, manifesting floor and ceiling effects, refractory period estimates obtained by measuring response rates are dependent of the arbitrary choice of stimulation frequency. Yeomans proposed a technique which requires that a full range of frequencies be tested at each C-T interval,

thus yielding a family of frequency-response curves. A scaling procedure is then employed which determines the amount of stimulation required to maintain a constant level of responding at different C-T intervals. The rationale behind this procedure rests on the assumption that at long C-T intervals, both pulses will contribute equally to the behavior. However, at short C-T intervals, the T-pulse will fall within the refractory period of some cells and will fail to trigger action potentials. In this case, action potentials lost to refractoriness must be replaced by additional pulse pairs in order to maintain a constant behavioral output.

The purpose of this second experiment will be to estimate the refractory periods of those reward-relevant fibers undergoing collision in the first experiment. Using these estimates, it will be possible to estimate the conduction velocity of these same fibers. By estimating the refractory periods of the same sites and with the same currents that were used for the collision test, the fibers which are stimulated in the two experiments are kept constant./ The results of this second experiment will therefore directly characterize those reward-relevant fibers linking rostral mesencephalic and pontine sites.

Method

Subjects

The same subjects were used as in experiment 1.

Procedure

Whenever possible, refractory periods were estimated for both anterior and posterior sites. Refractory period estimation consisted of single- and double-pulse frequency threshold determinations. A session began with two warm-up single-pulse threshold determinations. Eight additional single-pulse thresholds were determined throughout the session, interspersed among paired-pulse frequency thresholds at 17 different C-T intervals that ranged from 0.2 to 10.0 msec. The data from a session were discarded if the standard error of the mean for single-pulse thresholds varied by more than 10%. Refractory period tests were replicated six times for each site. The order in which different C-T intervals were tested was counterbalanced from day to day.

In order to reduce the contribution of local potential summation, refractory periods were, whenever possible, estimated using pulses of unequal amplitude (C>T) (see

Yeomans, 1979). Although the use of C-pulses of greater
amplitude than T-pulses results in poor definition of the
end of recovery, due to the presence of the supernormal
period, it has been shown to reduce the contribution of
local potential summation at short C-T intervals and
therefore allows a more precise estimate of the end of the
absolute refractory period of the most excitable neurons
(see Miliaressis and Rompré, 1980). In cases where
refractory periods were estimated using this technique
(C>T), relative T-pulse effectiveness was estimated using
the formula of Bielajew et al. (1981):

$$E = (FT_{SP_L}/FT_{C-T}) - 1/(FT_{SP_L}/FT_{SP_H})$$

where   E = relative T-pulse effectiveness,

FT_{SP_L} = lower of the two single-pulse frequency

thresholds,

FT_{C-T} = frequency threshold for a given C-T

interval,

FT_H = higher of the two single-pulse frequency

thresholds.

In cases where refractory periods could not be estimated
using unequal pulses (due to the animal's reaction to the
high intensity of the C-pulse), refractory periods were
estimated using pulses of equal amplitude. Under these

conditions, SP_L and SP_H in the above formula are the same and thus their ratio reduces to 1. This in turn reduces the above formula to the one used for pulses of equal amplitude:

$$E=(FT_{SP}/FT_{C-T})-1$$

where E = relative T-pulse effectiveness,

FT_{SP} = average frequency threshold for single

pulses,

FT_{C-T} = frequency threshold for a given C-T

interval.

In the above formulas, the effectiveness of the T-pulse in triggering neural responses is scaled relative to the effectiveness of the C-pulse. If the T-pulse falls within the absolute refractory period of all the cells stimulated by the C-pulse, its effectiveness in triggering neural responses will be 0. Under these conditions, paired-pulse stimulation will have the same behavioral weight as single-pulse stimulation. At long C-T intervals, all cells will have recovered from refractoriness. The T-pulse will now contribute equally to the behavior as the C-pulse, and its relative effectiveness will thus be 1. In this case, the frequency threshold for paired pulses will be one-half that of single pulses.

Curve Fitting

Using the Biomedical Data Package (BMDP), a curve-fitting procedure was employed to non-arbitrarily determine the function which best represented the general trend of the refractory period data. The procedure fits three segments to the data: an exponentially decaying function to those points characterizing local potential summation, a linear function extending from the lowest E-value to the E-value at which an asymptote is reached, and a horizontal line which maintains this asymptotic value. The curve-fitting procedure, PAR (Derivative-Free Nonlinear Regression), estimates the parameters of a nonlinear function by calculation of the residual sum of squares. Estimation of these parameters is based on five initial values supplied by the experimenter based on visual inspection of the curve: 1) the time constant of the decay 2) the y-intercept of the exponential function, 3) the C-T interval corresponding to the lowest E-value among the data points, 4) the E-value at which an asymptote is reached and 5) its corresponding C-T interval. Using these initial estimates, and then systematically varying them, the program calculates the resultant residual sum of squares. When no significant change in the residual sum of squares is observed, the program indicates the parameters that yield the smallest residual sum of squares. These parameters were then used to fit the data.

In some cases where pulses of unequal amplitude were used to estimate refractory periods, the lack of local potential summation prevented the fitting of an exponentially decaying function to those points before the rise. In these cases, a straight line which yielded the smallest residual sum of squares was fit to those points at short C-T intervals.

Results

Refractory period estimates were obtained for every subject except M6 and M8. Subject M6 lost a considerable amount of weight near the end of the first experiment, and it was judged best to sacrifice the animal once enough replications of the collision curves were obtained. Subject M8 lost the electrode assembly at the end of the first experiment. For five of the remaining six subjects, refractory periods were estimated using pulses of unequal amplitude. For the remaining subject, MO, it was not possible to use unequal pulses due to undesirable side-effects induced by the higher intensity of the C-pulse. Figures 23 to 30 show the refractory period curves obtained for each subject. The left panel shows the site from which the estimates were obtained. The right panel shows the refractory period curve that was obtained from that site. The curve fitted to the data is shown below individual graphs. The distortions in the fitted curves result from plotting linear-based graphs onto semi-logarithmic space.

Figure 23 shows the refractory period data obtained from the posterior stimulation site of subject MO. Pulses of equal amplitude were used for estimating the refractory period (C & T = 346 uA). The curve derived from this site conforms well to the predicted phases of the excitability cycle of a stimulated bundle of axons. The initial decline

Figure 23. Refractory period data obtained from the posterior stimulation site of subject MO.

MO

A.

B.
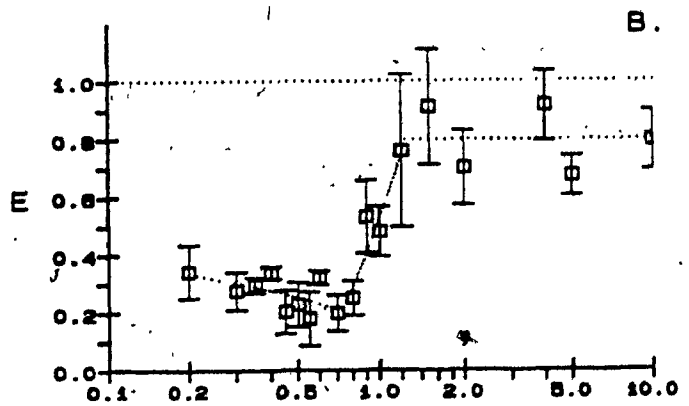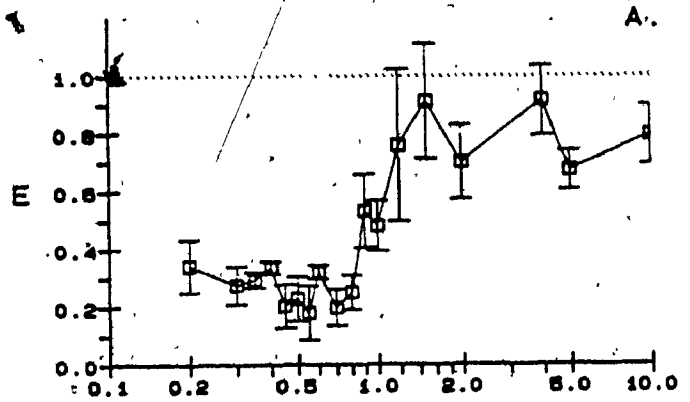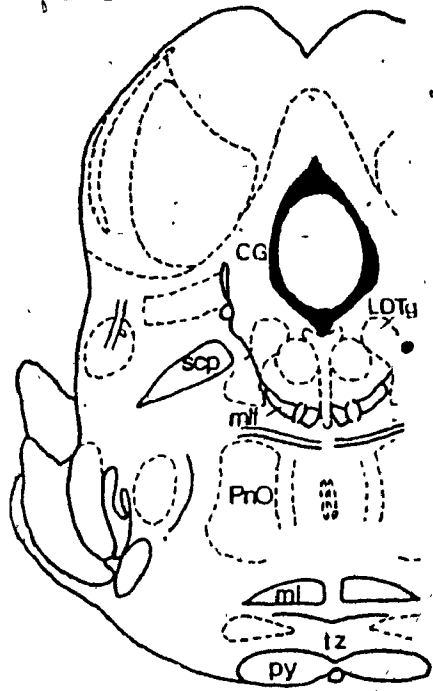
C-T INTERVAL (msec)

Figure 24.   Refractory period data obtained from the
anterior stimulation site of subject MO.

MO
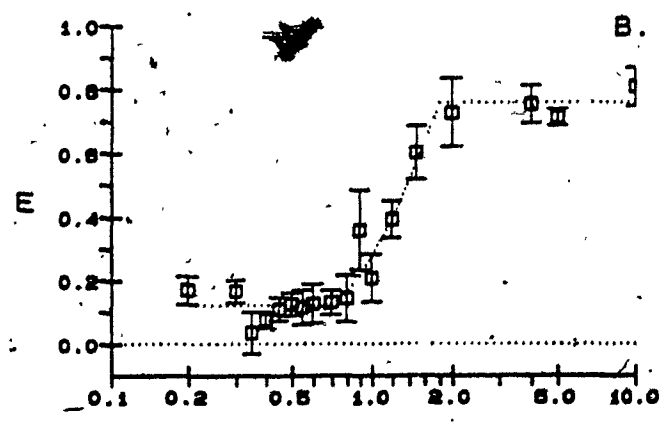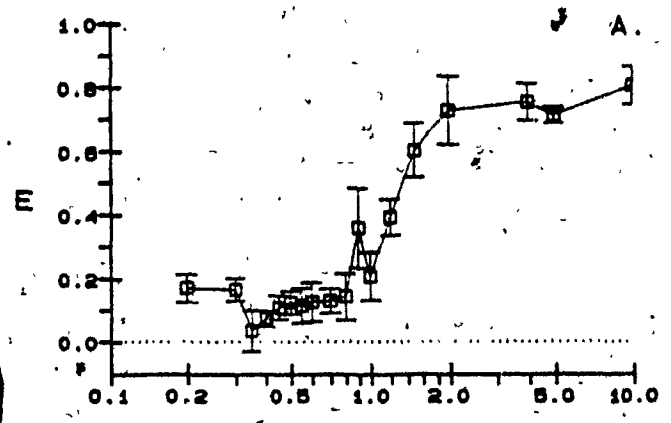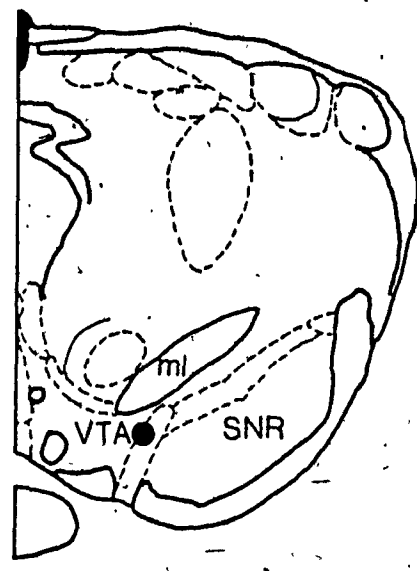
C-T INTERVAL (msec)

Figure 25 shows the data for subject M4. Pulses of
unequal amplitude were used to estimate the refractory
period of the ventral tegmental site (C = 732 uA, T = 516
uA). Accordingly, there is no evidence of local potential
summation at short C-T intervals and a supernormal period is
first evident at 4.0 msec. A supernormal period is
sometimes observed when C-pulses that are larger than T-
pulses are used. Fibers contributing to the supernormal
period are located outside of the suprathreshold region of
the T-pulse. These fibers will be stimulated above
threshold by the C-pulse and will fire again to the
subthreshold T-pulse due to a state of hyperexcitability
immediately following the end of the relative refractory
period. The data from subject M4 could not be fit with a
curve comprising an exponentially decaying function
describing local potential summation. Those points before
the rise were therefore fit with a straight line which
yielded the smallest residual sum of squares. The end of
the absolute refractory period was estimated by the curve-
fitting procedure at 0.52 msec.

The curve obtained from subject M1 is presented in Figure
26. C-pulses of greater amplitude than T-pulses were used
to estimate the refractory period of the ventral tegmental
site (C = 599 uA, T = 402 uA). It was not possible to
estimate the refractory period of the posterior stimulation
site of this subject due to aversive reactions induced by

Figure 25. Refractory period data obtained from the anterior stimulation site of subject M4.

M4

C-T INTERVAL (msec)

Figure 26. Refractory period data obtained from the anterior stimulation site of subject M1.

M1
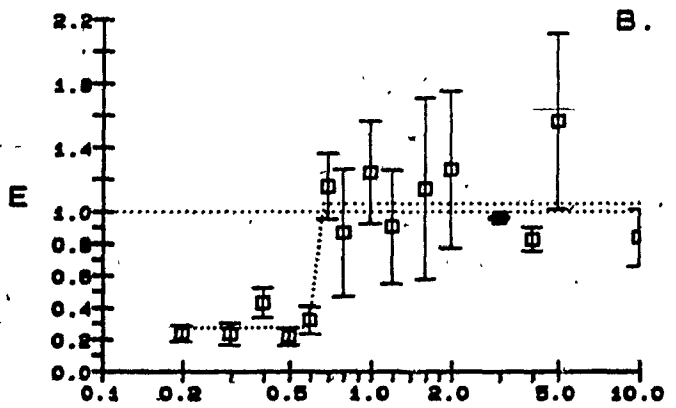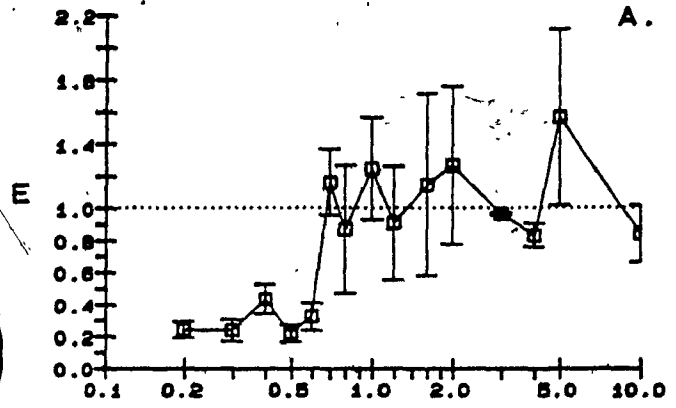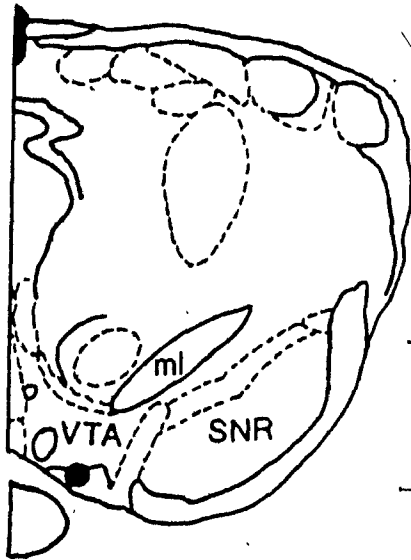
C-T INTERVAL (msec)

the C-pulse. The use of C-pulses of greater intensity than T-pulses eliminated the contribution of local potential summation, evidenced by the flatness of the curve at C-T intervals shorter than 0.6 msec. The curve-fitting procedure estimated the end of the absolute refractory period at 0.60 msec.

Figure 27 shows the refractory period curve obtained from the central gray stimulation site of subject M7. Although C-pulses were used that were larger than T-pulses (C = 402 uA, T = 300 uA), there appears to be some residual contribution of local potential summation between the C-T intervals of 0.2 and 0.6 msec. A supernormal period is observed at 5.0 msec. The fitted curve estimated the end of the absolute refractory period of the most excitable neurons at 0.60 msec.

Figure 28 shows the refractory period data for the posterior lateral hypothalamic site of subject M7. The use of C-pulses larger than T-pulses (C = 599 uA, T = 300 uA) reduced the contribution of local potential summation. This portion of the curve was therefore fit with the straight line yielding the smallest residual sum of squares. The fitted curve estimated the end of the absolute refractory period at 0.60 msec.

Figure 27.   Refractory period data obtained from the
posterior stimulation site of subject M7.

M7

A.

B.
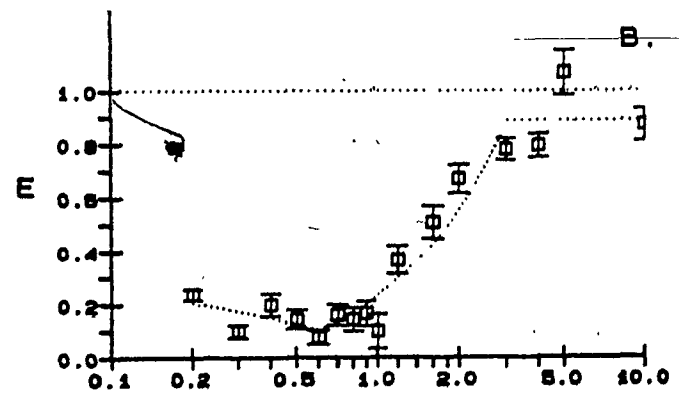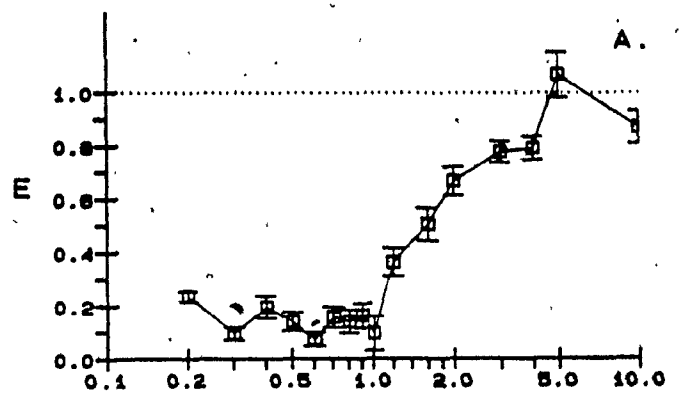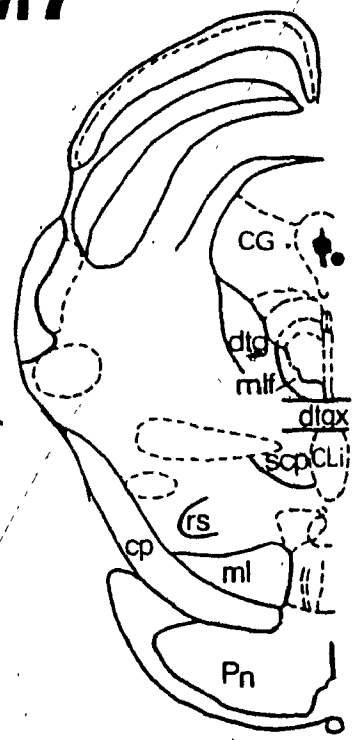
C-T INTERVAL (msec)

Figure 28. Refractory period data obtained from the anterior stimulation site of subject M7.

M7
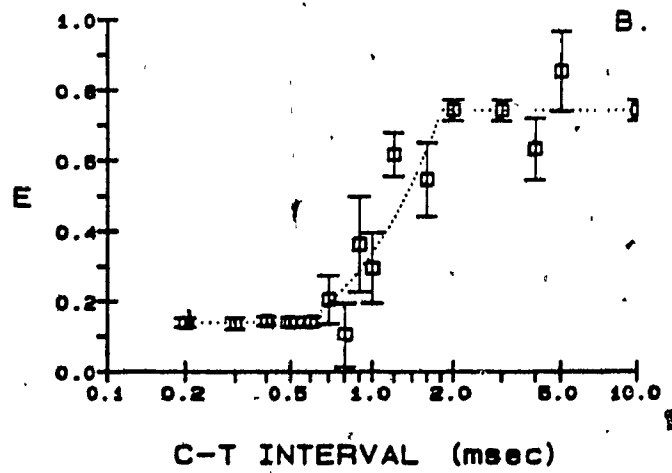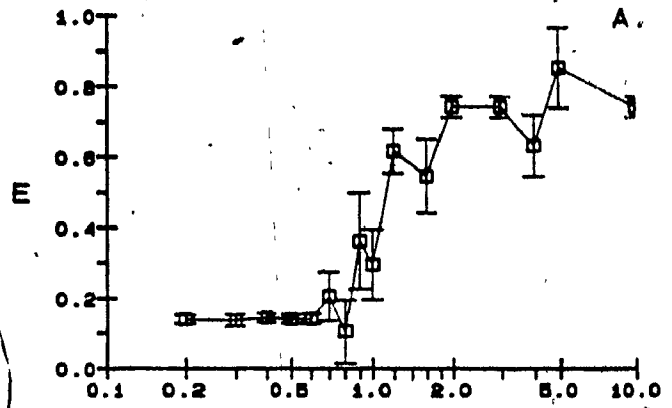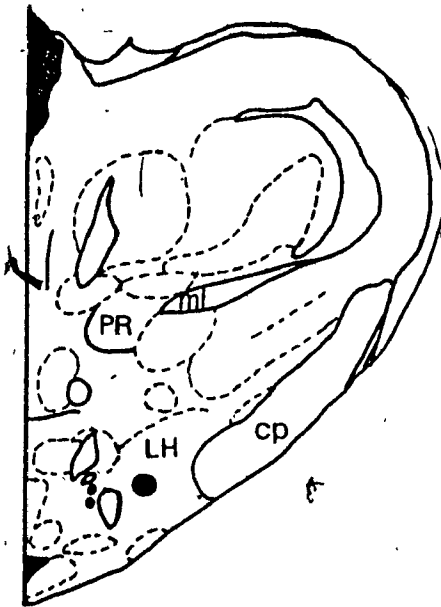
C-T INTERVAL (msec)

Figure 29 shows the refractory period data obtained from the ventral tegmental stimulation site of subject X2. For this subject, the refractory period estimate was erroneously obtained using T-pulses that were larger than C-pulses (C = 542 uA, T = 769 uA). Because the T-pulse intensity used to estimate the refractory period was larger than the intensity used for that same site during the collision test, the refractory period curve contains the contribution of neurons that did not contribute to the collision effect. Furthermore, reward-relevant fibers responsible for collision were stimulated at many times their thresholds during the refractory period test. This therefore results in a shorter estimate of the beginning of recovery of the most excitable fibers. The curve-fitting procedure estimated the end of the absolute refractory period at 0.35 msec.

The refractory period data obtained from the ventral tegmental site of subject Bl is presented in Figure 30. C-pulses were used that were greater in intensity than T-pulses (C = 346 uA, T = 232 uA). The use of unequal pulses did not completely eliminate the contribution of local potential summation as can be observed at C-T intervals between 0.2 and 0.6 msec. A small supernormal period was observed at 5.0 msec. The fitted curve estimated the end of the absolute refractory period at 0.53 msec.
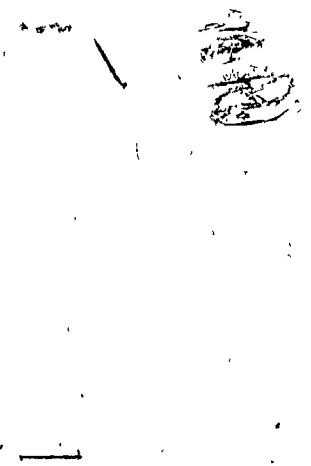
Figure 29.   Refractory period data obtained from the
anterior stimulation site of subject X2.
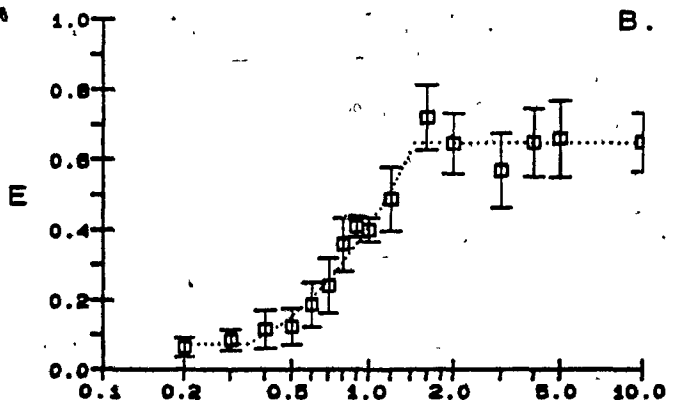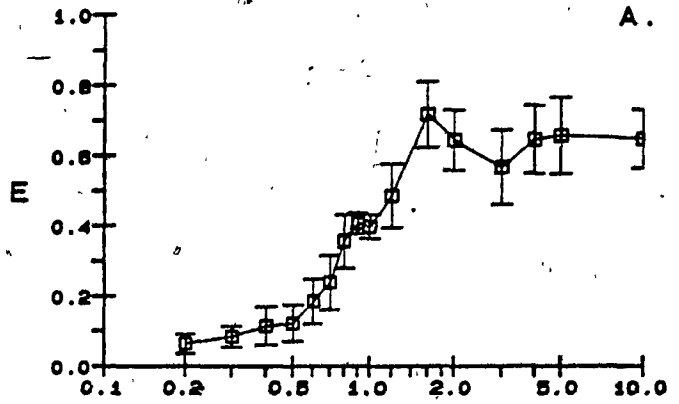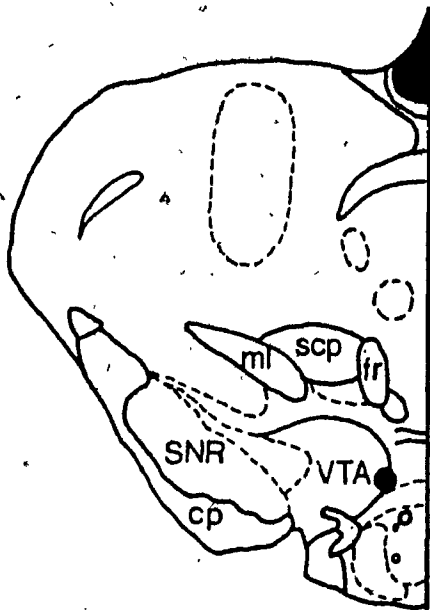
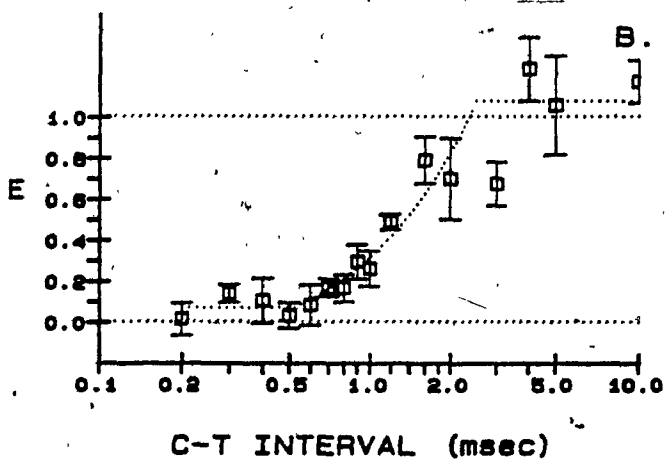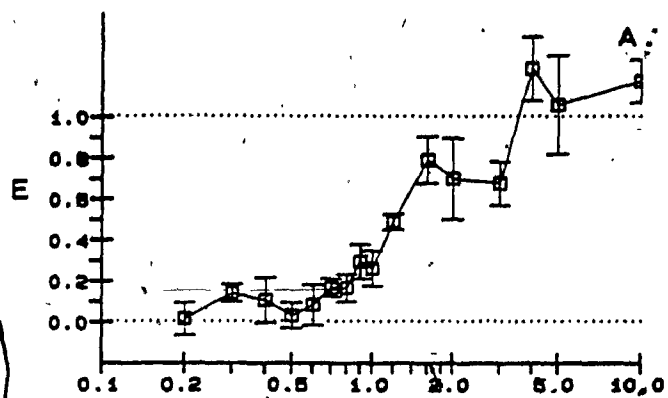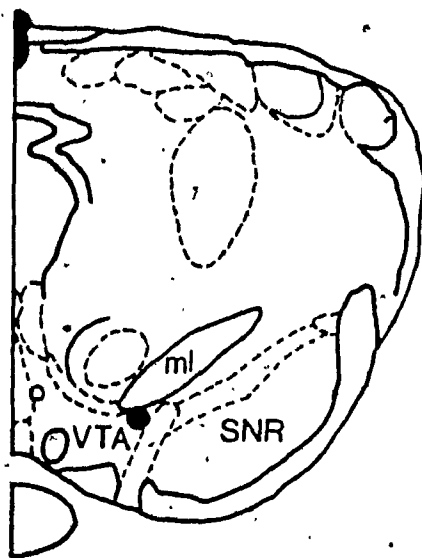

Figure 30. Refractory period data obtained from the anterior stimulation site of subject B1.

B1

A.

B.
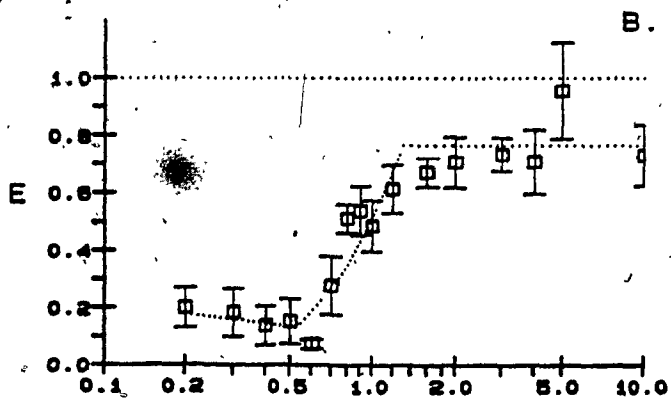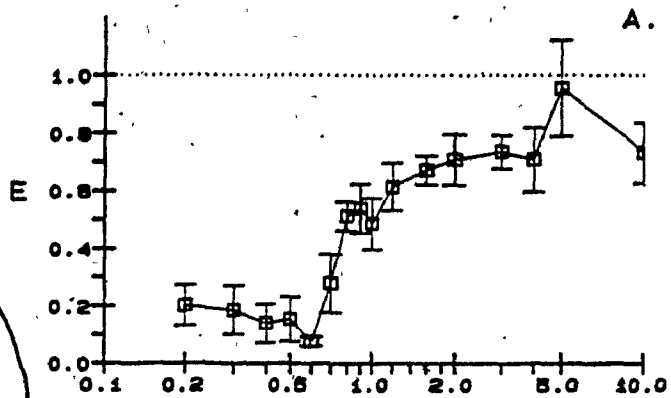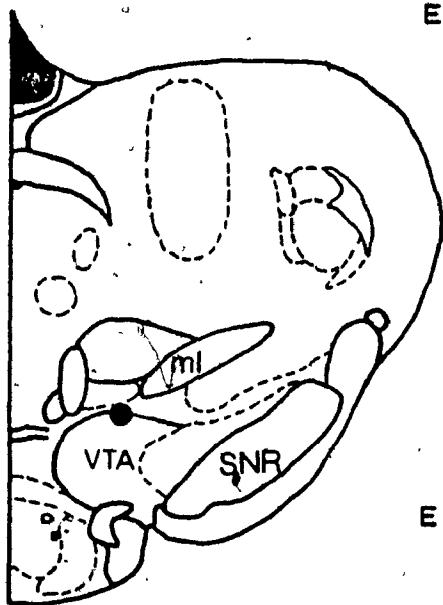
C-T INTERVAL (msec)

The refractory period estimates obtained in this second
experiment have been combined with the appropriate collision
curves in order to obtain an estimate of the conduction
velocity of those fibers responsible for the collision
effect. Because in some cases refractory periods were
obtained for only one of the two stimulation sites, this
determined which collision curve (anterior-posterior vs
posterior-anterior) was used in the estimation of conduction
velocities. For subject M4, the inter-electrode distance
was measured directly from the tips of the two electrodes
following removal of the electrode assembly during
perfusion. For the remaining subjects, the distance between
electrode tips was estimated by locating the lesion at the
tip of each stimulating electrode on fresh coronal sections
and then using the Pythagorean theorem. All relevant
information pertaining to the derivation of conduction
velocities are presented in Table 1. Estimates of
conduction velocities for reward-relevant axons undergoing
collision in the first experiment range from 3.96 to 14.00
m/sec.

Table 1

Estimates of Conduction Velocity for
Reward-Relevant Fibers Linking the Lateral Hypothalamus-
Ventral Tegmental Area and Pontine Sites

I.D.	Coll. interval		Refract. period (msec)	Conduct. time (msec)	Interelec. distance (mm)	Conduct. velocity (m/sec)
	AP	PA				
M0		1.0	0.73	0.27	3.78	14.00
M0	1.0		0.72	0.28	3.78	13.50
M1(E)		0.8	0.60	0.20	2.42	12.10
M4(H)		1.0	0.52	0.48	1.95	4.06
M4(I)		1.0	0.52	0.48	1.9	3.96
M7	1.0		0.60	0.40	4.36	10.90
M7		1.0	0.60	0.40	4.36	10.90
X2		1.0	0.35	0.65	4.03	6.20
B1		1.0	0.53	0.47	3.90	8.30

Discussion

Refractory period estimates obtained in the present experiment overlap with the range of estimates reported in previous studies (Rompré and Miliaressis, 1980; Shizgal et al., 1980; Bielajew and Shizgal, 1982, 1986; Bielajew, Lapointe, Kiss and Shizgal, 1982; Schenk and Shizgal, 1982; Macmillan et al., 1985; Durivage and Miliaressis, 1987; Rompré and Miliaressis, 1987; Gratton and Wise, 1988). For most of the refractory period curves, the estimates obtained with the curve-fitting procedure correspond well with the beginning of recovery that can be inferred de visu. Only in one case, subject M7, were the estimates derived with the curve-fitting procedure shorter than the C-T interval at which recovery, based on visual inspection, appears to begin. The reliability of the estimates derived with the curve-fitting procedure is supported first by the results of previous experiments and second, by the fact that the collision interval is equal to 1.0 msec. If the end of the absolute refractory period of the most excitable fibers were indeed 1.0 msec, this would imply that the time required for action potentials to travel from one electrode tip to the other (4.36 mm) would be 0 msec. In addition, the refractory period curves obtained at the rostral and caudal placements are characterized by a decline in T-pulse effectiveness that follows the initial recovery. This

unusual decrease in T-pulse effectiveness is likely to mask the initial recovery.

The conduction velocity estimates obtained in this second experiment have a wide range, suggesting that reward-relevant fibers linking rostral mesencephalic and pontine areas are heterogeneous. Although these estimates are faster than those reported in previous collision studies, the four slowest estimates (M4 sites H and I, X2 and B1) fall within the previously reported range of 1-8.3 m/sec for MFB reward-relevant fibers. In the case of subject X2, the estimates may be slightly biased. In effect, the refractory periods were estimated with T-pulses that were larger in amplitude than C-pulses. In such a case, there could be a reduction or elimination of relative refractory period contributions which could result in a shorter recovery of the most excitable fibers. The 0.35 msec refractory period estimate obtained with subject X2 might have resulted in an underestimation the conduction velocity.

The use of the curve-fitting procedure has allowed us, to a certain extent, to obtain non-arbitrary estimates of the collision interval and the end of the absolute refractory period of the most excitable neurons. The decision as to where recovery begins or collision block ends was therefore displaced from the experimenter's judgement to the parameters obtained from the curve-fitting procedure.

However, the conduction velocity estimates are nevertheless
biased in that the point chosen along the fitted line to
represent either the begining of recovery or the end of the
collision block was dependent on arbitrary criteria.   In
keeping with criteria used in previous collision studies in
which conduction velocities were also estimated (Shizgal et
al., 1980; Bielajew and Shizgal, 1982, 1986; Durivage and
Miliaressis, 1987; Gratton and Wise, 1988), our criteria for
the end of either the collision block or the absolute
refractory period of the most excitable neurons was the
longest C-T interval before the rise occurs in the
respective curves.   In estimating the end of the collision
block, had we used any point along the rise of the collision
curve to represent the collision interval, conduction time
would have been judged to be longer, and the estimated
conduction velocities slower.   For example, the use of the
midway point between the lower and higher portion of the
collision curve would not be a weak estimate of the
collision interval in view of the fact that the observed
collision interval in any given collision curve is
determined by the C-T intervals that are tested.   The end of
the collision block could therefore be thought of as
occuring anywhere along the rising portion of the curve.   In
the case of refractory periods, if to estimate the end of
the absolute refractory period of the most excitable
neurons, we had chosen any point along the rise in the
refractory period curve, the estimated conduction time would

have been shorter, and the resulting conduction velocity estimates faster.

Conduction velocity estimates are further biased due to the assumption that is made about the trajectory of the reward-relevant fibers linking the two stimulation sites. When estimating the distance that neural signals triggered at one stimulation site must travel in order to reach the other stimulation site, the distance between electrode tips is measured and it is assumed that reward-relevant fibers undergoing collision link the two brain sites by a straight line. Although the collision technique does not allow us to know the actual trajectory of these fibers, it should be recognized that meandering trajectories would imply faster conduction velocities than those obtained in the present study. It should be noted that although the procedure employed in the present study for locating the electrode tips allows us to be confident of their locations, greater precision can be achieved by measuring the inter-electrode distance straight from the electrode assembly.

One point of interest is the observation that most of the collision intervals occur at 1.0 msec eventhough there are differences in inter-electrode distances across subjects. One possible explanation is that the resolution in the inter-pulse intervals employed in the present study is not sufficient to allow us to detect subtle differences in the

collision intervals. For example, the inter-electrode
distances for subjects M0, M7, X2 and B1 range from 3.78 to
4.36 mm. If we assume that the conduction velocity of the
reward-relevant neurons is 8 m/sec (see Bielajew and
Shizgal, 1982), then the collision interval should differ by
less than 0.07 msec, a difference too small to be detected
with the resolution used in the present study.

The inter-electrode distance for subject M1 was 2.42 mm,
that is, 1.36 mm less than the shortest distance measured
for the previous subjects. Assuming again a conduction
velocity of 8 m/sec, the collision interval should be close
to 0.83 msec; indeed, the collision interval of subject M1
is 0.8 msec.

Subject M4 also had a collision interval of 1.0 msec.
However, this subject's inter-electrode distance was even
shorter, and inferred to be 1.9 mm. If these estimates are
correct, we then have to assume that collision in this case
is due to reward-relevant neurons that have slower
conduction velocities.

General Discussion

The results of this study provide anatomical and physiological criteria which could be used to select, among candidate neural pathways, those which best fit the profile of the reward substrate. The candidate neural pathway should, first, travel between the lateral hypothalamus-ventral tegmental area and the medial pons. Second, it should be composed of neurons having absolute refractory periods between 0.35 and 0.73 msec and conduction velocities that range from 3.96 to 14 m/sec. Some likely candidate neural pathways are reviewed below.

Descending pathways

In a study tracing efferent projections of the ventral tegmental area and substantia nigra, Beckstead, Domesick and Nauta (1979) described descending fibers which originate in the ventral tegmental area and extend to the ventral part of the central gray and dorsal raphe nucleus, parabrachial nuclei, locus coeruleus, and dorsolateral tegmental nucleus. In a similar study, Hosoya and Matsushita (1981) described fibers that originate in the lateral hypothalamic area and descend through the medial forebrain bundle to the ventral tegmental area. A portion of these fibers were further observed to project caudally, enter the central gray, and

terminate densely in the dorsal raphe. Although efferent projections from lateral hypothalamic areas to the central gray-dorsal raphe region are well documented (e.g., Beitz, 1982; Villalobos and Ferssiwi, 1987; Veening, Te Lie, Posthuma, Geeraedts and Nieuwenhuys, 1987) and seem to fit the anatomical criteria established in the present study, the physiology of these fibers has not been studied in sufficient detail to allow comparison of their physiological characteristics to those established in the present study.

Nauta and Domesick (1982) described the distribution of descending components of the medial forebrain bundle; such fibers are described to have origins within various forebrain structures. Upon entering the ventral tegmental area, descending fibers were observed to bifurcate into a lateral and a medial subdivision. The medial subdivision is of interest in the present context, because it travels caudally to the interpeduncular nucleus, the median and dorsal raphe, and other ventral regions of the central gray such as the dorsolateral tegmental nucleus and the locus coeruleus. In a recent electrophysiological study (Rompré and Shizgal, 1986), it was shown that neurons originating in the medial septum, diagonal band of Broca and other forebrain structures, send fibers through the medial forebrain bundle that descend at least as far as the ventral tegmental area. Furthermore, some of these cells were considered as likely mediators of the reward signal in that

they were found to exhibit physiological characteristics (i.e., refractory periods, conduction velocities) that were comparable to criteria that have been established with behavioral methods.

These anatomical and physiological data would suggest that some reward-relevant neurons linking the mesencephalon and the medial pons might be part of a descending neural pathway originating from the basal forebrain.

Ascending pathways

Ascending fibers have also been shown to link the dorsal raphe to sites within the medial forebrain bundle. Phillipson (1978) showed that efferents from the dorsal raphe constitute one of the densest projections to the ventral tegmental area. Similar results were obtained by Taber-Pierce, Foote and Hobson (1976). Takagi, Shiosaka, Tohyama, Senba and Sakanaka (1980) proposed two ascending components: one extending from the dorsal raphe to areas between the anterior commissure and anterior hypothalamic nucleus, and another from the dorsal raphe to areas between the ventromedial and posterior hypothalamic nuclei. These authors also showed that ascending fibers from the dorsolateral tegmental nucleus ascend through the MFB. Although these fibers travel from brain stem regions to the MFB, it is not known, based on the description afforded by

these authors, if they directly link these caudal sites to the ventral tegmental area. In a separate study, ascending fibers with origins within the dorsolateral tegmental nucleus, dorsal raphe, and caudal linear nucleus were found to ascend through the MFB to the level of the most anterior part of the dorsal hippocampus (Vertes, 1984). Again, the trajectory of these fibers was not described in sufficient detail to know if they link directly to the ventral tegmental area.

Noradrenergic pathways

Early hypotheses involved a role for noradrenaline as a mediator of reward after it was observed that self-stimulation could be obtained from sites near the locus coeruleus or its major rostral efferent, the dorsal tegmental bundle (see Crow, Spear and Arbuthnott, 1972; Ritter and Stein, 1973). Much of the available data are correlational, however, and inconclusive (see Wise, 1978). A major catecholamine system, however, known as the tegmental catecholamine radiations and described by Lindvall and Björklund (1974), corresponds well with the anatomical constraints placed by our collision data. The tegmental catecholamine radiations are fed by the major ascending noradrenergic pathways originating in the brain stem such as the dorsal tegmental bundle, central tegmental tract and the periventricular system. When passing from dorsal to ventral

regions, these tegmental radiations are described to diverge into a fanlike arrangement, in an area immediately rostral to the decussation of the superior cerebellar peduncles. The radiating fibers are described to diverge into median, medial and lateral components. The median flow of fibers was traced by these authors from the rostral part of the dorsal raphe, between the two medial longitudinal fasciculi, to the region dorsal to the interpeduncular nucleus.

Although the trajectory of the tegmental catecholamine radiations conforms to the anatomical constraints placed by the collision data, neurophysiological characteristics of noradrenergic neurons are not compatible with the criteria established in the present study. First, the refractory periods of noradrenergic neurons are longer than 2.0 msec (Takigawa and Mogenson, 1977; Guyenet, 1980), values too long to account for the rising portion of the refractory period curves. Noradrenergic neurons may, however, contribute to the late part of the refractory period curve (C-T > 2.0 msec). Stronger evidence against a first-stage role for noradrenergic neurons is that they are fine and unmyelinated (Foote, Bloom and Aston-Jones, 1983) and consequently, have slower conduction velocities (0.4-0.86 m/sec) than those obtained in the present study (Takigawa and Mogenson, 1977; Guyenet, 1980).

Serotonergic pathways

A role for serotonergic neurons in the mediation of brain stem reward was proposed following the observation that self-stimulation could be obtained from the dorsal and median raphe, nuclei rich in serotonergic cell bodies (see Miliaressis, 1977). Parent, Descarries and Beaudet (1981) described a major system of ascending serotonergic fibers, known as the transtegmental system, which conforms to the anatomical boundaries set by the present study. This serotonergic system was observed to originate in the dorsal raphe, and less prominently form the median raphe. The fibers of this system were described to course ventrally, either medial to or through the medial longitudinal fasciculi, and penetrate the decussation of the superior cerebellar peduncles. These serotonergic fibers were observed to follow the trajectory of the tegmental catecholamine radiations, but were mostly confined to the median and medial components of the system. Transtegmental fibers were further observed to sweep rostrally through the ventral tegmental decussation and enter the ventral tegmental area.

As is the case with noradrenergic fibers, neurophysiological characteristics of serotonergic fibers are not compatible with the criteria established in this study. The refractory periods of serotonergic neurons are estimated to

range from 1.2 to 5.0 msec (Wang and Aghajanian, 1977).
Furthermore, only about 0.7% of MFB serotonergic neurons are
myelinated (Azmitia and Gannon, 1983). Although fast-
conducting serotonergic fibers project from the raphe magnus
to the spinal cord (3.1-6.0 m/sec) (Wessendorf, Proudfit and
Anderson, 1981), the conduction velocities of ascending
serotonergic neurons have been estimated to range from 0.5
to 1.7 m/sec (Wang and Aghajanian, 1977; Crunelli and Segal,
1982). As with the noradrenergic neurons, these
neurophysiological characteristics make it unlikely that
serotonergic neurons constitute the directly stimulated
reward substrate.

An important characteristic of the reward substrate that
would help narrow the selection of candidate pathways would
be knowledge of the normal direction of propagation of
action potentials within reward-relevant neurons linking the
ventral tegmental area with the pons. This can be achieved
with the hyperpolarization block technique developed by
Bielajew and Shizgal (1986). Using this technique, these
authors showed that at least some reward-relevant neurons
within the MFB conduct orthodromic action potentials in a
rostro-caudal direction. If, in future work, application of
this technique to the areas studied in the present work
yield similar results, this would provide support for the
notion that brain stem reward shares a common substrate with
medial forebrain bundle reward. Indeed, the overlap in

estimates of refractory periods and conduction velocities
seem to suggest such continuity. Moreover, the collision
data of subject M7 further strengthen the idea of a
continuous substrate.

A more direct way to test for continuity between the
substrate mediating MFB and brain stem reward is to extend
the present collision findings in a rostral direction by
testing for collision between anterior MFB sites and sites
in the brain stem. Based on the results obtained from
subject MO, the collision data obtained in the present study
could also be extended to caudal and lateral areas. Recall
that this subject's posterior electrode was located
approximately 1.0 mm lateral to the midline. Replication of
such a finding could be followed by application of the
collision test to posterior sites at different bilateral
distances from the midline but with the anterior electrode
implanted at a fixed location. Findings of such a study
would yield further information about the trajectory of the
reward substrate in pontine regions.

The results of the present study have extended our
knowledge about the neural circuitry responsible for brain
stimulation reward. It was shown that reward-relevant
fibers directly link the lateral hypothalamus-ventral
tegmental area to sites in the pons. Furthermore, these
fibers were shown to be fast-conducting and have refractory

periods that overlap with estimates obtained from reward-
relevant fibers in the MFB. These results bring us one step
forward towards the identification of the reward
substrate(s).

References

Azmitia, E. and Gannon, P. (1983). The ultrastructural localization of serotonin immunoreactivity in myelinated and unmyelinated axons within the medial forebrain bundle of rat and monkey. The Journal of Neuroscience, 3 (10), 2083-2090.

Beckstead, R. M., Domesick, V. B. and Nauta, W. H. (1979). Efferent connections of the substantia nigra and ventral tegmental area in the rat. Brain Research, 175, 191-217.

Beitz, A. J. (1982). The organization of afferent projections to the midbrain periaqueductal gray of the rat. Neuroscience, 7 (1), 133-159.

Bielajew, C., Jordan, C., Ferme-Enright J. and Shizgal, P. (1981). Refractory periods and anatomical linkage of the substrates for lateral hypothalamic and periaqueductal gray self-stimulation. Physiology and Behavior, 27, 95-104.

Bielajew, C., Lapointe, M., Kiss I. and Shizgal, P. (1982). Absolute and relative refractory periods of the substrates for lateral hypothalamic and ventral midbrain self-stimulation. Physiology and Behavior, 28, 125-132.

Bielajew, C. and P. Shizgal. (1980). Dissociation of the substrates for medial forebrain bundle self-stimulation and stimulation-escape using a two-electrode stimulation technique. Physiology and Behavior, 25, 707-711.

Bielajew, C. and Shizgal, P. (1982). Behaviorally derived measures of conduction velocity in the substrate for rewarding medial forebrain bundle stimulation. Brain Research, 237, 107-119.

Bielajew, C. and Shizgal, P. (1986). Evidence implicating descending fibers in self-stimulation of the medial forebrain bundle. The Journal of Neuroscience, 6 (4), 919-929.

Bielajew, C., Thrasher, A. and Fouriezos, G. (1987). Self-stimulation sites in the lateral hypothalamic and lateral preoptic areas are functionally connected. Canadian Psychology, 28, abstract No. 36.

Bower, G. H. and Miller, N. E. (1958). Rewarding and
    punishing effects from stimulating the same place in the
    rat's brain. Journal of Comparative and Physiological
    Psychology, 51, 669-674.

Caggiula, A. R. and Hoebel, B. G. (1966). Copulation-
    reward site in the posterior hypothalamus. Science, 153
    (3741), 1284-1285.

Chung, J. M. and Wurster, R. D. (1978). Neurophysiological
    evidence for spatial summation in the CNS from
    unmyelinated afferent fibers. Brain Research, 153,
    596-601.

Crow, T. J., Spear, P. J. and Arbuthnott, G. W. (1972).
    Intracranial self-stimulation with electrodes in the
    region of the locus coeruleus. Brain Research, 36,
    275-287.

Deutsch, J. A. (1964). Behavioral measurement of the
    neural refractory period and its application to
    intracranial self-stimulation. Journal of Comparative
    and Physiological Psychology, 58 (1), 1-9.

Durivage, A. and Miliaressis, E. (1987). Anatomical
dissociation of the substrates of medial forebrain
bundle self-stimulation and exploration. Behavioral
Neuroscience, 101 (1), 57-61.

Foote, S. L., Bloom, F. E. and Aston-Jones, G. (1983).
Nucleus locus coeruleus: new evidence of anatomical and
physiological specificity. Physiological Reviews, 63,
844-914.

Gallistel, C. R., Shizgal, P. and Yeomans, J. (1981). A
portrait of the substrate for self-stimulation.
Psychological Review, 88 (3), 228-273.

Gratton, A. and Wise, R. A. (1988). Comparisons of
connectivity and conduction velocities for medial
forebrain bundle fibers subserving stimulation-induced
feeding and stimulation reward. Brain Research, 438,
264-270.

Guyenet, P. G. (1980). The coeruleospinal noradrenergic
neurons: anatomical and electrophysiological studies in
the rat. Brain Research, 189, 121-133.

Hoebel, B. G. and Teitelbaum, P. (1962). Hypothalamic
control of feeding and self-stimulation. Science, 135,
375-377.

Hosoya, Y. and Matsushita, M. (1981). Brainstem
projections from the lateral hypothalamic area in the
rat, as studied with autoradiography. Neuroscience
Letters, 24, 111-116.

Lindvall, O. and Björklund, A. (1974). The organization of
the ascending catecholamine neuron systems in the rat
brain. Acta Physiologica Scandinavica, Supplement 412,
1-48.

MacDonnel, M. F. and Flynn, J. P. (1964). Sensory control
of hypothalamic attack. Animal Behavior, 14, 339-405.

Macmillan, C. J., Simantirakis, P. and Shizgal, P. (1985).
Self-stimulation of the lateral hypothalamus and
ventrolateral tegmentum: Excitability characteristics of
the directly stimulated substrates. Physiology and
Behavior, 35, 711-723.

Malette, J. and Miliaressis, E. (1987). Evidence for
ascending and descending rewarding axons in the medial
forebrain bundle. Canadian Psychology, 28, abstract No.
364.

Miliaressis, E. (1977). Serotonergic basis of reward in
median raphe of the rat. Pharmacology Biochemistry and
Behavior, 7, 177-180.

Miliarressis, E. and Rompré, P. P. (1980). Self-stimulation and circling: differentiation of the neural substrata by behavioral measurement with the use of the double pulse technique. Physiology and Behavior, 25, 939-943.

Miliaressis, E. (1981). A miniature, moveable electrode for brain stimulation in small animals. Brain Research Bulletin, 7, 715-718.

Miliaressis, E. and Philippe, L. (1983). A dual moveable stimulating electrode and its application to the behavioral version of the collision test. Brain Research Bulletin, 10, 573-577.

Mogenson, G. J. and Stevenson, J. A. F. (1966). Drinking and self-stimulation with electrical stimulation of the lateral hypothalamus. Physiology and Behavior, 1, 251-254.

Mundl, W. J. (1980). A constant-current stimulator. Physiology and Behavior, 24, 991-993.

Nauta, W. J. H. and Domesick, V. B. (1982). Neural associations of the limbic system. In: The Neural Basis of Behavior. Beckman, A. L. (Ed.) Spectrum Publications Inc., New York.

Nieuwenhuys, R., Geeraedts, L. M. G. and Veening, J. G. (1982). The medial forebrain bundle of the rat. I. General introduction. Journal of Comparative Neurology, 206, 49-81.

Olds, J. and Milner, P. (1954). Positive reinforcement produced by electrical stimulation of septal area and other regions of rat brain. Journal of Comparative and Physiological Psychology, 47, 419-427.

Parent, A., Descarries, L. and Beaudet, A. (1981). Organization of ascending serotonin systems in the adult rat brain. A radioautographic study after intraventricular administration of $(^3H)5$-hydroxytryptamine. Neuroscience, 6, 115-138.

Paxinos, G. and Watson, C. (1986). The rat brain is stereotaxic coordinates (2nd ed.) Australia: Academic Press.

Phillipson, O. T. (1978). Afferent projections to A10 dopaminergic neurones in the rat as shown by the retrograde transport of horseradish peroxidase. Neuroscience Letters, 9, 353-359.

Ritter, S. and Stein, L. (1973). Self-stimulation of
noradrenergic cell group (A6) in locus coeruleus of
rats. Journal of Comparative and Physiological
Psychology, 85, 443-452.

Rolls, E. T. and Kelly, P. H. (1972). Neural basis of
stimulus-bound locomotor activity in the rat. Journal
of Comparative and Physiological Psychology, 81,
173-182.

Rompré, P. P. and Miliaressis, E. (1980). A comparison of
the excitability cycles of the hypothalamic fibers
involved in self-stimulation and exploration.
Physiology and Behavior, 24, 995-998.

Rompré, P. P. and Miliaressis, E. (1985). Pontine and
mesencephalic substrates of self-stimulation. Brain
Research, 359, 246-259.

Rompré, P. P. and Shizgal, P. (1986). Electrophysiological
characteristics of neurons in forebrain regions
implicated in self-stimulation of the medial forebrain
bundle in the rat. Brain Research, 364, 338-349.

Rompré, P. P. and Miliaressis, E. (1987). Behavioral determination of refractory periods of the brainstem substrates of self-stimulation. Behavioural Brain Research, 23, 205-219.

Rompré, P. P. and Boye, S. M. (1988) Localization of reward-relevant neurons in the pontine tegmentum: A moveable electrode mapping study. Submitted.

Schenk, S. and Shizgal, P. (1982). The substrates for lateral hypothalamic and medial pre-frontal cortex have different refractory periods and show poor spatial summation. Physiology and Behavior, 28, 133-138.

Shizgal, P., Bielajew, C., Corbett, D., Skelton R. and Yeomans, J. (1980). Behavioral methods for inferring anatomical linkage between rewarding brain stimulation sites. Journal of Comparative and Physiological Psychology, 94 (2), 227-237.

Taber-Pierce, E., Foote, W. E. and Hobson, T. A. (1976). The efferent connections of the nucleus raphe dorsalis. Brain Research, 107, 137-144.

Takagi, H., Shiosaka, S., Tohyama, M., Senba, E. and
Sakanaka, M. (1980). Ascending components of the medial
forebrain bundle from the lower brain stem in the rat,
with special reference to raphe and catecholamine cell
groups. A study by the HRP method. Brain Research,
193, 315-337.

Takigawa, M. and Mogenson, G. J. (1977). A study of inputs
to antidromically identified neurons of the locus
coeruleus. Brain Research, 135, 217-230.

Veening, J. G., Te Lie, S., Posthuma, P., Geeraedts, L. M.
G. and Nieuwenhuys, R. (1987). A topographical
analysis of the origin of some efferent projections from
the lateral hypothalamic area in the rat. Neuroscience,
22 (2), 537-551.

Vertes, R. P. (1984). A lectin horseradish peroxidase
study of the origin of ascending fibers in the medial
forebrain bundle of the rat. The upper brainstem.
Neuroscience, 11 (3), 669-690.

Villalobos, J. and Ferssiwi, A. (1987). The differential
descending projections from the anterior, central and
posterior regions of the lateral hypothalamic area: An
autoradiographic study. Neuroscience Letters, 81,
95-99.

Wang, R. Y. and Aghajanian, G. K. (1977). Antidromically identified serotonergic neurons in the rat midbrain raphe: evidence for collateral inhibition. *Brain Research*, 132, 186-193.

Wessendorf, M. W., Proudfit, H. K. and Anderson, E. G. (1981). The identification of serotonergic neurons in the nucleus raphe magnus by conduction velocity. *Brain Research*, 214, 168-173.

Wise, R. A. (1978). Catecholamine theories of reward: A critical review. *Brain Research*, 152, 215-247.

Yeomans, J. (1975). Quantitative measurement of neural post-stimulation excitability with behavioral methods. *Physiology and Behavior*, 15, 593-602.

Yeomans, J. (1979). The absolute refractory periods of self-stimulation neurons. *Physiology and Behavior*, 22, 911-919.

APPENDIX A

Currents Used For Collision Test

Subject	Site	Anterior Current (uA)	Posterior Current (uA)
M1	A	900	420
	B	900	420
	C	900	420
	D	900	420
	E	402	516
M4	A	500	1000
	B	500	1000
	C	500	599
	D	500	599
	E	500	467
	F	500	402
	G	500	402
	H	516	269
	I	516	269
M6	A	402	402

	B	402	402
AP	C	363	363
PA	C	269	363
M7	A	300	300
M8	A	809	199
	B	732	402
	C	516	402
	D	444	402
	E	444	382
	F	444	329
	G	444	313
	H	444	313
	I	444	313
	J	444	313
	K	444	313
	L	444	313
	M	444	313
	N	732	244
X2	A	542	516
	B	542	491
B1	A	232	570
M0	A	599	346